

UNIVERSITÀ DEGLI STUDI DI NAPOLI FEDERICO II

Dipartimento di Ingegneria Strutturale

PH.D. PROGRAMME IN SEISMIC RISK

COORDINATOR PROF. ALDO ZOLLO

XXIII CYCLE



CARMINE GALASSO

PH.D. THESIS

**Consolidating record selection for
earthquake resistant structural design**

TUTOR PROF. IUNIO IERVOLINO

2010

*A Maria, Ernesto
e Salvatore*

Acknowledgements¹

Da qualche giorno ho sottomesso la versione finale ed “ufficiale” di questa tesi. Tuttavia, prima della stampa, posso ancora aggiungere qualche riga, anche se il rischio è di scrivere un intero nuovo capitolo. Ho aspettato qualche giorno per essere sicuro di aver definitivamente superato lo stress e l'ansia (e l'influenza!) da “consegna” degli ultimi giorni. E per essere sicuro di essere lucido il più possibile nel ricordare tutte le persone che, a vario titolo, hanno contribuito a rendere “speciali” questi ultimi tre anni. Tre anni trascorsi forse troppo rapidamente, ricchissimi di esperienze, di viaggi in tutto il mondo, di crescita intellettuale e umana.

Il primo pensiero va sicuramente a Iunio, un grande scienziato e maestro, il tutor spesso severo ma, soprattutto, colui che mi ha dato e continua a darmi tante opportunità di crescita. Tanti “successi” raggiunti insieme in questi anni, tanti traguardi importanti, dall'esame di Tecnica delle Costruzioni fino alla laurea in Ingegneria Gestionale e poi a questo dottorato. Anche qualche incomprensione e delusione, ma credo che tutto questo sia normale ed inevitabile quando c'è una fiducia reale e reciproca ed una grande e profonda stima. Spero che, nei prossimi mesi, anche a distanza, continui ad essere per me un punto di riferimento fondamentale. E spero di avere la possibilità di collaborare con lui ancora a lungo, certo che nessuno, meglio di lui, sappia veramente essere un eccellente tutor.

Una delle più grandi opportunità in assoluto è stata sicuramente quella di collaborare con Edoardo Cosenza. Nonostante i suoi ruoli sempre più importanti, negli anni, ha saputo creare un rapporto diretto, fatto di chiacchierate ma anche di decine di mail ed sms. Credo, forse con un po' di presunzione, che insieme siamo riusciti a creare una intesa perfetta dal punto di vista umano e didattico ed è stata percepita dai tantissimi allievi dei “nostri” corsi. Ci siamo “divertiti” a “sperimentare” formule, a fare “esercizi” apparentemente semplici ma che ci hanno aiutato a capire meglio molte questioni complicate. Confesso che la sua nomina ad assessore, se da un lato mi ha riempito di orgoglio e di entusiasmo, allo stesso tempo mi ha un po' spaventato, per la paura di

¹ I have chosen to write these few pages in Italian for better express myself, my feelings and my thoughts.

Acknowledgements

“perdere” (inevitabilmente forse, a causa dei mille nuovi impegni) una guida importante per il nostro gruppo. Tuttavia, guardando a questi primi mesi del suo assessorato e ai primi successi, credo che persone come lui siano fondamentali in certe posizioni e possano dare un contributo veramente importante da ogni punto di vista.

Grazie ad Edoardo Cosenza e all’enorme attività didattica che ho svolto in questi tre anni per i corsi di Tecnica delle Costruzioni e Teoria e Progetto delle Costruzioni in c.a che ho avuto la possibilità di interagire con Maria, Salvatore A., Francesco, Antonio N., Biagio, Oliver, Antonio P., Michele, Alfredo, Alessandra, Ilario, Rossella, Gennaro M., Gennaro N., Stefania, Giusy, Nicola, Raffaella, Mario, Salvatore M., Angelo, Carmine, Gaetano, Marco, i miei “tesisti”, che mi hanno insegnato quanto sia faticoso fare bene questo “lavoro” ma anche quante soddisfazioni possa dare se alla base di tutto ci sia grande passione e soprattutto tanto e durissimo impegno.

Un ringraziamento particolare va ad Angelo e Carmine, per il contributo importante, fondamentale, dato a questa tesi attraverso le loro tesi di laurea specialistica ma, soprattutto, per il rapporto di fiducia, stima ed amicizia creatosi in questi ultimi mesi. Due persone semplici ed umili ma soprattutto due brillanti neo-ingegneri a cui auguro tutto il meglio.

Grazie a Gaetano Manfredi. Pochi incontri “formali”, innumerevoli incontri in ascensore, tra i corridoi ed, ogni volta, un solo sguardo, un sorriso o poche parole di persona che, nonostante i mille impegni, è continuamente informata e conosce tutto del percorso di ognuno di noi, ci guida e guida al meglio una delle realtà scientifiche più importanti a livello nazionale e internazionale. E credo che nessuno sarebbe altrettanto bravo.

Al DISt ho incontrato e conosciuto Fabio e Ludovica che mi hanno accolto nonostante la mia provenienza “incivile”, mi hanno supportato e supportato, consigliato e continuano a mostrarmi affetto e stima e a credere in me. In particolare, ringrazio Fabio, un grande amico ma soprattutto uno straordinario ricercatore, sempre pronto ad aiutarmi e a mettersi in discussione, contando solo sulle sue forze, nonostante le tante condizioni al contorno non sempre favorevoli al massimo. Spero che saremo colleghi ancora a lunghissimo.

Al DISt ho incontrato Fulvio, che ho imparato a conoscere ancora meglio in questo ultimo anno di “convivenza” al terzo piano e che ammiro molto per il suo modo di procedere e di impegnarsi senza limiti, spinto spesso solo da una smisurata passione.

Acknowledgements

Al DIST ho re-incontrato Simona, dopo qualche anno. Dopo una iniziale diffidenza, ho scoperto una persona veramente speciale, solare, determinata, dolce. Forse è la persona più in crisi per la mia partenza, ma sa che potrà contare sempre su di me, anche a distanza e sa bene che anche io conto e conterò su di lei sempre.

Grazie a Giuseppe Maddaloni che mi ha passato il testimone dei vari corsi di Cosenza. Sempre pronto ad aiutarmi, a fornire consulenze, anche notturne, prima di una lezione, anche quando era oltreoceano. Grazie a Raffaele che, a sua volta, ha raccolto il testimone ed in tantissime occasioni mi ha mostrato e continua a mostrarmi la sua stima e il suo affetto, ovviamente ampiamente ricambiati. La sua bravura è un dato di fatto; la sua crescita scientifica e umana, è sotto gli occhi di tutti e sono fiero di aver contribuito, nel mio piccolo (e forse minimamente), a trasmettergli la passione per la ricerca e la didattica.

Grazie a Fatima, una grande e brillante ricercatrice ma ormai anche un'ottima moglie ed una straordinaria mamma per il piccolo Arman. Dolcissima, sempre pronta ad aiutare tutti, a consigliarmi, a sorridere anche nei momenti più difficili.

Ringrazio il prof. Paolucci, Francesca Pacor e Andrea Spinelli per la collaborazione a REXELite. In particolare, ringrazio Andrea, per l'accoglienza e per le piacevoli settimane nella valle Brembana, per l'enorme pazienza con cui continua a rispondere sempre ad ogni mail/richiesta mia e di Iunio, anche a quelle più scoccianti.

Grazie a Catia e Cristina, una conferma ormai. Non abbiamo segreti, mi comprendono sempre (anche quando sbaglio oggettivamente!), mi incoraggiano continuamente e costantemente. Grazie a Roberto.

Grazie ai miei genitori, a mio fratello e ad Eleonora. Per il loro amore, la loro pazienza nel sopportarmi, per il loro sostegno e perché hanno sempre creduto in me e continuano a farlo, nonostante le tante difficoltà e nonostante siamo, e saremo, spesso lontani.

Ringrazio infine tutte le persone che non ho menzionato ma che mi hanno incoraggiato in questi anni, perché mi hanno spinto ad impegnarmi fino al limite. Ringrazio anche chi mi ha deluso e scoraggiato (o hanno provato a farlo), perché mi ha spinto a superare quel limite e ad impegnarmi ancora di più nelle cose che faccio ed in cui credo.

Carmine

Summary

Seismic assessment of existing, generally under-designed, structures and of proposed design of new structures is usually based on nonlinear static (i.e., pushover) analysis procedures, but nonlinear dynamic analysis (NLDA) is now being increasingly used in assessing the seismic structural performance. In NLDA, once an appropriate and accurate model for the structure is created, the seismic demand is determined by nonlinear response history analysis of the structure for several earthquake ground motions.

The issue of selecting recorded earthquake ground motions as input for NLDA is seen to be one of the most critical and it is sometimes considered more important even than structural modeling. Procedures for selecting and scaling ground motions records for a site-specific hazard are described in building codes and have been the subject of much research in recent years.

As non-linear dynamic analysis becomes a more frequently used procedure in research, international codes and practice for assessing the demand on a structure due to earthquakes, ground motion selection becomes increasingly relevant (Chapter 1).

In order to select representative ground motions to effectively assess structural performance, it is important, first of all, to understand which properties of a recorded ground motion are mostly strongly related to the response caused in the structure and, consequently, have to take into account (Chapter 2). Then, it is important to develop and introduce into the practice of structural engineering, tools which may effectively help to address the basic issues related to seismic input selection, trying to reconcile research achievements and code-based practice (Chapter 3-5).

Based on these remarks, the aim of this study is to consolidate the state of research and to shed some light on a number of aspects involved when selecting and, eventually, manipulating ground motions for NLDA. Practical guidance and software tools are developed and provided to the engineering community for choosing appropriate ground motions in predicting structural response by NLDA.

The provisions on which the whole thesis is based are those of Eurocode 8, i.e., the main seismic design code in Europe, and the new Italian building code, one of the most advanced with respect to seismic hazard issue, at least in Europe.

Keywords: *Performance-Based Earthquake Engineering • Italian Building Code • Eurocode 8 • Hazard • Record Selection • Nonlinear Dynamic Analysis • REXEL • Cumulative Damage.*

Tables of contents

| | |
|--------------------------------|-----------|
| Summary | 8 |
| Tables of contents..... | 10 |
| List of figures | 13 |
| List of tables | 17 |

Chapter 1

| | |
|---|-----------|
| INTRODUCTION | 19 |
| 1.1 Motivation..... | 19 |
| 1.2 Record selection for non-linear seismic analysis of structures: some key concepts . | 21 |
| 1.3 Organization and contributions to code-based record selection | 30 |
| References..... | 34 |

Chapter 2

| | |
|--|-----------|
| Code-based real record selection: what really matters? | 37 |
| 2.1 Introduction | 38 |
| 2.2 Findings of previous investigations about record selection for NLDA..... | 41 |
| 2.3 Case-study structure..... | 44 |
| 2.4. Record classes | 50 |
| 2.5 Results and discussion | 58 |
| 2.6. Conclusions..... | 69 |
| References..... | 71 |

Chapter 3

| | |
|--|-----------|
| Improving seismic action assessment: conditional design maps for secondary intensity measures | 74 |
| 3.1 Introduction | 75 |
| 3.2 Ground motion prediction equation for I_D | 77 |
| 3.3 Joint normality and conditional distributions of the logarithms of I_D and PGA | 82 |

Table of contents

| | |
|------------------------------------|----|
| 3.4 Illustrative application | 85 |
| 3.5 Conclusions | 91 |
| Data and resources | 92 |
| References..... | 92 |

Chapter 4

| | |
|---|-----------|
| Including research advances into practice: REXEL | 95 |
| 4.1 Introduction | 95 |
| 4.2 Record selection in EC8..... | 98 |
| 4.3 Seismic input according to NIBC..... | 102 |
| 4.4 REXEL | 104 |
| 4.5 Illustrative applications..... | 118 |
| 4.6 Comparison with the classification in seismic zones | 134 |
| 4.7 Conclusions | 137 |
| References..... | 139 |

Chapter 5

| | |
|---|------------|
| Using the ITalian ACcelrometric Archive from earthquake engineering perspective | 142 |
| 5.1 Introduction | 142 |
| 5.2 The ITalian ACcelrometric Archive (ITACA)..... | 144 |
| 5.3 European and Italian standards for record selection for dynamic structural analysis | 146 |
| 5.4 REXELite..... | 150 |
| 5.5 Applications..... | 154 |
| 5.6 CONCLUSIONS..... | 165 |
| References..... | 167 |

Chapter 6

| | |
|--------------------------|------------|
| Conclusions | 169 |
| 6.1 Main findings..... | 169 |

Table of contents

Appendix A

| | |
|--------------------------------------|------------|
| Target spectra | 174 |
| A1. Eurocode 8 target spectra | 174 |
| A.2 Italian code target spectra..... | 175 |

Appendix B

| | |
|--|------------|
| Earthquake ground motions used for analysis | 181 |
|--|------------|

Appendix C

| | |
|--|------------|
| Ground motions sets used for analysis | 190 |
|--|------------|

List of figures

| | |
|--|----|
| Figure 1. Schematic illustration of the Performance-Based Earthquake Engineering model and the “link” variables IM, EDP and DM. | 20 |
| Figure 2. Combining hazard curves from individual periods to generate a uniform hazard spectrum with 0.0021 annual rate of exceedance (i.e., 10% probability of exceedance in 50 years) for a site in Sant’Angelo dei Lombardi (southern Italy). (a) Hazard curves for different periods, with an example UHS point identified ($T = 0.75s$). (b) Uniform hazard spectrum (adapted from Iervolino and Manfredi, 2008)..... | 24 |
| Figure 3. Steps to define seismic action according to the hazard at the site (<i>best practice</i>); from (1) to (3): target spectrum for the limit-state of interest, hazard disaggregation for the spectral ordinate at the period of the first mode of the structure, selection of a set of records compatible to disaggregation and matching the target spectrum at that same period (adapted from Iervolino, 2010)..... | 25 |
| Figure 4. Steps to define seismic action according to the hazard at the site (alternative, code-based, procedure); from (1) to (3): target spectrum for the limit-state of interest, hazard disaggregation for the spectral ordinate at the period of the first mode of the structure, selection of a set of records compatible to disaggregation and matching the target spectrum in a range of periods. | 26 |
| Figure 5. Italian map of first (left) and second design earthquakes (right) in terms of M (top) and R (bottom) for $S_a(1.0sec)$ with a return period of 475 yr. For further details see Chioccarelli et al. (2010)..... | 28 |
| Figure 6. Geometry of the case-study building: (left) tri-dimensional view and (right) plan. | 44 |
| Figure 7. (a) Schematic diagram of the monotonic behavior of plastic hinge model used in this study; (b) static pushover of the case-study building. | 48 |
| Figure 8. Disaggregation results for Ponticelli for $S_a(T=1s)$ and for a 2475-years return period..... | 54 |
| Figure 9. Average spectra for each individual set of seven records selected (and eventually scaled) to be compatible (on average) with the target spectrum in [0.15-2s] periods range (a) Group I (1 st disaggregation mode-based); (b) Group II (2 nd disaggregation mode-based). | 55 |
| Figure 10. Individual and average spectra for each individual set of seven records selected and scaled to match precisely $T=1s$ -ordinate of the target spectrum (a) Group III (1 st disaggregation mode-based); (b) Group IV (2 nd disaggregation mode-based).... | 56 |
| Figure 11. Summary of MIDR responses for the selected ground motions sets..... | 59 |
| Figure 12. Summary of RD responses for the selected ground motions sets..... | 59 |

List of figures

| | |
|---|-----|
| Figure 13. Summary of E_H responses for the selected ground motions sets..... | 60 |
| Figure 14. SEE/median EDP as a function of set size. | 61 |
| Figure 15. E_H versus (a) I_A and (b) I_D for the considered sets..... | 67 |
| Figure 16. Distribution of the records with respect to moment-magnitude and epicentral distance. | 78 |
| Figure 17. Plot of I_D as a function of epicentral distance..... | 81 |
| Figure 18. (a) Example of joint distribution of PGA and I_D for an M 7 event and for a site at 50 km from the source in terms of epicentral distance. (b) Contours of joint distribution of PGA and I_D for different M values ($R_{epi} = 50$ km). | 84 |
| Figure 19. (a) Seismic zones considered in the analysis; (b) 475 years return period PGA on rock hazard map for the Campania region (southern Italy). | 86 |
| Figure 20. (a) Hazard map in term of I_D with a 50% exceedance probability given PGA of panel 19b; (d) hazard map in terms of I_D with a 10% exceedance probability given PGA of panel 19b. | 87 |
| Figure 21. Modal values of magnitude and epicentral distance from disaggregation of seismic hazard in terms of PGA given in Figure 19b and used to compute the conditional distribution of I_D whose percentiles are in Figure 20a and Figure 21b..... | 89 |
| Figure 22. Probability of exceedance of I_D given PGA for five scenarios for S. Angelo dei Lombardi (a) and Ponticelli (b)..... | 90 |
| Figure 23. Image of the software GUI. | 106 |
| Figure 24. Magnitude (M_W only for ESD, M_W or M_L for ITACA) vs epicentral distance distribution for the ESD (a) and ITACA (b) records featured in REXEL. The records are grouped by site class according to EC8 classification. | 110 |
| Figure 25. Disaggregation of the $S_a(T=1s)$ with 475 years return period on rock for Sant'Angelo dei Lombardi..... | 119 |
| Figure 26. Plot of the spectra found in the ESD for the selected M and R bins in the case of site class A..... | 120 |
| Figure 27. Unscaled combinations found for the assigned example in Sant'Angelo dei Lombardi using the <i>I'm feeling lucky</i> option in the case of horizontal 1-component (a) and 2-components (b) GMs. | 121 |
| Figure 28. Last of 1000 and 520 unscaled combinations found for the assigned example in Sant'Angelo dei Lombardi in the case of horizontal 1-component (a) and 2-components (b) GMs..... | 123 |
| Figure 29. Scaled combinations found for the assigned example in Sant'Angelo dei Lombardi using the <i>I'm feeling lucky</i> option in the case of horizontal 1-component (a) and 2-components (b) GMs. | 124 |

List of figures

| | |
|--|-----|
| Figure 30. First scaled combination found for the assigned example in Sant' Angelo dei Lombardi which includes the two horizontal (a) and the third vertical (b) components of GM matching the respective target spectra..... | 125 |
| Figure 31. Scaled pair of combinations without overlapping events, (a) and (b). | 126 |
| Figure 32. Scaled triplet without overlapping records 31a, 32a and 32b, for the considered example..... | 127 |
| Figure 33. Unscaled combinations found for the assigned example in case of EC8 selection using the <i>I'm feeling lucky</i> option in the case of horizontal 1- (a) and 2-components (b) GMs..... | 129 |
| Figure 34. Scaled combinations found for the assigned example in case of EC8 selection using the <i>I'm feeling lucky</i> option in the case of horizontal 1-component (a) and 2-components (b) GMs..... | 130 |
| Figure 35. Plot of the spectra found in the ESD for the selected M and R bins in the case of site class B. | 131 |
| Figure 36. Unscaled combinations found for the assigned example in case of user-defined spectrum selection using the <i>I'm feeling lucky</i> option in the case of horizontal 1-component (a) and 2-components (b) GMs..... | 132 |
| Figure 37. Scaled combinations found for the assigned example in case of user-defined spectrum selection using the <i>I'm feeling lucky</i> option in the case of horizontal 1-component (a) and 2-components (b) GMs..... | 133 |
| Figure 38. PGA on rock with a 475 years return period a) in Campania (southern Italy) and various spectra for two close sites in the region (b)..... | 136 |
| Figure 39. Magnitude (moment or local) vs epicentral distance distribution for the ITACA dataset on which REXELite operates. The records are grouped by site class according to EC8 classification..... | 146 |
| Figure 40. Steps to define seismic action according to the hazard at the site; from (1) to (3): target spectrum for the limit-state of interest, hazard disaggregation for the spectral ordinate at the period of the first mode of the structure, selection of a set of records compatible to disaggregation and matching the target spectrum in a range of periods. | 147 |
| Figure 41. REXELite user interface..... | 152 |
| Figure 42. Definition of spectral matching parameters and illustration of REXELite output as it appears to the user..... | 153 |
| Figure 43. Disaggregation of PGA with 50 years return period on rock for L'Aquila (http://esse1.mi.ingv.it). | 155 |
| Figure 44. 1-component combination found for the assigned example in L'Aquila in the case of damage limit state..... | 156 |

List of figures

| | |
|--|-----|
| Figure 45. Essential record data returned by REXELite for the combination of Figure 44..... | 157 |
| Figure 46. Scaled 1-component combination found for the assigned example in L'Aquila in the case of damage limit state..... | 160 |
| Figure 47. Essential record data returned by REXELite for the combination of Figure 46..... | 160 |
| Figure 48. Screenshot of web-based waveform visualization..... | 161 |
| Figure 49. 2-component combination found for the assigned example in L'Aquila in the case of damage limit state..... | 162 |
| Figure 50. Scaled 2-component combination found for the assigned example in L'Aquila in the case of damage limit state..... | 163 |
| Figure 51. Preliminary record search criteria..... | 163 |
| Figure 52. 1-component combination (only digital, normally triggered records) found for the assigned example in L'Aquila in the case of damage limit state..... | 164 |
| Figure 53. Scaled 1-component combination (only digital, normally triggered records) found for the assigned example in L'Aquila in the case of damage limit state..... | 165 |
| Figure 54. Essential record data returned by REXELite for the combination of Figure 53..... | 165 |
| Figure 55. EC8 spectra for Sant'Angelo dei Lombardi (site class B, $a_g = 0.27g$) (a), NIBC spectra for Sant'Angelo dei Lombardi (site class A) and UHS for a 50 years return period on rock (b)..... | 180 |

List of tables

| | |
|---|-----|
| Table 1. Summary of records sets of Group I | 57 |
| Table 2. Summary of records sets of Group II | 57 |
| Table 3. Summary of records sets of Group III..... | 57 |
| Table 4. Summary of records sets of Group IV..... | 57 |
| Table 5. Aspin-Welch test results in terms of MIDR; p -values lower than 0.05 are reported in bold..... | 63 |
| Table 6. Aspin-Welch test results in terms of RD; p -values lower than 0.05 are reported in bold. | 64 |
| Table 7. Aspin-Welch test results in terms of E_{H_i} ; p -values lower than 0.05 are reported in bold. | 65 |
| Table 8. I_D values for rejection cases of Table 7. | 68 |
| Table 9. Regression coefficients for PGA, PGV and $I_A (R_{epi})$ | 79 |
| Table 10. Regression coefficients for PGA, PGV and $I_A (R_{jb})$ | 79 |
| Table 11. Regression coefficients for $I_D (R_{epi})$ | 81 |
| Table 12. Regression coefficients for $I_D (R_{jb})$ | 81 |
| Table 13. Tests for joint normality of the logarithms of PGA and $I_D (R_{epi})$ | 83 |
| Table 14. Tests for joint normality of the logarithms of PGA and $I_D (R_{jb})$ | 83 |
| Table 15. Parameters of the selected seismogenic zones shown in Figure 4a..... | 88 |
| Table 16. Considered scenarios for S. Angelo dei Lombardi and Ponticelli. | 90 |
| Table 17. Essential record data returned by REXEL for the combination of Figure 27a. | 122 |
| Table 18. Essential record data returned by REXEL for the combination of Figure 27b. | 122 |
| Table 19. Results of comparison, in terms of search for unscaled combinations, for Sant'Angelo dei Lombardi according to the new and the former seismic classifications. | 137 |
| Table 20. Sample from the <i>data.txt</i> file for the combination of Figure 44. | 158 |
| Table 21. Sample of <i>data.txt</i> file for the combination of Figure 46. | 159 |
| Table 22. Values of the parameters describing the recommended elastic type 1 EC8 response spectra. | 175 |

List of tables

| | |
|---|-----|
| Table 23. Recommended values of parameters describing the vertical elastic response spectra. | 175 |
| Table 24. Recommended values of parameters describing the vertical elastic response spectra. | 177 |
| Table 25. Possible values for P_{V_R} , C_U and V_N | 177 |
| Table 26. Expressions defining S_S and C_C | 179 |

Chapter 1

INTRODUCTION

1.1 Motivation

Earthquake-resistant design represents the *art* of balancing the seismic capacity of a structure with the expected seismic demand to which it may be subjected. In this sense, earthquake-resistant design contributes to mitigation of seismic risk.

Quantitative assessment of seismic risk is a very broad field, including seismology and geotechnical engineering to quantify the shaking which a structure might experience at its base (*seismic hazard*), structural engineering to quantify the structure's response and the resulting damage (*vulnerability*), as well as finance and public policy to quantify social and economic consequences of earthquake induced damage (*exposure*). All these aspects present several uncertainties, requiring that the assessment is made in probabilistic terms, adding a further layer of complexity.

A sound methodology for solving this problem has been proposed by Pacific Earthquake Engineering Research (PEER) Center. Without enter into details of the probabilistic framework and dropping the idea of introducing the apparently complicated (but very fine) equations on which this framework is based, this opening speech will be restricted to a simple and schematic illustration of this Performance-based Earthquake Engineering (PBEE) model and a few remarks to introduce the aim of this dissertation.

There are four basic steps in PEER methodology (Figure 1), consisting of quantifying the seismic ground motion hazard, assessing the structural response, estimating the damage to building and contents and resulting consequences in terms of financial losses, fatalities and business interruption.

Each step of the process have to be performed in formal probabilistic terms and may be carried out independently. This four independent “modules” are then linked together using intermediate output variable, i.e., *Intensity Measures* (IMs), *Engineering Demand Parameters* (EDPs) and *Damage Measures* (DMs).

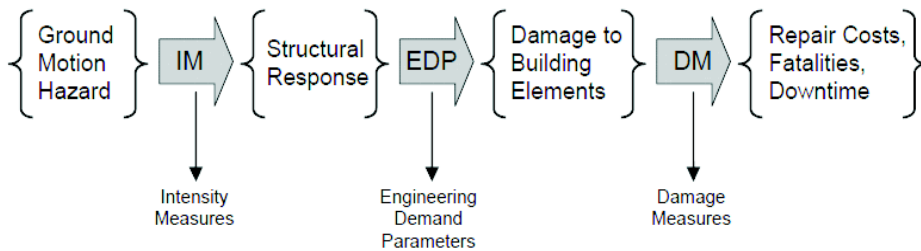


Figure 1. Schematic illustration of the Performance-Based Earthquake Engineering model and the “link” variables IM, EDP and DM.

Seismic input selection, in terms of accelerograms, represents the bridge between seismic hazard and structural response, the first two components in PBEE methodology, providing ground motion input for a structure at a specific site for non-linear structural time history analysis.

As non-linear dynamic analysis (NLDA) gains popularity in research, codes and practice, ground motions selection becomes increasingly relevant. In order to select representative ground motions to effectively assess structural performance, it is important, first of all, to understand *which ground motion properties have the greatest effect on structural response* and, consequently, have to take into account (Chapter 2). Then, it is important to develop and introduce into the practice of structural engineering, tools (Chapter 3-5) which may effectively help to address the basic issues related to seismic input selection, trying to reconcile research achievements and code-based practice. The provisions on which the whole thesis is based are those of Eurocode 8, abbreviated in the following as EC8 (CEN, 2003), i.e., the main seismic design code in Europe, and the new Italian building code, abbreviated in the

following as NIBC (CS.LL.PP., 2008), one of the most advanced with respect to seismic hazard issue, at least in Europe².

Based on these preliminary remarks, the aim of this study is to consolidate the state of research and to shed some light on a number of aspects involved when selecting and, eventually, manipulating ground motions for NLDA. Practical guidance and tools are developed and provided to the engineering community for choosing appropriate ground motions in predicting structural response by code-based NLDA.

1.2 Record selection for non-linear seismic analysis of structures: some key concepts

This dissertation focuses on code-based record selection which links the ground motion hazard with the structural response.

Ground motion hazard is computed using Probabilistic Seismic Hazard Analysis (PSHA) and the typical output is the mean annual frequency of exceeding various levels of a chosen IM, e.g., peak ground acceleration, PGA, or a spectral response value at a given period (spectral acceleration at first-mode period of the structure, $S_a(T_1)$ is the intensity measure used most frequently today for seismic structural analysis). Structural analysis is then performed to obtain a probabilistic model (or simple, as in codes approach, some statistics) for structural response as a function of this intensity measure.

Ground motion parameters are essential for describing the important characteristics of strong ground motion in compact, quantitative form for engineering purposes; many parameters have been proposed to characterize the amplitude (e.g. PGA and other peak parameters), frequency content (e.g. spectral ordinates) and duration of strong ground motions: some describe only

² When reviewing different codes, it becomes obvious that guidelines have been copied from codes used in other part of the world, without significant review of the recommendations given therein; see Beyer and Bommer (2007) for a detailed analysis on the topic.

one of these characteristics, while others may reflect two or three; see Kramer, 1996 and Iervolino and Manfredi (2008) for a detailed discussion. Because of complexity of earthquake ground motions, identification of a single parameter that accurately describes all important ground motion characteristics is regarded as impossible. However, a preferred IM should be both *sufficient* with respect to the ground motion characteristics and also *efficient*. A sufficient IM renders the structural response conditionally statistically independent on other ground motion characteristics such as event magnitude, while an efficient IM predicts the structural response with (relatively) small record-to-record variability. Theoretically, careful record selection is not essential if the IM is demonstrated to be sufficient. Useful strategy, in cases where the adopted scalar IM does not prove to be sufficient, is to introduce an additional intensity measure, thus adopting a vector-valued IM, consisting of two scalar IMs, in order to render a more complete description of the ground motion characteristics.

At same time, there are several possible methods to estimate probabilistic (i.e., in terms of a probability distribution) structural response as a function of ground motion IMs using the results of NLDA. Options include using regression analysis on structural analysis results from a set of unscaled (or uniformly scaled) ground motions or fitting a probability distribution to the analysis results from a set of records, each of which has been scaled to a target ground motion intensity level.

Codes do not provide detailed guidance on how accurately select ground motions records and how estimate structural response based on NLDA results. Herein, a very brief overview, with key references, is presented with the aim of introducing the key concepts on which this thesis is based.

1.2.1 Uniform hazard spectra and code-based record selection

A common goal of PSHA is to identify a design response spectrum to use for structural or geotechnical analysis. One approach for developing a spectrum is to compute a uniform hazard spectrum (UHS). This spectrum is

developed by firms performing the PSHA calculations for spectral accelerations at a range of periods (e.g., McGuire, 1995; Bazzurro and Cornell, 1999), commonly, 5% critically damped. Then, a target rate (i.e., probability) of exceedance is chosen (e.g., 10%), depending on the limit state of interest, and for each period the spectral acceleration amplitude corresponding to that rate is identified. Those spectral acceleration amplitudes are then plotted versus their periods, as illustrated in Figure 2.

This spectrum is called a uniform hazard spectrum because every ordinate has an equal rate of being exceeded. But it should be clear that, for PSHA integral nature, this spectrum is an envelope of separate spectral acceleration values at different periods, each of which may have come from a different earthquake event. For example, short-periods ordinates are controlled by nearby moderate-magnitude earthquake and the longer-period part of the UHS is dominated by larger and more distant events.

Although these inherent limitations, currently, UHS, or an approximation of it (e.g., in NIBC), is, in the most advanced seismic codes, the basis for the definition of design seismic action on structures and to select input ground motions for seismic structural analysis. Given the UHS for the limit-state of interest (i.e., the specified exceedance probability) most advanced practice today would select a set of records reflecting the *likely* magnitudes, distances and other earthquake parameters thought to drive the PSHA for the site (i.e. the UHS ordinate of interest) and which are believed to matter with respect to structural response. Finally, the records are usually manipulated (e.g., linearly scaled) to match the UHS, individually or in average sense, at the period of the first mode of the structure, T_1 or in a range of periods (Figure 3).

The engineer will subsequently run time-history analysis for each accelerograms and observe the structural response. If the average³ (then, simply a statistic for structural response rather than the full distribution)

³ According to many international code, if the sample size of the record set is at least seven, the analyst may consider as design value the average structural response to the ground motions.

exceeds a certain limit, he may conclude the structure does not withstand the design ground motion.

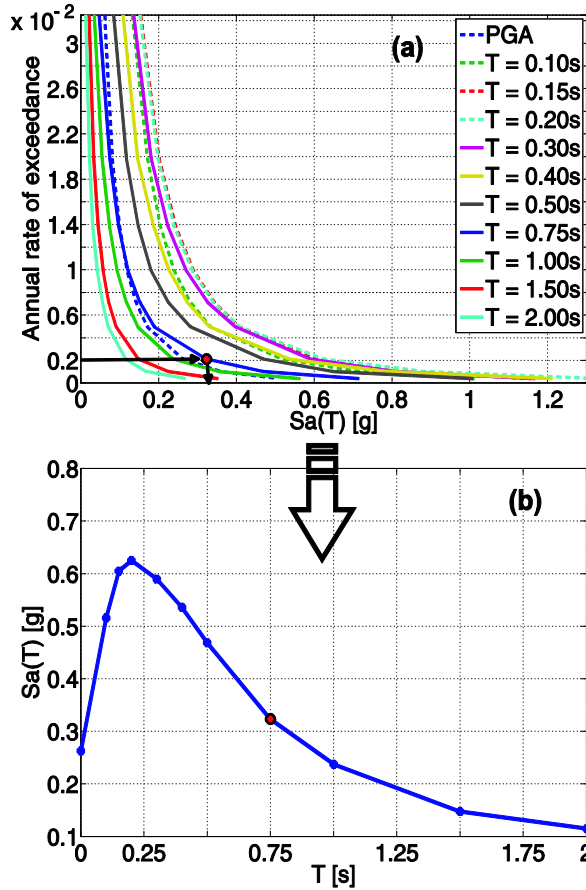


Figure 2. Combining hazard curves from individual periods to generate a uniform hazard spectrum with 0.0021 annual rate of exceedance (i.e., 10% probability of exceedance in 50 years) for a site in Sant’Angelo dei Lombardi (southern Italy). (a) Hazard curves for different periods, with an example UHS point identified ($T = 0.75s$). (b) Uniform hazard spectrum (adapted from Iervolino and Manfredi, 2008).

International codes, at least in principle, may be seen as not very far from that. In fact, once the design spectrum has been defined, the main criterion is that the records have to match it in a range of periods (Figure 4). This extended range (beyond T_1) accounting for both the contributions to the response for

higher modes and also for the elongation of response period due to high inelastic deformations.

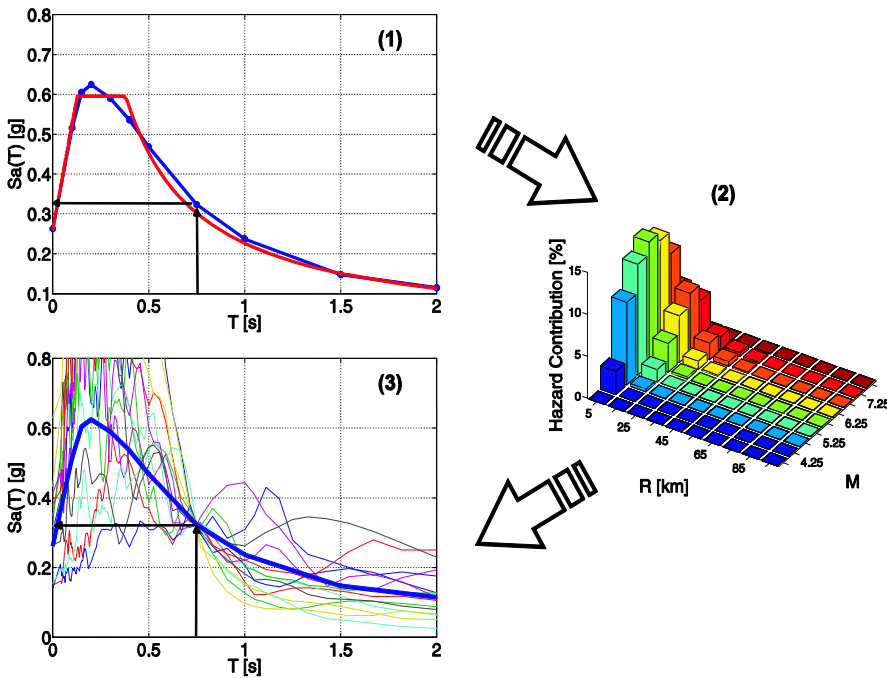


Figure 3. Steps to define seismic action according to the hazard at the site (*best practice*); from (1) to (3): target spectrum for the limit-state of interest, hazard disaggregation for the spectral ordinate at the period of the first mode of the structure, selection of a set of records compatible to disaggregation and matching the target spectrum at that same period (adapted from Iervolino, 2010).

In applying code prescriptions, some issues may impair the job of the practitioner in defining seismic action. For example, it may be hard to select real records matching on average the design spectrum in a broad range of periods; moreover, it is unlikely that engineer is able to qualify the input ground motion with respect to the seismological features of the source driving the hazard, even supposing that these ground motions features really matter in structural response assessment (Iervolino et al., 2008, 2008).

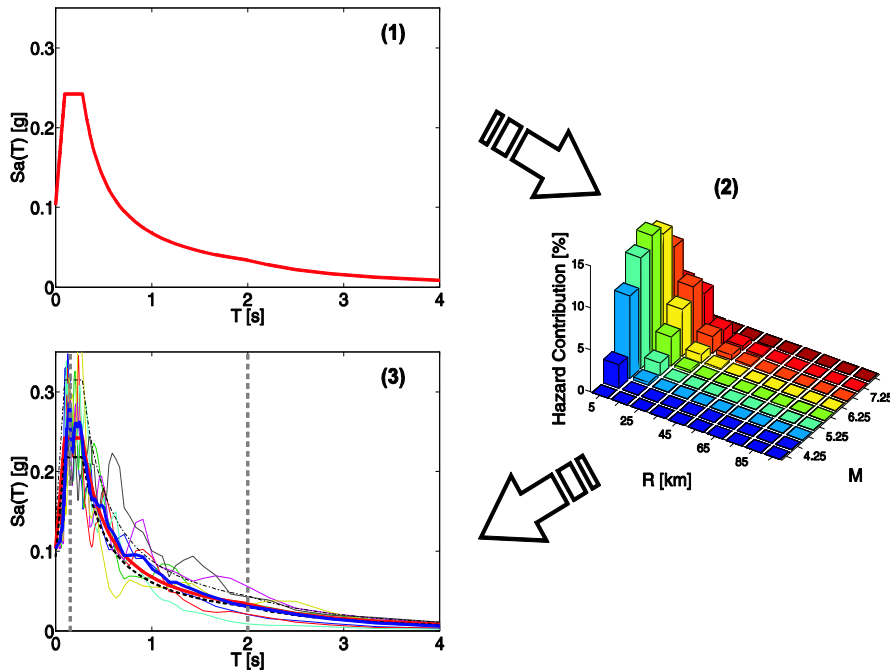


Figure 4. Steps to define seismic action according to the hazard at the site (alternative, code-based, procedure); from (1) to (3): target spectrum for the limit-state of interest, hazard disaggregation for the spectral ordinate at the period of the first mode of the structure, selection of a set of records compatible to disaggregation and matching the target spectrum in a range of periods.

Then, some practical guidance and some east-to-adopt tools, intended as attempts to reconcile code-based record selection to the practice, are needed.

1.2.2 Disaggregation

As discussed above, in the most advanced codes, the UHS is the basis for the definition of design seismic actions on structures. On the other hand, accelerograms to be employed in structural analysis, not only are recommended to match such a spectrum, but also to be compatible with the earthquake source features relevant for the site of interest. This may be intended as identifying the *design earthquakes*, which may be done via disaggregation of PSHA. In fact, once the UHS has been defined, it is possible

to identify one or more values of magnitude (M), source-to-site distance (R) and epsilon⁴ (ϵ) providing the largest contributions to the hazard in terms of exceeding a specified S_a value (e.g., Convertito et al., 2009).

Disaggregation results depend on the hazard level being disaggregated (i.e., the rate of exceedance, or, equivalently, the return period, T_R), and on the structural period the spectral acceleration refers to. In fact, UHS for different T_R are characterized by different design earthquakes and, within the UHS for a given T_R , short and long period ranges may display different M , R and ϵ from disaggregation. Therefore, useful tools for record selection may be maps, which for several probabilities of exceedance of spectral ordinates at structural periods of interest to earthquake engineering, map the design earthquakes from disaggregation. An example is given in Chioccarelli et al. (2010) where, disaggregation of 10% in 50 years hazard (i.e., an annual rate of exceedance equal to 0.0021 or, equivalently, a return period equal to 475 years) for the whole Italy, and for structural periods equal to 0 sec (PGA) and 1.0 sec is presented.

Disaggregation for these two periods is intended to help in identifying design earthquakes for the short and moderate/long period ranges of the UHS related to the life safety limit-state of ordinary constructions. In Figure 5 these maps are partially given. They report, for each site and for $S_a(1 \text{ sec})$, the first two design earthquakes in terms of M and R ; in fact, the most of sites hazard is contributed by more than a single earthquake source.

⁴ Epsilon is the number of standard deviations by which the logarithmic ground motion (in terms of spectral acceleration) departs from the median predicted by an appropriate attenuation relationship. Epsilon may be important because in the case of time histories to be used as the input for structural dynamic analysis, high epsilon values are associated with peaks in the response spectrum of the record. During shaking, the effective period of the structure lengthens, lowering the peak toward a less energetic portion of the frequency content; therefore, ground-motion records with high epsilon values may be associated with a more benign structural response. The opposite happens to negative epsilon records. Therefore, when selecting waveforms for structural analysis, one should consider choosing them among those having the right epsilon, that is, the one dominating the hazard at the site, for an unbiased estimation of structural response (e.g., Cornell, 2004; Baker and Cornell, 2006).

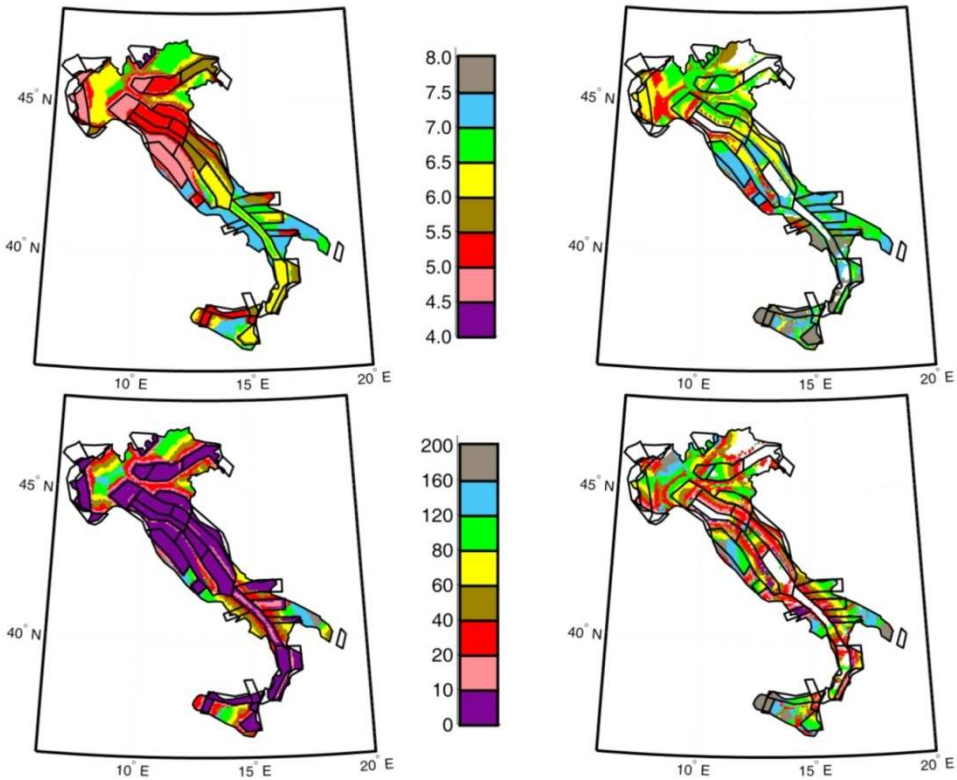


Figure 5. Italian map of first (left) and second design earthquakes (right) in terms of M (top) and R (bottom) for $S_a(1.0\text{sec})$ with a return period of 475 yr. For further details see Chioccarelli et al. (2010).

1.2.3 Acceleration time-histories

Generally, the signals that can be used (e.g., EC8 and NIBC) for the seismic structural analysis are of three types: (1) artificial waveforms; (2) simulated accelerograms; and (3) natural records (Bommer and Acevedo, 2004; Iervolino and Manfredi, 2008).

Spectrum-compatible signals of type (1) are obtained, for example, generating a power spectral density function from the code response spectrum (which is, in some cases, the only information available to the practitioner regarding the characteristics of the ground motions to be considered), and deriving signals compatible to that. However, this approach may lead to

accelerograms not reflecting the real phasing of seismic waves and cycles of motion, and therefore energy (Iervolino et al., 2010). Moreover, because UHS is strongly influenced by more than one source of seismicity (as discussed above), perfectly spectrum-compatible artificial records tend to be particularly unrealistic.

Simulation records (2) are obtained via modeling of the seismological source and may account for path and site effects. These methods range from stochastic simulation (Boore, 2003) of point or finite sources to dynamic models of rupture.

Synthetics may be the only way to obtain appropriate records for rare scenarios, such as large magnitude events “close” to the site and give the benefit that one can produce from them large samples of nominally similar events. However, effort should be employed to insure that their spectra are appropriate for nonlinear analysis, e.g., non smooth (Cornell, 2004). Moreover, they often require setting of some rupture parameters, such as the *rise-time*, which are hard to determine. Some state-of-the-art simulation methods seem to overcome these shortcomings, but they are not yet readily available to engineers.

Finally, of type (3) are ground-motion records from real events. The availability of on-line, user-friendly, databases of strong-motion recordings, and the rapid development of digital seismic networks worldwide, have increased the accessibility to recorded accelerograms. However, due to the large variability in records representing a scenario, a number of points arise regarding the criteria for appropriate selection and manipulation of such records. In particular, an issue regarding the use of real recordings, whose spectra are generally non smoothed, is the selection of a set compatible with a code-specified spectrum.

To overcome this, various approaches have been developed to manipulate real records to match a target spectral shape, either by frequency-domain or by time-domain modification methods such as the *wavelet* transform. The wavelet transform basically consists of using modulating functions, selectively located in time to modify the spectrum of the signal,

where and when it is needed in order to match the target spectrum (see Hancock et al., 2006, for details). Although these methods produce records perfectly compatible with code's prescriptions and have the additional advantage of reducing the dispersion in the response, and hence the required sample size, some studies show that they may lead to a non conservative estimation of the seismic response (Carballo and Cornell, 2000; Bazzurro and Luco, 2003).

Based on these remarks, the ground motions selection and modification methods considered in this thesis are only those that rely on selecting natural (i.e. recorded) ground motions and (possibly) linearly scaling their amplitude.

1.3 Organization and contributions to code-based record selection

This thesis aims, through its chapters, to address the challenges mentioned above. The major contributions of this work are summarized below.

Identifying parameters that most affect the structural response (Chapter 2)

As NLDA is becoming more prevalent in codes and practice, there is a need to consolidate ground motion record selection and scaling (or more generally the "modification") procedures from a structural engineering perspective.

As discussed above, the seismic input selection represents one of the main issues in assessing the seismic performance of a structure through NLDA. There are currently many options in seismic input selection and modification for NLDA available but little guidance is available to practitioners on which methods are appropriate for their specific application.

In this thesis, the non-linear response of a modern, code-conforming four-story reinforced concrete (RC) frame building is analyzed; the aim is to compare, in terms of inelastic seismic response, different options to obtain sets of accelerograms for NLDA. The study is code-based and then spectral-shape based; all the considered sets of records match, on average (in a range of

periods) or individually (at the fundamental vibration period of the structure), the same target (i.e. design) spectrum for a case-study site in southern Italy. Additional criteria in terms of earthquake magnitude, source-to-site distance and site classification are considered.

Results show little evidence to support the need for a careful site-specific process of record selection by magnitude, distance and soil class once spectral matching is assured. Moreover, results indicate that the linearly scaled records do not show significant differences with respect to the unscaled records, for both peak and cyclic response parameters, suggesting that linear scaling is a fair procedure, as many studies point out, if the spectral shape is controlled.

Finally, it is discussed how, when selecting and scaling ground motion records, one can improve the resulting structural response prediction by taking into account integral record properties, other than spectral accelerations, that may be important to the non-linear cyclic response.

Hazard-consistent inclusions of additional IMs in selection (Chapter 3)

Vector-valued ground motion IMs have been the focus of a significant deal of research recently. Proposed measures are mainly function of spectral ordinates which have been shown to be useful in the assessment of structural response. This is especially appropriate in the case of structures following modern earthquake resistant design principles, in which structural damage is mainly due to peak displacements experienced during nonlinear dynamics. On the other hand, as discussed above, there may be cases in which the cumulative damage potential of the earthquake is also of concern, even if it is generally believed that integral ground motion IMs, associated with duration, are less important with respect to peak parameters of the record. For these IMs, it seems appropriate to develop conditional hazard maps; i.e., maps of percentiles of a secondary IM (e.g., duration-related) given the occurrence or exceedance of a primary parameter (e.g., peak acceleration), for which a design hazard map is often already available. In this thesis, this concept is illustrated and a conditional hazard is developed for a parameter which may account for the cumulative damage potential of ground motion, the so-called *Cosenza and*

Manfredi index (I_D), given PGA. To this aim, a ground motion prediction relationship was derived for I_D first. Subsequently, the residuals of PGA and I_D were tested for correlation and for joint normality. Finally, the study obtained analytical distributions of I_D conditional on PGA and on the corresponding design earthquake in terms of magnitude and distance from hazard disaggregation. As shown by the some application, I_D maps conditional on the code design values of PGA may be useful, for example, for a more refined ground motion record selection as an input for NLDA of structures.

Aiding selection of spectrum matching real records (Chapters 4-5)

In code-based seismic design and assessment it is often allowed the use of real records as an input for NLDA. On the other hand, as, discussed above, international seismic guidelines, concerning this issue, have been found hardly applicable by practitioners. This is related to both the difficulty in rationally relating the ground motions to the hazard at the site and the required selection criteria, which do not favor the use of real records, but rather various types of spectrum matching signals. To overcome some of these obstacles a software tool for code-based real records selection was developed. REXEL, freely available at the website of the Italian network of earthquake engineering university labs (<http://www.re Luis.it>), allows to search for suites of waveforms, currently from the European Strong-motion Database (ESD) and the Italian ACcelerometric Archive (ITACA), compatible to target spectra being either user-defined or automatically generated according to Eurocode 8 (EC8) and the recently released new Italian seismic code (NIBC). The selection reflects the provisions of the considered codes and others found to be important by research on the topic. Via some examples (Chapter 4), it is shown how REXEL can effectively be a contribution to code-based real records selection for seismic structural analysis. Moreover, an internet version of REXEL, termed REXELite, was also developed, operating on ITACA web portal (<http://itaca.mi.ingv.it>). REXELite (Chapter 5) aims at integrating an advanced earthquake records' repository with an automatic tool to define seismic input for engineering seismic analysis according to modern standards.

Chapter 1

Introduction

REXEL and REXELite seem successful in standardizing and aiding professional engineering in seismic input definition.

The chapters of this thesis are developed to be largely self-contained because they have been or will be published as individual journal articles. Because of this, there is some repetition in introductions and background material. In addition, notational conventions were chosen to be simple and clear for the topic of each chapter rather than for the thesis as a whole; because of this, the notational conventions may not be strictly identical for each chapter. Apologies are made for any distraction this causes when reading the thesis as a continuous document.

References

Baker, J.W., and Cornell, C.A. (2006). Spectral shape, epsilon and record selection. *Earthquake Engineering and Structural Dynamics*, 35, 1077–1095.

Bazzurro, P., and Cornell, C.A. (1999). Disaggregation of seismic hazard. *Bulletin of the Seismological Society of America*, 89, 501–520

Bazzurro, P., and Luco, N. (2003). Report for Pacific Earthquake Engineering Research (PEER), Center Lifelines Program Project 1G00, December, 2003.

Beyer, K., and Bommer, J.J. (2007). Selection and scaling of real accelerograms for bi-directional loading: a review of current practice and code provisions. *Journal of Earthquake Engineering*, 11, 13–45.

Bommer, J.J., and Acevedo, A.B. (2004). The use of real earthquake accelerograms as input to dynamic analysis. *Journal of Earthquake Engineering*, 8, 43–91.

Boore, D.M. (2003). Simulation of ground-motion using the stochastic method. *Pure and Applied Geophysics*, 160, 635–676.

Carballo, J.E., and Cornell, C.A. (2000). Probabilistic seismic demand analysis: spectrum matching and design, Report No. RMS-41, Reliability of Marine Structures Program, Department of Civil and Environmental Engineering, Stanford University, Stanford, CA.

CEN, European Committee For Standardisation (2003). Eurocode 8: Design provisions for earthquake resistance of structures, part 1.1: general rules, seismic actions and rules for buildings, prEN 1998-1.

Chioccarelli, E., Iervolino, I., Convertito, V. (2010). Italian Map of Design Earthquakes from Multimodal Disaggregation Distributions: Preliminary

Results. *Proc. of 14th European .Conference on Earthquake Engineering*, Ohrid, Republic of Macedonia.

Convertito, V., Iervolino, I., Herrero, A. (2009) The importance of mapping the design earthquake: insights for southern Italy. *Bulletin of the Seismological Society of America*, 99, 2979–2991.

Cornell, C.A. (2004). Hazard, ground-motions and probabilistic assessment for PBSD, In *Performance Based Seismic Design Concepts and Implementation*, PEER Report 2004/05, Pacific Earthquake Engineering Research Center University of California Berkeley.

CS.LL.PP. (2008). DM 14 Gennaio 2008. Norme tecniche per le costruzioni. *Gazzetta Ufficiale della Repubblica Italiana*, 29. (in Italian)

Hancock, J., Watson-Lamprey, J., Abrahamson, N.A., Bommer, J.J., Markatis, A., McCoy, E., and Mendis, R. (2006). An improved method of matching response spectra of recorded earthquake ground-motion using wavelets. *Journal of Earthquake Engineering*, 10, 67–89.

Iervolino, I., De Luca, F., Cosenza, E. (2010). Spectral shape-based assessment of SDOF nonlinear response to real, adjusted and artificial accelerograms. *Engineering Structures*, 32, 2776-279.

Iervolino, I., Maddaloni, G., Cosenza, E. (2008). Eurocode 8 compliant real record sets for seismic analysis of structures. *Journal of Earthquake Engineering*, 12, 54-90.

Iervolino, I., Maddaloni, G., Cosenza, E. (2009). A note on selection of time-histories for seismic analysis of bridges in Eurocode 8. *Journal of Earthquake Engineering*, 13, 1125–1152.

Iervolino, I., and Manfredi, G. (2008). Review of ground motion record selection strategies for dynamic structural analysis. In *Modern Testing*

Chapter 1

Introduction

Techniques of Mechanical and Structural Systems, Oreste S. Bursi, David J. Wagg (Editors), CISM Courses and Lectures 502, Springer.

Iervolino, I. (2010). Hazard, ground motions, and code-based structural assessment: a few proposals and yet unfulfilled needs. *Proc. of 14 th European Conference on Earthquake Engineering*, Ohrid, Republic of Macedonia.

Kramer, S.L. (1996). Geotechnical earthquake engineering, Prentice Hall, Upper Saddle River, N.J., 653 pp.

McGuire, R.K. (1995). Probabilistic seismic hazard analysis and design earthquakes: closing the loop. *Bulletin of the Seismological Society of America*, 85, 1275–1284.

Chapter 2

Code-based real record selection: what really matters?

ABSTRACT

As non-linear dynamic analysis (NLDA) is becoming more prevalent in codes and practice, there is a need to consolidate ground motion record selection and scaling (or more generally the “modification”) procedures from a structural engineering perspective.

The seismic input selection represents one of the main issues in assessing the seismic performance of a structure through NLDA. There are currently many options in seismic input selection and modification for NLDA available but little guidance is available to practitioners on which methods are appropriate for their specific application.

In this chapter, the non-linear response of a code-conforming four-story reinforced concrete (RC) frame building is analyzed; the aim is to compare, in terms of inelastic seismic response, different options to obtain sets of accelerograms for NLDA. The study is code-based and then spectral-shape based; all the considered sets of records match, on average (in a range of periods) or individually (at the fundamental vibration period of the structure), the same target (i.e. design) spectrum for a case-study site in southern Italy. Additional criteria in terms of earthquake magnitude, source-to-site distance and site classification are considered.

Results here show little evidence to support the need for a careful site-specific process of record selection by magnitude, distance and soil class once spectral matching is assured. Moreover, results indicate that the linearly scaled records do not show significant differences with respect to the unscaled records, for both peak and cyclic response parameters, suggesting that linear scaling is a fair procedure, as many studies point out, if the spectral shape is controlled.

Finally, it is discussed how, when selecting and scaling ground motion records, one can improve the resulting structural response prediction by taking into account integral record properties, other than spectral accelerations, that may be important to the non-linear cyclic response.

2.1 Introduction

The modern seismic codes, such as Eurocode 8, or EC8 (CEN, 2003), and the new Italian Building Code, or NIBC (CS.LL.PP., 2008), allow the designer to use different analysis methodologies for both earthquake-resistant design and seismic assessment of existing structures, in particular: (1) lateral force and (2) multi-modal elastic ones and (3) static and (4) dynamic non-linear ones. Their level of reliability decreases from (4) to (1) and, consequently, the safety margin with respect to the same limit state increases according to the same order, see for example Magliulo et al. (2007).

In equivalent lateral forces or spectral modal methods of analysis, the earthquake-induced ground shaking is generally represented in the form of a response spectrum of acceleration; the design spectrum is usually obtained by scaling an elastic spectrum by a factor that accounts for, amongst other phenomena, the influence of inelastic structural response. On the other hand, seismic assessment of structures via nonlinear dynamic analysis requires a suitable suite of ground motion accelerograms to represent the seismic excitation. Non-linear structural response is often highly sensitive to the selection and modification of input ground motions and many options do exist in both research and codes.

Modern seismic codes suggest different procedures to select ground motions signals, most of those assuming spectral compatibility to the uniform hazard spectrum (UHS)⁵, or other elastic design spectrum, as the main criterion. For example, EC8 requires the average spectrum of the chosen set to be above 90% of the design code spectrum in the range of periods $0.2T_1 - 2T_1$, where T_1 is the fundamental period of the structure. Practitioners have several options to get input signals for their structural analysis: e.g., real or real manipulated records and various types of synthetic and artificial

⁵ Although the use of UHS was only recently acknowledged by engineering practice and/or codes for design and assessment purposes (e.g., in Italy), some studies have already investigated the shortcomings of this kind of representation of ground motion and propose more sound alternative (see, e.g., Baker, 2011).

accelerograms. All these options are usually acknowledged by codes which may provide additional criteria or limitations for some of them.

In NIBC, for example, artificial records, generated by random vibration theory, should have a duration of at least 10s in their pseudo-stationary part, and they cannot be used in the assessment of geotechnical structures. Synthetic records, generated by simulation of earthquakes rupture process, should refer to a characteristic scenario for the site in terms of magnitude, source-to-site distance and seismological source characteristics; finally, real records should reflect the earthquake dominating the hazard at the site. This choice may be guided by the disaggregation of seismic hazard for the site of interest (Convertito et al., 2009).

However, practitioners cannot always accurately characterize the seismological threat to select real records or generate synthetic signals or it is not possible to find a set of real records that fits the code requirements properly in terms of a specific hazard scenario. Moreover, limitations of the existing earthquake ground motion databases lead often to scaling of records to obtain accelerograms consistent with a ground motion target for structural design and evaluation.

This study tries to address these matters and to provide some guidance to engineers regarding code-based methods for real record selection and scaling. To this aim, the approach followed in this study is (1) to select (and eventually scale) real ground motions sets using a wide variety of code-allowable options; (2) to use these ground motions sets as inputs to NLDA of a case-study structure and then (3) to analyze the differences in the resulting structural response predictions in order to identify what really matters in real record selection criteria.

The ground motions selection and modification methods considered in this study are those that rely on selecting natural (i.e. recorded) ground motions and (possibly) linearly scaling their amplitude. Other methods that use modification of the frequency content of ground motion (i.e. artificial records) or simulate ground motion are not included here but are analyzed in other studies (e.g. Iervolino et al., 2010).

More specifically, 18 sets of seven (only) Italian and European real records are considered, matching, on average in the range of periods 0.15-2s, or individually at the fundamental vibration period of the structure (equal to 1s), the same target, code-based, spectrum for a case-study site in southern Italy. Additional criteria in terms of earthquake magnitude, source-to-site distance and site classification are considered and discussed.

The seismic response of a modern, code-conforming four-story reinforced concrete frame building is analyzed. As structural response measures, or engineering demand parameters (EDPs), maximum inter-story drift ratio (MIDR), roof drift (RD) and the total (cumulative) hysteretic energy (E_H) are considered to relate the ground motions to both peak and cyclic structural demand.

Analyses here aims at comparing statistically the differences, if any, in the EDPs associated to each set of records. Hypothesis tests are carried out to assess the statistical significance of the results found in terms of both peak and cyclic response.

The result shown herein are, for the sake of brevity, limited to a single site and a single structure, completely fulfils codes' provisions, but they are confirmed by analyses performed on different variants of the same building, considering different geometry/details and designed according to different levels of seismic action (i.e., for different sites in Italy).

Moreover, the specific results of the study are intended to provide an initial step toward practical guidance in selecting and scaling ground motions for buildings; the overall methodology provides a general framework for future evaluation of other ground motion selection and scaling techniques and other classes of engineered structures. Similar results, in terms of prediction of median MIDR response of buildings, are provided by PEER Ground Motion Selection and Modification Working Group (2009) considering also advanced (not only code-based) methods of ground motion selection and scaling⁶.

⁶ The study demonstrated that code-approaches can lead to highly conservative over-prediction of structural response.

2.2 Findings of previous investigations about record selection for NLDA

Many performance-based assessments of seismic response require that one (a) use probabilistic seismic hazard analysis (PSHA) to identify an $Sa(T_1)$ amplitude (i.e. spectral acceleration at T_1) that is exceeded with a given probability in a reference period, (b) use disaggregation to identify the most likely (e.g., the modal pair) casual magnitude (M) and distance (R) for that $Sa(T_1)$ level, and then (c) select records reflecting these magnitude and distance values and scale ground motions to match precisely the target $Sa(T_1)$ value.

This procedure represents one of the best practices in selecting accelerograms for assessing the non-linear demand of structures but it is somewhat different from the simplified *criteria* specified in current international building codes (e.g., EC8, NIBC). These code requirements provide a fixed target spectrum, typically based on an UHS and then require the use of ground motions which *exceed* (only some small tolerances are accepted), on average, that spectrum over a *range of periods*⁷ around T_1 . Moreover, codes suggest that it is reasonable to choose ground motion records whose magnitude, distance, site conditions and fault mechanisms are representative for the seismic hazard at the site of the structure under consideration.

Lack of knowledge of the influence of seismological parameters on the structural response had driven the seismologist to be prudent and assume that all features matter to structural response

In particular, earthquake magnitude and distance of the rupture zone from the site of interest are the most common parameters related to a seismic event; then, it is evident that the simplest selection procedure involves

⁷ This extended range accounting for both the contributions to the response for higher modes and also for the elongation of response period due to high inelastic deformations: since the structure is non-linear, the effective first mode period increases as it yields and then the spectral shape beyond the original fundamental period is important when predicting structural response.

identifying these parameters. However, a structural designer who attempts to select records based on some seismological features, not being a seismology expert and knowing little detail about the PSHA framework used to assemble the design spectra and which ground motions contributed most significantly to these spectra, could be confronted with a difficult task, even in the case of “well trained” practitioners or designers with many years of experience.

Moreover, given the limited availability of recorded ground motions within relatively narrow magnitude and distance range appropriate to a given site condition, there is often a need to relax these constraints in favor of other parameters that are believed to be better predictor of the non-linear response, i.e., spectral shape.

Based on all these considerations, recent studies have questioned the effectiveness of the (M, R) based selection procedure. More specifically, in Iervolino and Cornell (2005) the dependence of structural response on (M, R) pair was studied. In their work, real accelerograms are arranged in two main classes. The first comprised six sets of ten accelerograms formed from available records characterized by comparatively high magnitudes and small distances (defined as the closest distance to a rupture greater than 15 km), thus simulating the case of a carefully chosen scenario. The records in the second class, comprising ten *arbitrary* set of ten accelerograms, are chosen randomly from a large catalog of real records without limitation, other than being scaled to the median, first-mode spectral acceleration period of the first class of *target* sets. In order to generalize the conclusions of the study, a series of structures with (a) different fundamental periods, (b) hysteresis relationships, (c) target ductility, (d) number of degrees of freedom, i.e., single (SDOF) and multiple (MDOF) and (e) structural type, i.e., concrete or steel frames, are chosen. The key response parameter considered was the maximum drift and inter-story drift of the SDOF and MDOF systems, respectively. Conclusions based on investigating the non-linear response of these model structures to sets of records selected by matching a specific moderate-magnitude and distance scenario and other records selected arbitrarily, showed no evidence that the

first, site-specific (M, R) record pair selection process was different (and then superior) in terms of predicted structural response.

Before, Shome et al. (1998) pointed out the insensitivity of some post-elastic damage indices (i.e., three local and three global measures) to the (M, R) parameter pair of a 5-story steel structure subjected to real records. In particular, the choice of the (M, R) pair in selection was shown to be of no consequence in the estimation of displacement-based damage indices. This conclusion, however, is not quite valid in the case of cumulative damage measures (i.e., energy-based indices), since these damage measures shown some form of dependency on record duration and then, indirectly, on (M, R).

In Iervolino et al. (2006) this conclusion was confirmed by examining the non-linear response of a number of SDOF systems and considering six different demand indices. By selecting real accelerograms (three sets comprising 20 records characterized by short, moderate and large duration) as representative of specific duration scenarios, it was concluded that duration is insignificant for displacement-based demand indices while it influences energy-based measures such as hysteretic ductility and equivalent number of cycles.

Other studies (e.g., Luco and Bazzurro, 2007, Iervolino et al., 2010) demonstrated that scaling is not only legitimate (i.e. no bias is induced in median response) but also useful for assessing structural response, reducing the record-to-record spectral variability within a set, which is a desirable feature if one has to estimate the seismic demand on the basis of 7 analyses only, as discussed below. In general, the belief that scaling procedures bias non-linear structural response is mostly based on unquestionable difference in ground motion characteristics (e.g., response spectral shape, duration, ecc) and much less on their effects on structures.

The study presented here is aimed at consolidating all the concepts illustrated and at improving the knowledge on the topic from a structural engineering perspective; moreover, here, code-based procedures in record selection are specifically considered and code-based criteria are taken into

account; special attention is given also to additional selection criteria in terms, for example, of soil profile.

2.3 Case-study structure

A modern, NIBC-conforming, four-storey RC frame building is selected as case-study; the design of the selected structure is carried out based on realistic criteria, representative of what would be done in practice, as discussed in the following.

2.3.1 Geometry, elastic analysis and design principles

The geometry of the case-study four-storey RC frame building is reported in Figure 6; it is regular (both in plan and in elevation) with 4-bay by 2 bay and with total dimensions in plan equal to $19 \times 10 \text{ m}^2$.

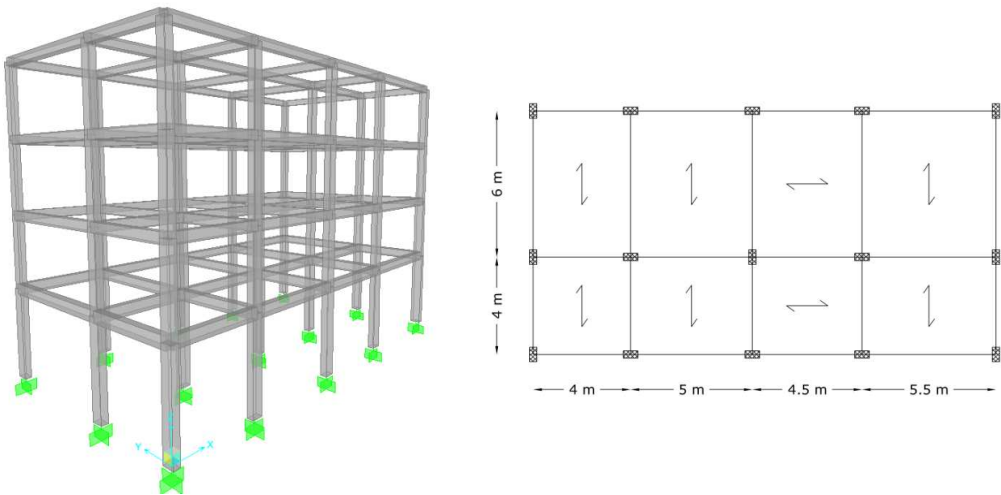


Figure 6. Geometry of the case-study building: (left) tri-dimensional view and (right) plan.

The bottom interstorey height is equal to 4m, while at other levels it is equal to 3.2m; at the first storey the dimensions of the cross-sections⁸ of all the columns are 30 x 55 cm², of all the beams are 30 x 50 cm², at the second storey such dimensions are respectively 30 x 50 cm² and 30 x 45 cm², at the third 30 x 45 cm² and 30 x 40 cm², while at the top level they are 30 x 40 cm² both for column and beam sections. A low variation of the element dimensions between adjacent floors is assigned in order to favour the structure's vertical regularity, while columns dimensions are kept larger than beam ones in order to take into account the capacity design.

The dimensions of the frame elements are assigned in order to satisfy the damage limitation requirement, in particular the limitation for buildings having non-structural elements of brittle materials attached to the structure (i.e., MIDR for a 50-years return period spectrum less than 0.5%).

In the elastic analysis, beams and columns are modelled as massless one dimensional finite elements: the mass is concentrated in the floor levels, assumed rigid in their own planes; consequently, the structure is characterized by three degree of freedoms (DoFs) for each floor. As imposed by the code, a 5% accidental eccentricity is considered and then four models are analyzed with the centre of mass placed in four different positions.

In order to take the cracking into account, the elements stiffness is assigned to be one-half of the corresponding uncracked one. The first two modes are translational, whereas the third mode is torsional; the periods of the first three modes of such models are 1.06s (X dir), 0.98s (Y dir) and 0.74s (rot.).

The building is designed according to NIBC and EC8 by modal response spectrum analysis; gravity load is represented by the uniformly distributed load on the beams and live load of 2 kN/m² is adopted in the design of the structure.

A design spectrum according to NIBC is considered for a case-study site in Ponticelli, Naples (latitude: 40.8516°, longitude: 14.3446°), southern Italy. The elastic spectrum considered is that corresponding to the life-safety limit

⁸ All the beams and columns have rectangular cross-sections.

state of an ordinary construction with a nominal life of 50 years (i.e., corresponding to a return period of 475 years) on B-type soil class, according to EC8 classification.

The design is performed following the High Ductility Class (DCH) rules and assuming a behavior factor equal to 5.85, also considering that the frame is regular in elevation.

Concrete characteristic cylindrical strength equal to $f_{ck} = 25$ MPa (medium value, according to NIBC, equal to 33 MPa) and steel characteristic yielding strength equal to $f_{yk} = 450$ MPa are adopted. The concrete Young modulus and its maximum tensile strength are also computed according to NIBC; steel Young modulus is assumed equal to 200000 MPa.

The orthogonal effects are considered by the 30% rule: 8 combinations for each of the 4 models are computed.

The columns are reinforced by 16mm bars, with a total reinforcement ratio equal to 1% (minimum longitudinal reinforcement in columns according to both NIBC and EC8) for all cross-sections; stirrups $\phi 8/10$ have been defined in all the critical regions of the columns based on codes' limitation. Beams are reinforced by 14mm bars with symmetric reinforcement; also for beams, stirrups $\phi 8/10$ have been defined in all the critical regions. Also for beams, the design meets the code requirements as closely as possible to the minimum values.

As provided by the code, all nodes of the frame structure, unless the top floor ones and those at foundation, satisfy the design condition of Eq. (1).

$$\sum M_{Rc} \geq 1.3 \sum M_{Rb} \quad (1)$$

$\sum M_{Rc}$ and $\sum M_{Rb}$ are the sum of design values of moment of resistance of respectively the column and the beam framing the joint; this is satisfied along both the orthogonal directions and considering both sign of seismic action.

2.3.2 Non-linear model

Since the structure meets fully the regularity requirement, the main central frame in the structure is extracted and used as the structural model for NLDA; due to symmetry, only one direction of seismic action is analyzed and the fundamental period $T_1 = 1\text{s}$ for plane frame is obtained.

Non-linear analyses are performed by means of the Open System for Earthquake Engineering Simulation (OpenSees) software. Non-linearity regards flexural rotations while all the other deformations (i.e. axial, shear and torsional) are assumed linear. Both beams and columns are modelled by one-component lumped plasticity elements, i.e., the non-linear behavior in the structure is concentrated in plastic hinges located at element ends; no axial force-bending moment interaction is considered at the plastic hinge.

Plastic hinges are characterized by a tri-linear backbone curve (Figure 7a), defined by yielding (M_y) and maximum (M_{\max}) moment and the corresponding rotations⁹; the moment-rotation relationship in the positive and negative direction is symmetrical for both beams and columns due to symmetrical reinforcement.

Such moments and the corresponding curvatures are computed by analyzing the cross-sections of the elements considering the Mander-Priestly (1988) constitutive relation for confined concrete under compression; an elastic-perfectly plastic steel stress-strain diagram is considered, characterized by a maximum strength equal to 548 MPa, computed as mean of tests on more than 200 bars made by steel 430 MPa grade.

The yielding (θ_y) and ultimate (θ_u) chord rotations and the plastic hinge length are evaluated as provided by EC8 semi-empirical equations (A.10b) and (A.1) respectively, where the already cited medium values are assigned to concrete maximum (f_c) and steel yielding (f_y) strength. Zero axial force and the axial load due to gravity loads are taken into account when determining the

⁹ Codes do not provide an expression for rotation at maximum moment, θ_{\max} . This rotation value is therefore assumed arbitrarily equal to $0.5\theta_u$, where θ_u is the ultimate rotation. Some researchers (e.g., Haselton, 2006) have proposed empirically-based formulas for the prediction of the rotation at maximum moment.

moment-rotation relationship for beams and columns, respectively. The possibility of shear failure is not taken into account.

As it regards the post-peak behavior, it is assumed that the section resistance drops to a value of the moment equal to one tenth of the maximum moment (M_{max}) corresponding to a rotation value equal to 2.75 times the ultimate value (θ_u)¹⁰.

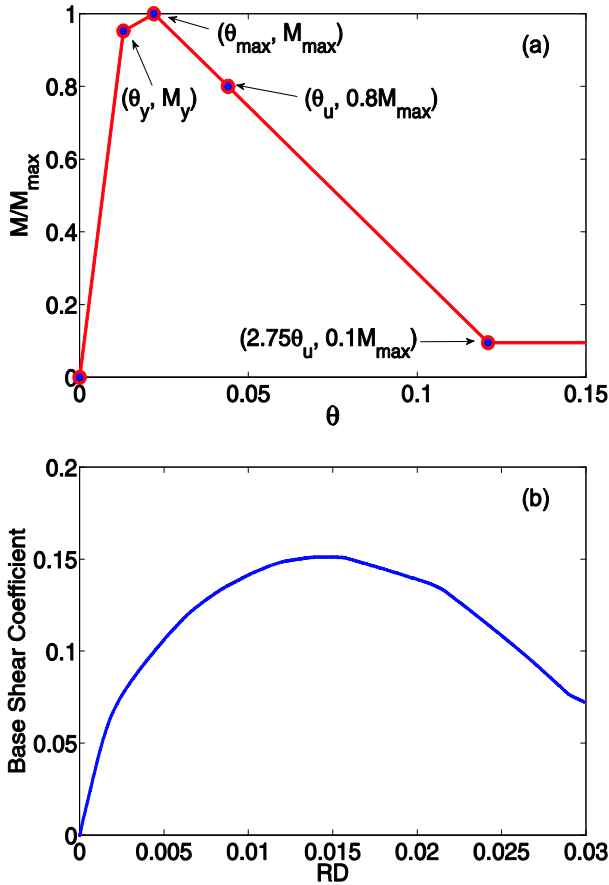


Figure 7. (a) Schematic diagram of the monotonic behavior of plastic hinge model used in this study; (b) static pushover of the case-study building.

¹⁰ These post-peak values for moment and rotation are chosen rather arbitrarily in order to avoid numerical in-convergence problem; they do not influence the results.

Given the scope of the present study, the assumed hysteresis rule accounts for stiffness deterioration in a simple way by modifying the path with which the reloading branch approaches the backbone curve, i.e. a peak-oriented model is assumed. The need to better simulate structural response far into elastic range, in which components deteriorate in both strength and stiffness (especially in members without modern structural details), led to the development of more advanced models, including various rules for stiffness and strength deterioration as well as pinching (see for example Ibarra et al., 2005 for a detailed review on the topic). The structural damping is modeled based on the Rayleigh model and it is assumed to be equal to 5% for the first two modes.

Figure 7b presents the static pushover curve for the case-study building. Non-linear static analysis is performed according to NIBC and EC8 considering a force distribution proportional to first modal shape in the frame direction. The curve is reported in terms of top centre of mass displacement divided by the total height of the structure along the horizontal axis of the diagram and base shear divided by the building seismic weight along the vertical axis. This figure is shown to illustrate the capability of the structural model to directly simulate response up to collapse. A detailed comparison between code-based static and dynamic non-linear analyses according to EC8 (for a very similar code-conforming building) is presented in Magliulo et al. 2007.

2.3.3 Nonlinear demand measures

As discussed in the introduction, the EDPs chosen are selected to investigate both the peak and the cyclic seismic response and then to be representative of the most common building damage measures. The displacement-based parameters are maximum inter-story drift ratio (MIDR),

i.e., the the maximum IDR over building height, and roof drift (RD)¹¹, i.e., the ratio of the maximum absolute displacement of the roof of structure (relative to the ground) compared to the height of the building.

Such parameters are of great interest for both code-based design checks as well as performance-bases engineering assessment and there is much research experience in prediction these response parameters. Moreover, displacement-based parameters are good proxies for measuring the earthquake induced damage to the buildings, as it should be reasonable that the greater the displacement of a building, the more damage is caused during the earthquake's shaking.

The cyclic response-related parameter is the cumulative hysteretic energy (E_H), evaluated as the sum, for all the plastic hinges in the model, of the areas of the hysteretic cycles. This parameter is chosen because the cyclic collapse of structure that show a degrading behavior (e.g., existing buildings) is strongly influenced by the amount of E_H dissipated under seismic action (Manfredi, 2001). Future studies should consider a broader range of the response parameters.

2.4. Record classes

As discussed above, code-consistent ground motion selection requires the definition of a “target” to compare the suitability of different ground motions and the consequent selection and, eventually, manipulation of records to match this target.

In an effort to push the structural response well into the non-linear range, a strong target ground motion level (in terms of elastic response

¹¹ Other EDPs (displacement ductility, rotational demand, ecc) are computed; the result in terms of these parameters, not reported for the sake of brevity, confirm the conclusions found in terms of MIDR and RD.

spectrum) have been defined for Ponticelli, corresponding to a return period of 2475 years¹².

All the sets averages are selected to be within [-10%, +30%] tolerance range¹³ with respect to the target spectrum and in most of the compatibility interval they approximated the target spectral shape very well. To measure such an approximation, the deviation (δ), Eq. (2), from the target spectrum have been used as criterion in selection.

$$\delta = \sqrt{\frac{1}{N} \sum_{i=1}^N \frac{Sa_{ave}(T_i) - Sa_{target}(T_i)}{Sa_{target}(T_i)}} \quad (2)$$

In Eq. (2), $Sa_{ave}(T_i)$ represents the pseudo-acceleration ordinate of the average real spectrum of the set corresponding to the period T_i , while $Sa_{target}(T_i)$ is the value of spectral ordinate of the target spectrum at the same period; N is the number of values within the considered range of period (0.15-2s). All the selected sets have similar δ -values.

The choice of seven records is based on international building code requirements because seven is the minimum set size for which it is possible to consider the average structural response as design value.

The investigate database are the European Strong-motion Database (ESD) (last updated on July 2007), whose URL is <http://www.isesd.cv.ic.ac.uk> and the ITalian ACcelerometric Archive (ITACA) (last updated on October 2010), whose URL is <http://itaca.mi.ingv.it>. All the records used satisfies the free-field conditions and are produced by earthquakes of moment magnitude larger than 4.

¹² Considering a target spectrum corresponding to a 475-years, the structure would remain elastic for most of the selected ground motions; the choice of higher return period of seismic action insure that nonlinear response results appropriate to the objectives of the study.

¹³ Few exception are allowed, especially for set of ITACA records.

ESD and ITACA have records in common although with different seismological processing. There was no attempt by the authors to combine records coming from the two database in defining record classes.

2.4.1 Selection strategies

All the sets of records selected for Ponticelli refer to the same 5% damped elastic design spectrum evaluated according to NIBC for a return period of 2475 years. The considered spectrum corresponds, for example, to the near collapse limit state (SLC) of an important structure with a nominal life of 100 years on B-type soil class, according to the EC8 classification; see Appendix A for details.

In Figure 8, the disaggregation of seismic hazard in terms of $S_a(T=1s)$ for the site is reported; the joint distribution of M and R for Ponticelli have a bimodal shape¹⁴, i.e., two relative maxima exist. In fact, the disaggregated hazard level at site (i.e., 0.38g) is affected by both the zone where the site is located and the nearest, most hazardous, zone (Convertito et al., 2009). As a consequence, for the selected spectral ordinate (coincident with the fundamental one for the case-study structure) at least two design earthquake do exist: one representing closer, smaller magnitudes and the other more distant, larger magnitudes.

Two groups of spectrum-compatible sets are identified and compared: the first group comprises 8 sets of seven records carefully chosen to reflect, within tolerable limits, the specific magnitude and distance scenario corresponding to the first mode of seismic hazard disaggregation; the second group comprises 6 sets of seven records chosen to reflect, within tolerable limits, the specific magnitude and distance scenario corresponding to the second mode of seismic hazard disaggregation. All the considered combinations belonging to the two first groups of accelerograms are

¹⁴ Disaggregation result change with the spectral ordinate and return period and, if multiple sources affect the hazard at the site, more than a single event may dominate the hazard; see Convertito et al., 2009 for a discussion.

compatible, in the average, with the target spectrum, in the range of periods 0.15-2s.

Within each group, the sets differs for the source database (ESD or ITACA), for the soil class of the records (same as target spectrum or any site class) and finally, for being not manipulated (original records) or linearly scaled in amplitude¹⁵, controlling the mean (for set) scale factors (SF_{mean}) that varies between 5 and 15. Detailed information on selected set, divided by groups, are summarized in Table 1-Table 4.

Two additional groups, each including 2 seven-record sets (one for each database) are considered: these records are selected to match, within tolerable limits, the values of magnitude and distance corresponding to the design earthquake and the soil condition of the site (i.e., B-type soil class) and are then scaled to match precisely the target spectrum level at the fundamental period of the structure ($T = 1\text{s}$), according to the practice described in section 2. Figure 9 and Figure 10 show the average spectra of each ground motions set, divided by groups, along with the target spectrum and the range of periods of interest.

¹⁵ More specifically, before the search of records has begun, the spectra are preliminarily normalized by dividing the spectral ordinates by the corresponding PGA. These non-dimensional spectra are compare to the target spectrum, also normalized. Records belonging to spectrum matching combinations found in this way require to be linearly scaled to comply with the original code spectrum.

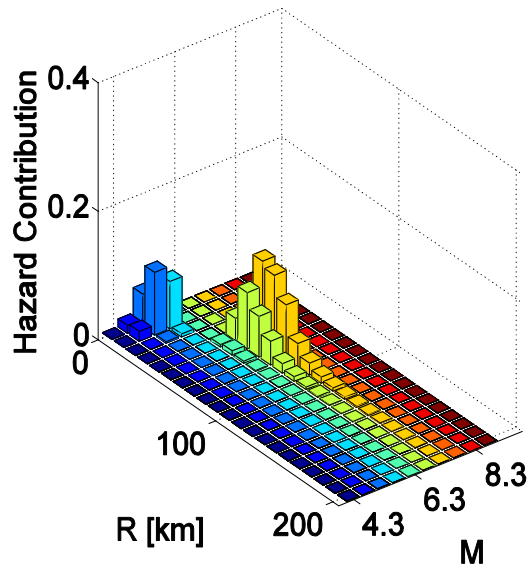


Figure 8. Disaggregation results for Ponticelli for $S_a(T=1s)$ and for a 2475-years return period.

In order to reduce the correlation or “overlapping” due to records commonality between sets, it is desirable to select combinations having no accelerograms in common (i.e., statistically independent); this requirement conflicts with limitations of the reference ground motion databases, especially if one looks at the relatively large target spectrum and the corresponding controlling earthquake scenarios. Then, some exceptions are allowed because complete avoidance of overlap is not feasible given the limited number of record available, see Appendix B for details.

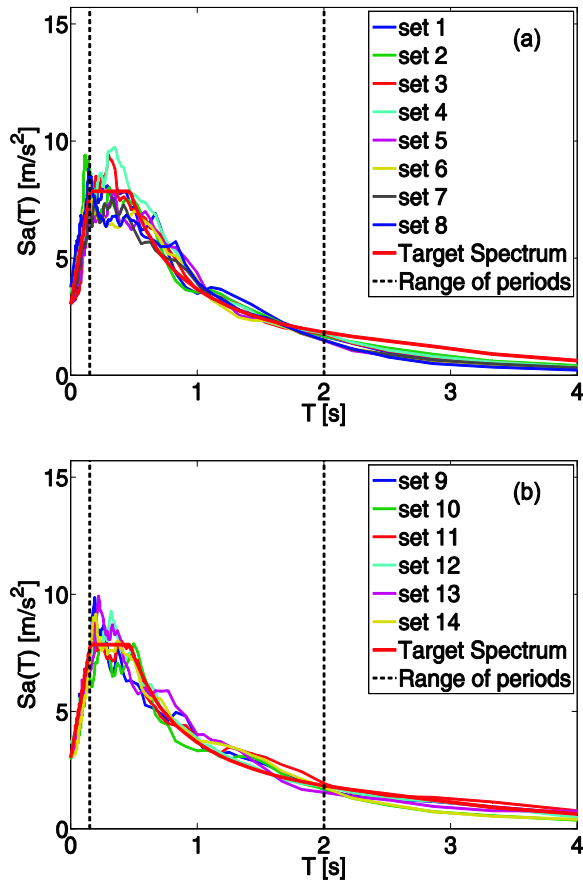


Figure 9. Average spectra for each individual set of seven records selected (and eventually scaled) to be compatible (on average) with the target spectrum in [0.15-2s] periods range (a) Group I (1st disaggregation mode-based); (b) Group II (2nd disaggregation mode-based).

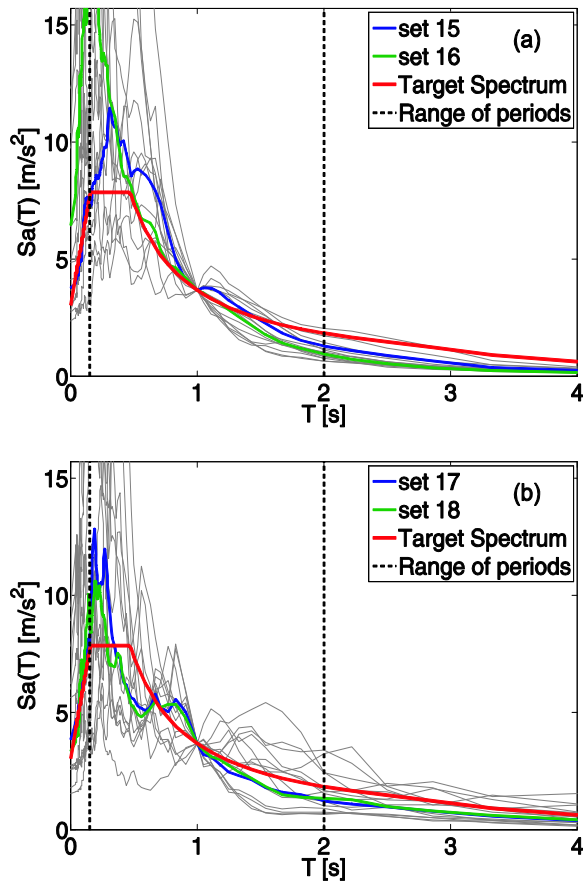


Figure 10. Individual and average spectra for each individual set of seven records selected and scaled to match precisely $T=1s$ -ordinate of the target spectrum (a) Group III (1st disaggregation mode-based); (b) Group IV (2nd disaggregation mode-based).

Chapter 2

Code-based real record selection: what really matters?

Table 1. Summary of records sets of Group I

| (matching target spectrum on average, with [-10%, +30%] tolerance, over the periods range 0.15-2s) | | | | |
|--|-----------------|-------------------|----------------------------------|-----------------------------|
| <i>Set no.</i> | <i>Database</i> | <i>Site class</i> | <i>Scaling/SF_{mean}</i> | <i>(M, R)</i> |
| 1 | ESD | B | Yes/5 | Disag. 1 st mode |
| 2* | ESD | B | No | Disag. 1 st mode |
| 3 | ESD | Any site class | Yes/5 | Disag. 1 st mode |
| 4 | ESD | Any site class | No | Disag. 1 st mode |
| 5** | ITACA | B | Yes/10 | Disag. 1 st mode |
| 6** | ITACA | B | No | Disag. 1 st mode |
| 7** | ITACA | Any site class | Yes/5 | Disag. 1 st mode |
| 8** | ITACA | Any site class | No | Disag. 1 st mode |

* Lower tolerance is increased to 15% to find a compatible set.

** Lower tolerance is increased to 20% to find a compatible set.

Table 2. Summary of records sets of Group II

| (matching target spectrum on average, with [-10%, +30%] tolerance, over the periods range 0.15-2s) | | | | |
|--|-----------------|-------------------|----------------------------------|-----------------------------|
| <i>Set no.</i> | <i>Database</i> | <i>Site class</i> | <i>Scaling/SF_{mean}</i> | <i>(M, R)</i> |
| 9** | ESD | B | Yes/5 | Disag. 2 st mode |
| 10*** | ESD | B | No | Disag. 2 st mode |
| 11 | ESD | Any site class | Yes/5 | Disag. 2 st mode |
| 12 | ESD | Any site class | No | Disag. 2 st mode |
| 13** | ITACA | Any site class | Yes/15 | Disag. 2 st mode |
| 14 | ITACA | Any site class | Yes/15 | Disag. 2 st mode |

** Lower tolerance is increased to 20% to find a compatible set.

*** Lower tolerance is increased to 25% to find a compatible set.

Table 3. Summary of records sets of Group III

| (matching target spectrum precisely at T = 1s) | | | | |
|--|-----------------|-------------------|----------------------------------|-----------------------------|
| <i>Set no.</i> | <i>Database</i> | <i>Site class</i> | <i>Scaling/SF_{mean}</i> | <i>(M, R)</i> |
| 15 | ESD | B | Sa(T ₁) scaling | Disag. 1 st mode |
| 16 | ITACA | B | Sa(T ₁) scaling | Disag. 1 st mode |

Table 4. Summary of records sets of Group IV

| (matching target spectrum precisely at T = 1s) | | | | |
|--|-----------------|-------------------|----------------------------------|-----------------------------|
| <i>Set no.</i> | <i>Database</i> | <i>Site class</i> | <i>Scaling/SF_{mean}</i> | <i>(M, R)</i> |
| 17 | ESD | B | Sa(T ₁) scaling | Disag. 2 st mode |
| 18 | ITACA | B | Sa(T ₁) scaling | Disag. 2 st mode |

2.5 Results and discussion

All records selected for each group are used as input for nonlinear dynamic analysis applied to case-study structure; a large amount of results is obtained.

As a general summary, the maximum inter-story drift ratios (MIDRs) for all the records sets are shown in Figure 11. Figure 11 shows the individual response predictions from each record (black x-markers) as well as the mean values for each set (red squares) and the mean plus (and minus) one standard deviation (red crosses). No collapses (i.e. dynamic instability where EDPs increase without bounds) are observed.

There is a large scatter in the MIDR values predicted for each record of a single ground motion suite; there is not large variability in the median predicted values from each set. This visual evidence will be confirmed by the hypothesis tests described in the following section.

The roof drift ratios and the total hysteretic energy for all the records sets are shown in Figure 12 and in Figure 13 respectively. As Figure 11, Figure 12 and Figure 13 show the individual response predictions from each record (black x-markers) as well as the mean values for each set (red squares) and the mean plus (and minus) one standard deviation (red crosses). Large variability in the median predicted values of E_H may be observed (Figure 13). The median of the response parameters, for each pair of sets, are compared statistically for equality (or not) in the next section.

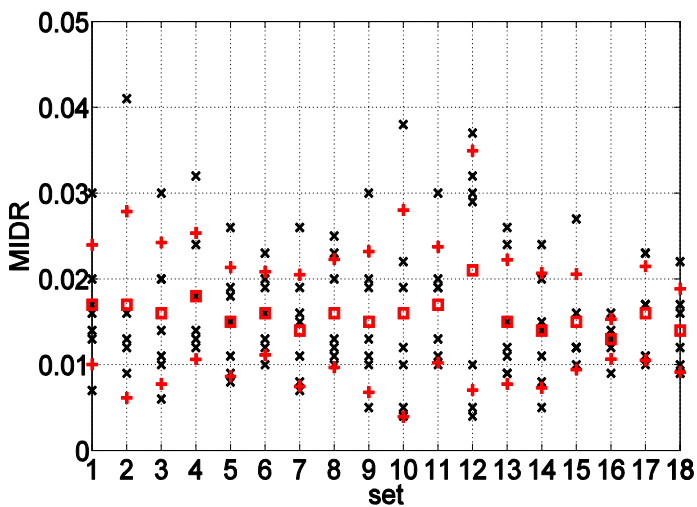


Figure 11. Summary of MIDR responses for the selected ground motions sets.

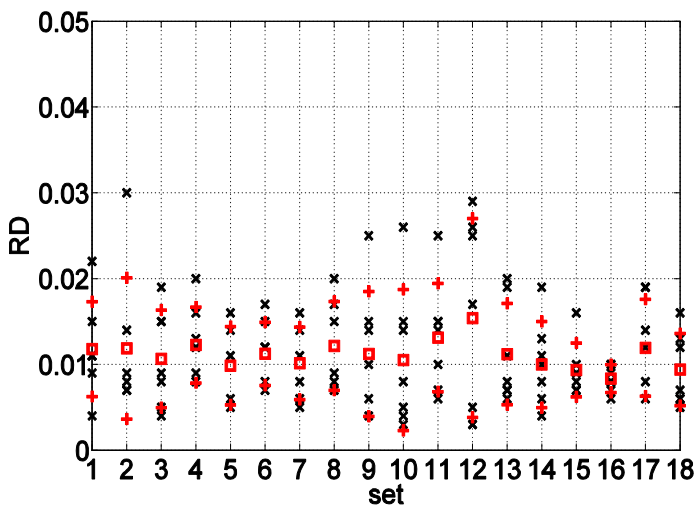


Figure 12. Summary of RD responses for the selected ground motions sets.

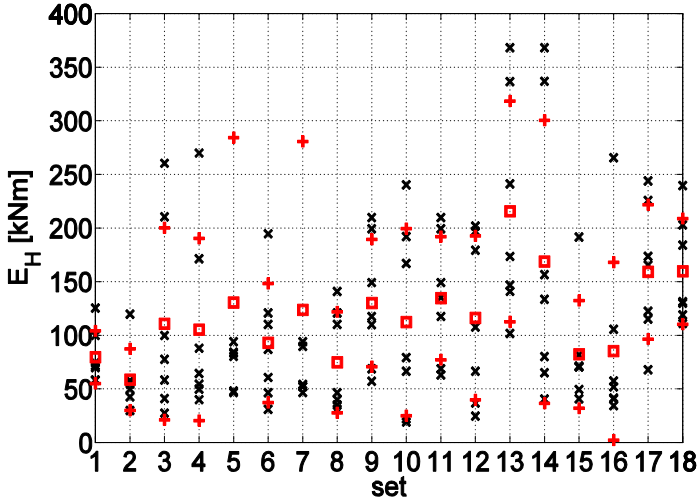


Figure 13. Summary of E_H responses for the selected ground motions sets.

Some general remarks are possible based on these results. In particular, Figure 11-Figure 13 show that the values of standard deviation for scaled combinations are generally smaller if compared with the values of standard deviation in the case of unscaled sets. This is a key issue if one is interested in how many records are required to obtain a stable and unbiased estimate of the inelastic response of a structure (e.g. Hancock et al., 2008). As many authors point out, the number of accelerograms required to obtain an estimate of the median response to within a defined confidence intervals depends on the standard deviation of response. Therefore, the number of record to be used should depend on both the procedure used to select and scale the record and the nature of the EDP being investigate: the larger the variance in the EDP, the greater the number of record that are required to obtain a robust estimate of the structural response.

All these concepts are summarized by Figure 14, where the ratio of the standard error of the estimate ($SEE = \frac{\sigma}{\sqrt{N}}$, where σ is the standard deviation¹⁶ of the considered EDP and N is the number of records in the considered set) to the median is given, for all the considered EDPs, as the size of the set increases (from 7 to 21, combining some of the sets of seven records discussed in the previous section). It is evident that scaled sets are characterized by smaller dispersion; moreover, as evident from Figure 14, the number of records required to predict the displacement-based measures may be significantly less than for the energy-based measures due to the large variability in these kind of damage-indices.

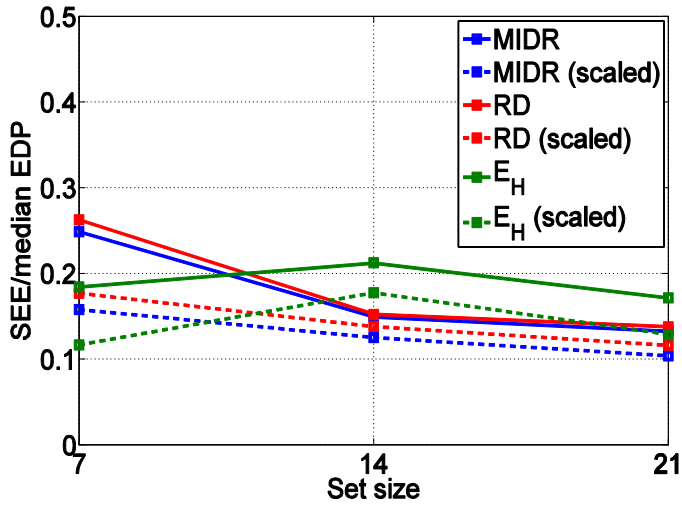


Figure 14. SEE/median EDP as a function of set size.

2.5.1 Hypothesis tests

To finally drawn conclusion from the results above, it may be helpful to try to quantitatively assess their significance. In particular, parametric

¹⁶ It is assume to be equivalent to the sample standard deviation for the purposes of the analysis.

hypothesis tests (Benjamin and Cornell, 1970) are performed to assess to what significance the median values¹⁷ of the response, from a given set of records, may be considered equal to that from another class. Hypothesis tests are performed for both peak and cyclic EDPs, assuming a lognormal distribution for all the response parameters of interest. This distribution assumption are checked with the Shapiro-Wilk (1965) test and could not be rejected at the 95% significance level.

The null hypothesis to check is whether the median EDPs for a given set (*i*) are equal (null hypothesis) or not (alternate hypothesis) to that from the set (*j*). To this aim, a two tail Aspin-Welch (Welch, 1938) test is preferred with respect to the standard Student t-test as the former does not require the assumption of equal, yet still unknown, variances of populations originating the samples, which would be an unreasonable assumption given the nature of the compared records sets.

The test statistic employed is reported in Eq. (3), in which z_i and z_j are the sample means, s_i and s_j are the sample standard deviations and n and m are the samples sizes (in this case always equal to 7). The test statistic, under the null hypothesis, has an approximate Student-t distribution with the number of degrees of freedom given by Satterthwaites's approximation (Satterthwaites, 1949).

$$t = \frac{z_x - z_y}{\sqrt{\frac{s_x^2}{n} + \frac{s_y^2}{m}}} \quad (3)$$

In the following Tabel 4-6, the *p*-values for each comparison are reported; red bold font values are the rejection cases assuming a 95% significance level, i.e., choosing I-type risk (α) equal to 0.05.

¹⁷ This focus on median responses is because median response (or the closely related mean or "average" response) is of primary interest in the NLDA requirements of current international building codes rather than the full probability distribution (e.g., average and standard deviation).

Chapter 2

Code-based real record selection: what really matters?

Table 5. Aspin-Welch test results in terms of MIDR; p -values lower than 0.05 are reported in bold.

| | <i>Group I</i> | | | | | | | | <i>Group II</i> | | | | | | <i>Group III</i> | | <i>Group IV</i> | |
|----|----------------|------|------|------|------|------|------|------|-----------------|------|------|------|-------------|------|------------------|------|-----------------|------|
| | 1 | 2 | 3 | 4 | 5 | 6 | 7 | 8 | 9 | 10 | 11 | 12 | 13 | 14 | 15 | 16 | 17 | 18 |
| 1 | 1.00 | 0.52 | 0.93 | 0.57 | 0.47 | 0.56 | 0.95 | 0.81 | 0.64 | 0.37 | 0.87 | 0.47 | 0.37 | 0.99 | 0.86 | 0.66 | 0.92 | 0.76 |
| 2 | | 1.00 | 0.36 | 1.00 | 0.93 | 0.95 | 0.38 | 0.58 | 0.91 | 0.91 | 0.61 | 0.91 | 0.95 | 0.44 | 0.61 | 0.78 | 0.37 | 0.62 |
| 3 | | | 1.00 | 0.45 | 0.10 | 0.39 | 0.96 | 0.55 | 0.52 | 0.06 | 0.74 | 0.09 | 0.02 | 0.92 | 0.74 | 0.44 | 0.96 | 0.48 |
| 4 | | | | 1.00 | 0.94 | 0.95 | 0.47 | 0.64 | 0.91 | 0.93 | 0.66 | 0.93 | 0.97 | 0.51 | 0.66 | 0.81 | 0.45 | 0.68 |
| 5 | | | | | 1.00 | 0.99 | 0.12 | 0.44 | 0.95 | 0.73 | 0.56 | 0.97 | 0.76 | 0.28 | 0.56 | 0.77 | 0.15 | 0.49 |
| 6 | | | | | | 1.00 | 0.41 | 0.63 | 0.95 | 0.85 | 0.65 | 0.98 | 0.89 | 0.47 | 0.66 | 0.83 | 0.40 | 0.67 |
| 7 | | | | | | | 1.00 | 0.59 | 0.54 | 0.08 | 0.76 | 0.12 | 0.04 | 0.95 | 0.76 | 0.46 | 0.93 | 0.52 |
| 8 | | | | | | | | 1.00 | 0.74 | 0.30 | 0.96 | 0.45 | 0.28 | 0.72 | 0.96 | 0.76 | 0.58 | 0.93 |
| 9 | | | | | | | | | 1.00 | 0.81 | 0.74 | 0.96 | 0.85 | 0.59 | 0.74 | 0.91 | 0.52 | 0.77 |
| 10 | | | | | | | | | | 1.00 | 0.44 | 0.70 | 0.91 | 0.19 | 0.44 | 0.60 | 0.10 | 0.34 |
| 11 | | | | | | | | | | | 1.00 | 0.57 | 0.45 | 0.82 | 1.00 | 0.77 | 0.74 | 0.91 |
| 12 | | | | | | | | | | | | 1.00 | 0.72 | 0.29 | 0.57 | 0.79 | 0.15 | 0.50 |
| 13 | | | | | | | | | | | | | 1.00 | 0.18 | 0.45 | 0.62 | 0.07 | 0.32 |
| 14 | | | | | | | | | | | | | | 1.00 | 0.82 | 0.56 | 0.90 | 0.66 |
| 15 | | | | | | | | | | | | | | | 1.00 | 0.78 | 0.73 | 0.92 |
| 16 | | | | | | | | | | | | | | | | 1.00 | 0.45 | 0.81 |
| 17 | | | | | | | | | | | | | | | | | 1.00 | 0.52 |
| 18 | | | | | | | | | | | | | | | | | | 1.00 |

The results presented in Table 5-Table 7 show that there are 2/153 (i.e., < 2%), 3/153 (i.e., \cong 2%) and 7/153 (i.e., \cong 5%) for MIDR, RD and E_H respectively. Study of patterns within the tables show that individual rows or columns (sets) tend to dominate in rejection (e.g., column 13 for MIDR, row 3 for RD, row 2 and column 15 for E_H); all these sets comprise scaled record (except for set 2), characterized by smaller dispersion and hence strongly conditioning the tests.

Entering in the detail, for both MIDR and RD, the results presented in Table 5 and Table 6 show that there are no rejections in comparing the seismic response to accelerograms selected based on magnitude, distance and soil condition and then scaled to match precisely the target spectrum (sets 15-18, Groups III-IV) and to accelerograms matching the target spectrum on average

Chapter 2

Code-based real record selection: what really matters?

in a broader range of period (sets 1-14), independently from the (M, R) pair of interest (Groups I and II), confirming that the two codes procedure are almost equivalent.

Table 6. Aspin-Welch test results in terms of RD; *p*-values lower than 0.05 are reported in bold.

| | <i>Group I</i> | | | | | | | | <i>Group II</i> | | | | | | <i>Group III</i> | | <i>Group IV</i> | |
|----|----------------|------|------|------|------|------|------|------|-----------------|-------------|------|-------------|-------------|------|------------------|------|-----------------|------|
| | 1 | 2 | 3 | 4 | 5 | 6 | 7 | 8 | 9 | 10 | 11 | 12 | 13 | 14 | 15 | 16 | 17 | 18 |
| 1 | 1.00 | 0.25 | 0.96 | 0.43 | 0.31 | 0.49 | 0.86 | 0.71 | 0.43 | 0.30 | 0.69 | 0.26 | 0.25 | 0.94 | 0.73 | 0.50 | 0.93 | 0.56 |
| 2 | | 1.00 | 0.11 | 0.86 | 0.70 | 0.71 | 0.18 | 0.33 | 0.85 | 0.72 | 0.47 | 0.80 | 0.80 | 0.20 | 0.36 | 0.60 | 0.17 | 0.47 |
| 3 | | | 1.00 | 0.33 | 0.06 | 0.37 | 0.64 | 0.51 | 0.32 | 0.05 | 0.56 | 0.03 | 0.02 | 0.85 | 0.57 | 0.32 | 0.79 | 0.35 |
| 4 | | | | 1.00 | 0.94 | 0.88 | 0.44 | 0.58 | 0.99 | 0.95 | 0.67 | 0.99 | 0.99 | 0.42 | 0.59 | 0.81 | 0.41 | 0.71 |
| 5 | | | | | 1.00 | 0.91 | 0.17 | 0.42 | 0.95 | 0.97 | 0.61 | 0.85 | 0.83 | 0.23 | 0.47 | 0.79 | 0.16 | 0.62 |
| 6 | | | | | | 1.00 | 0.50 | 0.67 | 0.89 | 0.90 | 0.76 | 0.83 | 0.82 | 0.48 | 0.68 | 0.93 | 0.46 | 0.82 |
| 7 | | | | | | | 1.00 | 0.76 | 0.43 | 0.15 | 0.74 | 0.11 | 0.08 | 0.90 | 0.79 | 0.48 | 0.89 | 0.55 |
| 8 | | | | | | | | 1.00 | 0.58 | 0.40 | 0.92 | 0.33 | 0.31 | 0.71 | 1.00 | 0.69 | 0.69 | 0.80 |
| 9 | | | | | | | | | 1.00 | 0.96 | 0.67 | 0.98 | 0.97 | 0.42 | 0.59 | 0.81 | 0.40 | 0.71 |
| 10 | | | | | | | | | | 1.00 | 0.59 | 0.87 | 0.86 | 0.21 | 0.45 | 0.77 | 0.15 | 0.60 |
| 11 | | | | | | | | | | | 1.00 | 0.53 | 0.51 | 0.69 | 0.92 | 0.81 | 0.68 | 0.91 |
| 12 | | | | | | | | | | | | 1.00 | 0.99 | 0.17 | 0.39 | 0.69 | 0.11 | 0.52 |
| 13 | | | | | | | | | | | | | 1.00 | 0.15 | 0.37 | 0.68 | 0.09 | 0.50 |
| 14 | | | | | | | | | | | | | | 1.00 | 0.74 | 0.47 | 0.99 | 0.54 |
| 15 | | | | | | | | | | | | | | | 1.00 | 0.71 | 0.72 | 0.81 |
| 16 | | | | | | | | | | | | | | | | 1.00 | 0.44 | 0.88 |
| 17 | | | | | | | | | | | | | | | | | 1.00 | 0.50 |
| 18 | | | | | | | | | | | | | | | | | | 1.00 |

Moreover, the non-linear response of case-study structure seems to be independent on M and R beyond the dependence through the intensity (i.e. spectral ordinates) level; in other words, non-linear response seems to be conditionally independent of M and R given spectral accelerations (i.e. spectral compatibility).

Chapter 2

Code-based real record selection: what really matters?

Table 7. Aspin-Welch test results in terms of E_H ; p -values lower than 0.05 are reported in bold.

| | <i>Group I</i> | | | | | | | | <i>Group II</i> | | | | | | <i>Group III</i> | | <i>Group IV</i> | |
|----|----------------|------|------|------|-------------|------|------|-------------|-----------------|------|------|-------------|-------------|------|------------------|------|-----------------|------|
| | 1 | 2 | 3 | 4 | 5 | 6 | 7 | 8 | 9 | 10 | 11 | 12 | 13 | 14 | 15 | 16 | 17 | 18 |
| 1 | 1.00 | 0.36 | 0.67 | 0.48 | 0.21 | 0.44 | 0.54 | 0.26 | 0.59 | 0.40 | 0.97 | 0.13 | 0.10 | 0.63 | 0.56 | 0.56 | 0.66 | 0.33 |
| 2 | | 1.00 | 0.07 | 0.89 | 0.03 | 0.16 | 0.10 | 0.02 | 0.83 | 0.07 | 0.43 | 0.01 | 0.01 | 0.07 | 0.69 | 0.16 | 0.18 | 0.07 |
| 3 | | | 1.00 | 0.31 | 0.22 | 0.56 | 0.72 | 0.21 | 0.32 | 0.51 | 0.67 | 0.10 | 0.06 | 0.91 | 0.18 | 0.72 | 0.88 | 0.41 |
| 4 | | | | 1.00 | 0.12 | 0.23 | 0.26 | 0.16 | 0.79 | 0.21 | 0.51 | 0.10 | 0.08 | 0.29 | 0.72 | 0.27 | 0.32 | 0.17 |
| 5 | | | | | 1.00 | 0.87 | 0.45 | 0.66 | 0.10 | 0.65 | 0.23 | 0.86 | 0.75 | 0.25 | 0.05 | 0.59 | 0.43 | 0.84 |
| 6 | | | | | | 1.00 | 0.72 | 0.92 | 0.26 | 0.87 | 0.45 | 0.78 | 0.71 | 0.59 | 0.23 | 0.79 | 0.67 | 0.99 |
| 7 | | | | | | | 1.00 | 0.63 | 0.27 | 0.79 | 0.55 | 0.32 | 0.25 | 0.78 | 0.19 | 0.93 | 0.90 | 0.64 |
| 8 | | | | | | | | 1.00 | 0.13 | 0.89 | 0.30 | 0.46 | 0.33 | 0.27 | 0.04 | 0.79 | 0.58 | 0.88 |
| 9 | | | | | | | | | 1.00 | 0.20 | 0.63 | 0.07 | 0.05 | 0.30 | 0.93 | 0.31 | 0.36 | 0.17 |
| 10 | | | | | | | | | | 1.00 | 0.42 | 0.50 | 0.41 | 0.56 | 0.13 | 0.89 | 0.71 | 0.83 |
| 11 | | | | | | | | | | | 1.00 | 0.16 | 0.13 | 0.64 | 0.62 | 0.56 | 0.66 | 0.34 |
| 12 | | | | | | | | | | | | 1.00 | 0.88 | 0.13 | 0.02 | 0.48 | 0.32 | 0.72 |
| 13 | | | | | | | | | | | | | 1.00 | 0.08 | 0.01 | 0.41 | 0.26 | 0.62 |
| 14 | | | | | | | | | | | | | | 1.00 | 0.17 | 0.76 | 0.93 | 0.45 |
| 15 | | | | | | | | | | | | | | | 1.00 | 0.26 | 0.30 | 0.12 |
| 16 | | | | | | | | | | | | | | | | 1.00 | 0.85 | 0.74 |
| 17 | | | | | | | | | | | | | | | | | 1.00 | 0.59 |
| 18 | | | | | | | | | | | | | | | | | | 1.00 |

This result is confirmed (also in terms of E_H) looking at pairs of *homologous* sets (e.g. 1-9, 2-10, 3-11, 4-12, 5-13, 7-14), i.e., sets that significantly differs in terms of average (M, R) pairs characterizing the set with all other conditions being equal; for all these comparisons no rejections are observed.

Similarly, considering pairs of sets that differs only for soil condition (*same as target spectrum vs. any site class*), i.e., 1-3, 2-4, 5-7, 6-8*, 9-11*, 10-12, 13-14 (pairs marked with an asterisk share more than 3 records and then the comparison is not statistically rigorous), with all other conditions being equal, no rejections are observed for both peak and cyclic response parameters: if the spectral shape is assigned by the code, the site class of real records may be of secondary importance.

In light of this consideration, there may be cases in which it may be useful to relax the matching criteria for site classification. This, should help to overcome some of the problems when for specific site conditions it is hard to find spectrum matching sets

Finally, note that the sets of linearly scaled records (i.e., 1, 3, 5, 7, 9, 11) do not show systematic difference with respect to those unscaled (with all other conditions being equal, i.e., 2, 4, 6, 8, 10, 12) for all the types of response considered, which seems to confirm that amplitude scaling is a legitimate practice, as many studies point out, if the spectral shape is controlled.

2.5.2 Including additional record selection criteria: Cosenza and Manfredi index

If the cyclic response is considered, some sets show significant differences in the prediction of seismic demand (i.e., p-values lower than 0.05). These differences were a predictable result looking at the integral intensity measures, characterizing each record (see also Iervolino et al., 2006).

To this aim, each record of the 18 sets is processed to evaluate its characteristics other than spectral shape; for each set, average values of the *Arias intensity*, I_A , Eq. (4), and of the *Cosenza and Manfredi index*, I_D (Manfredi, 2001), Eq. (5), taken as the average on the sample of seven records, are computed.

$$I_A = \frac{\pi}{2g} \int_0^{t_E} a^2(t) dt \quad (4)$$

$$I_D = \frac{2g}{\pi} \frac{I_A}{PGA \cdot PGV} \quad (5)$$

In Eq. (4), $a(t)$ is the signal's accelerometric time-history, whose duration is equal to t_E and PGV represents the peak ground velocity.

Figure 15a shows the I_A versus E_H plot; similarly, Figure 15b shows the I_D versus E_H plot¹⁸; the estimated linear regressions (for both I_A and E_H and I_D and E_H) are reported in the legend of the two panels of Figure 15. It is possible to note a fairly good correlation in both cases, confirmed by statistical tests on coefficients of regressions and on the estimate correlation coefficients (these results are not reported for the sake of brevity).

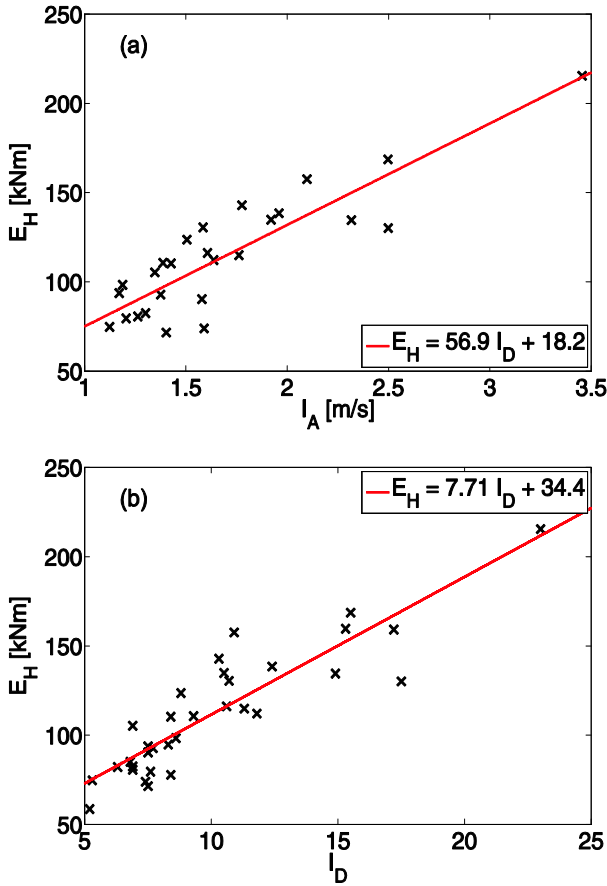


Figure 15. E_H versus (a) I_A and (b) I_D for the considered sets.

¹⁸ In this plots, to increase the significance of the results, 15 additional sets of records are considered, relating to another case-study site in southern Italy, i.e. S. Angelo dei Lombardi.

In Table 8, the values of Cosenza and Manfredi index for rejection cases of Table 7 are reported: generally, significant differences in I_D values characterizing the records, imply significant differences in the consequent E_H response.

Table 8. I_D values for rejection cases of Table 7.

| <i>Set</i> | I_D | <i>Set</i> | I_D | <i>p-value</i> |
|------------|-------|------------|-------|----------------|
| 2 | 5.2 | 5 | 10.7 | 0.03 |
| 2 | 5.2 | 12 | 10.6 | 0.01 |
| 2 | 5.2 | 13 | 23 | 0.01 |
| 15 | 6.3 | 8 | 5.3 | 0.04 |
| 15 | 6.3 | 12 | 10.6 | 0.02 |
| 15 | 6.3 | 13 | 23 | 0.01 |

As a conclusion, I_D can be suggested as an additional criterion in selection (or generation) procedures for accelerograms when the cyclic response represents a critical performance parameter for the structure to be analyzed.

A key issue in this direction consists in developing tools for a reliable assessment of the seismic hazard in terms of both peak and integral parameters of seismic motion, possibly (and explicitly) accounting for the correlation between the parameters of interest.

Probabilistic seismic hazard analysis has become a common tool in the engineering practice to determine the likelihood that ground motions of different amplitude may be observed at a given designed site but, conventionally, this computation is only done for scalar ground motion intensity measures, such as peak ground acceleration, spectral ordinates or some integral intensity measures (e.g. Arias intensity), considered independent. Nevertheless, the methodology for computing the joint (i.e. vector-valued) hazard at a given site has been proposed almost 10 years ago since the knowledge of joint hazard at a site is valuable in many applications where more than one ground motion parameters is needed for better predicting a structure's response, e.g. if one is interested in both displacement

and cyclic structural response. In these cases, an acceleration-duration vector-valued may be notably helpful in spite of the difficulties and the lack of computational tools to easily perform vector-valued seismic hazard analysis.

In Chapter 3 an easy yet hazard-consistent way of including secondary intensity measures in record selection will be presented. The proposed methodology requires mainly the manipulation of result from the scalar PSHA and allows to develop *conditional hazard maps*, i.e., maps of secondary ground motion intensity measures (e.g. integral parameters) conditional, in a probabilistic sense, to the design hazard for a primary parameter (e.g., a spectral ordinate).

2.6. Conclusions

In this study, different ways to obtain code-conforming real records sets are compared in terms of post elastic seismic peaks and cyclic responses. This was pursued by considering a modern code-conforming four-story RC frame building at high nonlinearity levels and a ground motion scenario (a reference site and the corresponding code-response spectra) as case study. More specifically, MIDR, RD and E_H are analyzed with respect to 18 sets of natural ground motion accelerograms obtained exploring all the possible options allowed by modern building codes in real record selection and modification.

Hypothesis tests are carried out with the aim of assessing quantitatively how significant there results are. Tests results show that no particular care is required in selecting records with respect to magnitude, distance and soil condition if accelerograms match, individually or in an average sense, a target spectral shape.

Moreover, results indicate that the linearly scaled records do not show any systematic trend with respect to the unscaled record results independently of response parameters, suggesting that scaling is a legitimate technique, as many studies point out, again if the spectral shape is controlled.

Finally, it worth noting that, as is well known, some differences in cyclic response may be observed. These differences may be predicted by some integral parameter of ground motion, which, if an appropriate hazard analysis tool is available, could be used as an additional criterion for record selection, especially in those cases when cyclic behavior has an important role in determining the seismic performances.

The analyses and results that are presented herein refer to a single structure at a single site; the possible limitations of this restricted analysis should be borne in mind when attempting to generalize these findings for other structures and scenarios. Further research should be conducted to verify that the results of this chapter also apply to alternative structures and sites/scenarios.

References

Baker, J.W. (2011). The Conditional Mean Spectrum: A tool for ground motion selection. *Journal of Structural Engineering*, (in press).

Benjamin, J., and Cornell, C. A. (1970). *Probability, statistics and decision for civil engineers*. NY (USA): Mc Graw-Hill.

CEN, European Committee for Standardization. (2003). Eurocode 8: Design provisions for earthquake resistance of structures, Part 1.1: general rules, seismic actions and rules for buildings, Pren1998-1.

Chioccarelli, E., Iervolino, I., Convertito, V. (2010). Italian Map of Design Earthquakes from Multimodal Disaggregation Distributions: Preliminary Results. *Proc. of 14th European Conference on Earthquake Engineering*, Ohrid, Republic of Macedonia.

Convertito, V., Iervolino, I., Herrero, A. (2009). The importance of mapping the design earthquake: insights for southern Italy. *Bulletin of the Seismological Society of America*. 99, 2979–2991.

CS.LL.PP. (2008). DM 14 Gennaio 2008. Norme tecniche per le costruzioni. *Gazzetta Ufficiale della Repubblica Italiana*, 29. (in Italian)

Hancock, J., Bommer, J.J., Stafford, P.J. (2008). Number of scaled and matched accelerograms required for inelastic dynamic analyses. *Earthquake Engineering and Structural Dynamics*, 37, 1585-607.

Haselton, C.B. (2006). *Assessing Seismic Collapse Safety of Modern Reinforced Concrete Moment Frame Buildings*, Ph.D. Dissertation, Department of Civil and Environmental Engineering, Stanford University.

Ibarra, L.F., Medina, R.A. and Krawinkler, H. (2005). Hysteretic Models that Incorporate Strength and Stiffness Deterioration. *Earthquake Engineering and Structural Dynamics*, 34, 1489-1511.

Iervolino, I., De Luca, F., Cosenza, E. (2010). Spectral shape-based assessment of SDOF nonlinear response to real, adjusted and artificial accelerograms. *Engineering Structures*, 32, 2776-279.

Iervolino, I., and Cornell, C.A. (2005). Record selection for nonlinear seismic analysis of structures. *Earthquake Spectra*, 21, 685-713.

Iervolino, I., Manfredi, G., Cosenza, E. (2006). Ground-motion duration effects on nonlinear seismic response. *Earthquake Engineering and Structural Dynamics*, 35, 21-38.

Luco, N., and Bazzurro, P. (2007). Does amplitude scaling of ground motion records result in biased nonlinear structural drift responses? *Earthquake Engineering and Structural Dynamics*, 36: 1813-1835.

Magliulo, G., Maddaloni, G., Cosenza, E., (2007). Comparison between non-linear dynamic analysis performed according to EC8 and elastic and non-linear static analysis. *Engineering Structures*, 9, 2893-2900.

Mander, J. B., Priestley, M. J. N., Park, R. (1988). Theoretical stress-strain model for confined concrete. *Journal of Structural Engineering*, 114, 1804-26.

Manfredi, G. (2001). Evaluation of seismic energy demand. *Earthquake Engineering and Structural Dynamics*, 30, 485-499.

PEER GSM, Haselton, C.B., Editor (2009). Evaluation of Ground Motion Selection and Modification Methods: Predicting Median Interstory Drift Response of Buildings, PEER Report 2009/01, Pacific Engineering Research Center, University of California, Berkeley, California.

Satterthwaite, F. E. (1941). Synthesis of variance. *Psychometrika*, 6, 309-16.

Shapiro, S.S., Wilk, M.B. (1965). An analysis of variance test for normality (complete samples). *Biometrika*, 52, 591-611.

Chapter 2

Code-based real record selection: what really matters?

Shome, N., Cornell, C. A., Bazzurro, P., and Carballo, J. E. (1998). Earthquakes, records and nonlinear responses. *Earthquake Spectra*, 14, 469–500.

Welch, BL. The significance of the difference between two means when the population variances are unequal. *Biometrika*, 1938:350-62.

Chapter 3

Improving seismic action assessment: conditional design maps for secondary intensity measures

ABSTRACT

Vector-valued ground motion intensity measures (IMs) have been the focus of a significant deal of research recently. Proposed measures are mainly function of spectral ordinates which have been shown to be useful in the assessment of structural response. This is especially appropriate in the case of structures following modern earthquake resistant design principles, in which structural damage is mainly due to peak displacements experienced during nonlinear dynamics. On the other hand, there may be cases in which the cumulative damage potential of the earthquake is also of concern, even if it is generally believed that integral ground motion IMs, associated with duration, are less important with respect to peak parameters of the record. For these IMs, it seems appropriate to develop conditional hazard maps, i.e., maps of percentiles of a secondary IM (e.g., duration-related) given the occurrence or exceedance of a primary parameter (e.g., peak acceleration), for which a design hazard map is often already available. In this chapter, this concept is illustrated and conditional hazard is developed for a parameter which may account for the cumulative damage potential of ground motion, the so-called Cosenza and Manfredi index (I_D), given peak ground acceleration (PGA). To this aim, a ground motion prediction relationship was derived for I_D first. Subsequently, the residuals of PGA and I_D were tested for correlation and for joint normality. Finally, the study obtained analytical distributions of I_D conditional on PGA and on the corresponding design earthquake in terms of magnitude and distance from hazard disaggregation. As shown by the application to the Campania region (southern Italy), I_D maps conditional on the code design values of PGA may be useful, for example, for a more refined ground motion record selection as an input for nonlinear dynamic analysis of structures.

3.1 Introduction

Intensity measures (IMs) should allow for a correct and accurate estimation of the structural performance on the basis of the seismic hazard at the considered site. An IM is a parameter which is considered to be a proxy for the potential effect of the ground motion on the structure. Typical ground motion IMs are the peaks of the ground acceleration and velocity, and conventional probabilistic seismic hazard analysis (PSHA) provides the mean annual frequency of exceeding a specified value of one of these parameters at the location of interest. Linear spectral ordinates are also often used as IMs for probabilistic assessment, especially those at the fundamental period of the structure, $S_a(T_1)$. This is mainly because $S_a(T_1)$, being the response of a linear single degree of freedom system (SDOF), should be, in principle, more correlated with the structural performance than, for example, peak ground acceleration (PGA).

More sophisticated IMs are currently under investigation by many researchers. For example, Baker (2007) discusses vector-valued IMs' potential in terms of efficiency in estimating structural response. Most of the proposed vector-valued IMs are comprised of spectral ordinates or other proxies for the spectral shape in a range of periods believed to be of interest for the nonlinear structural behavior. This helps to estimate the peak seismic demand especially in terms of displacements.

Integral parameters, as the *Arias intensity* or *significant ground motion duration*, are possible IMs, but they are considered to be related more to the cyclic energy dissipation rather than to the peak structural response (Chapter 2). Some studies (e.g., Iervolino et al., 2006; Hancock and Bommer, 2006) investigated how ground motion duration-related parameters affect nonlinear structural response. It was found that, generally, spectral ordinates are *sufficient* (i.e., duration does not add much information) if one is interested in the ductility demand, while duration-related measures do play a role only if the hysteretic structural response is that to assess; i.e., in those cases in which the cumulative damage potential of the earthquake is of concern. However, in

general, the integral ground motion parameters associated with duration are less important with respect to peak IMs, as damage to structures in general is more due to maximum displacement, and therefore the former IMs may be considered secondary with respect to the latter. In these cases, it seems appropriate to develop *conditional hazard maps*; i.e., maps of percentiles of the secondary IM given the occurrence or exceedance of the primary parameter for which a design hazard map is often already available by national authorities.

Herein, for illustration purposes, the primary intensity measure considered is PGA, while the secondary is a parameter which may account for the cumulative damage potential (i.e., damage related to the amount of cyclic shaking of the structure); the chosen cyclic response-related measure is the so-called *Cosenza and Manfredi index* (I_D) (Manfredi, 2001). To show the concept of conditional hazard, a ground motion prediction relationship had to be derived for I_D on the basis of an empirical dataset of Italian records already used for other well known ground motion prediction equations (GMPE) proposed in the past by Sabetta and Pugliese (1987, 1996). Subsequently, the residuals of the logarithms of PGA and I_D were tested for correlation and for joint normality. The study obtained distributions of I_D conditional on PGA and the corresponding design earthquake in terms of magnitude and distance from hazard disaggregation. Two percentiles (i.e. the 50th and the 90th) were extracted from the conditional probability density function (PDF) of I_D given PGA and mapped for the Campania region (southern Italy). The selected hazard level for PGA corresponds to a 10% exceedance probability in 50 years, which is a reference return period for the life-safety limit state of ordinary structures internationally.

The application to a case study region shows that the conditional hazard analysis may prove useful to complement the available acceleration hazard with maps providing suitable values of secondary IMs, to match in ground motion record selection (e.g., Iervolino and Cornell 2005; Iervolino et al., 2008a; Iervolino et al., 2010). In fact, apart from selecting seismic input for nonlinear dynamic analysis reflecting the design peak values of motion (e.g., PGA or spectral ordinates), one can benefit from this kind of information and consider

records featuring values of the secondary IM probabilistically consistent with the hazard of the primary IM.

3.2 Ground motion prediction equation for I_D

I_D has proven to be a good proxy for cyclic structural response (Manfredi, 2001). It is defined in Equation (1) where $a(t)$ is the acceleration time-history, t_E is the total duration of the ground motion recording, and PGV is the peak ground velocity. Therefore, the numerator of I_D is proportional to the Arias Intensity and it will be referred to as I_A .

$$I_D = \frac{\int_0^{t_E} a^2(t) dt}{PGA \cdot PGV} = \frac{I_A}{PGA \cdot PGV} \quad (1)$$

The best candidates to be ground motion intensity measures are those for which hazard analysis is easy to compute, which requires a GMPE to be available. Therefore, a GMPE was developed for I_D . The dataset used consists of 190 horizontal components from 95 recordings of Italian earthquakes used by Sabetta and Pugliese (1987, 1996). A representation in terms of magnitude, distance, and site conditions is given in Figure 16 (see Data and Resources section).

The empirical predictive equations for the logarithms of the terms (the generic dependent variable is indicated as Y) appearing in the definition of I_D were fitted by regression using the same functional form of Sabetta and Pugliese (1996), Equation (2), as a function of moment magnitude (M or M_W), source-to-site distance (closest distance to fault surface projection, R_{jb} , and epicentral distance, R_{epi} , both expressed in km), and recording site geology. In this form, h is a fictitious depth. The dummy variables S_1 and S_2 refer to the site classification and take the value of 1 for shallow and deep alluvium sites, respectively, and zero otherwise. The residual, $\varepsilon_{\log_{10}Y}$, is a random variable

which in ordinary least squares (OLS) regressions, is implicitly assumed to be Gaussian with zero mean and a standard deviation $\sigma_{\log_{10} Y}$.

$$\log_{10}(Y) = a + b M + c \log_{10} \left(R^2 + h^2 \right)^{\frac{1}{2}} + d S_1 + e S_2 + \varepsilon_{\log_{10} Y} \quad (2)$$

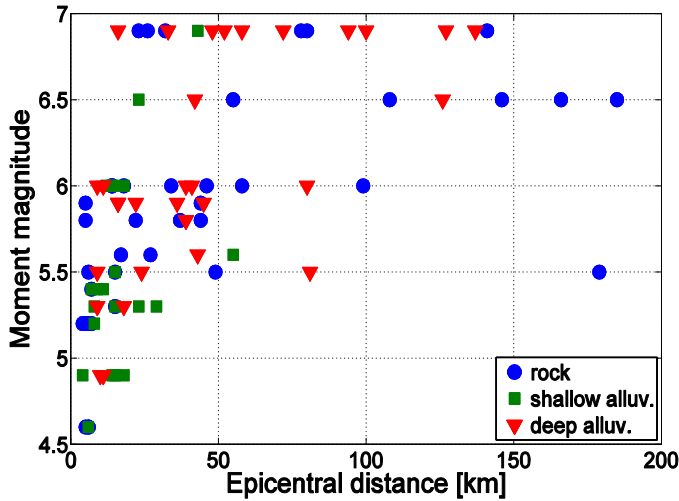


Figure 16. Distribution of the records with respect to moment-magnitude and epicentral distance.

The estimates for the coefficients¹⁹ for PGA, PGV and I_A , obtained using OLS regression²⁰, are given in Table 9 (R_{epi}) and Table 10 (R_{jb}). In the same tables also the estimated standard deviations of the respective residuals, are

¹⁹ Note that for some of the coefficients, those marked with an asterisk in the tables, the null hypothesis of being equal to zero could not be rejected at 0.05 significance level using a *Student's T-Test* (Mood et al., 1974), which means the variables associated to them could be dropped from Equation (2).

²⁰ A more refined model accounting for inter-event and intra-event variability (e.g., Joyner and Boore, 1993) was also used for the regressions on the considered database; however it did not change significantly the estimates of coefficients and variances with respect to those obtained with OLS. This is consistent with Sabetta and Pugliese (1996) who also could not find sufficient evidence supporting to use other fitting methods than OLS.

also given²¹. h values were not estimated and assumed to be coincident to those provided by Sabetta and Pugliese (1996); see also Iervolino et al. (2008b).

Table 9. Regression coefficients for PGA, PGV and I_A (R_{epi}).

| Y | a | b | c | d | e | h | $\sigma_{\log_{10} Y}$ |
|---|-------|------|-------|------|---------|-----|------------------------|
| PGA [cm/s ²] | 1.12 | 0.34 | -0.89 | 0.16 | -0.065* | 5.0 | 0.19 |
| PGV [cm/s] | -1.27 | 0.55 | -0.95 | 0.14 | 0.036* | 3.9 | 0.25 |
| I_A [cm ² /s ³] | 0.42 | 0.92 | -1.69 | 0.24 | -0.021* | 5.3 | 0.39 |

Table 10. Regression coefficients for PGA, PGV and I_A (R_{jb}).

| Y | a | b | c | d | e | h | $\sigma_{\log_{10} Y}$ |
|---|-------|------|-------|------|---------|-----|------------------------|
| PGA [cm/s ²] | 1.44 | 0.27 | -0.87 | 0.16 | -0.016* | 5.8 | 0.18 |
| PGV [cm/s] | -1.02 | 0.48 | -0.91 | 0.15 | 0.10 | 3.6 | 0.22 |
| I_A [cm ² /s ³] | 0.76 | 0.79 | -1.50 | 0.27 | 0.097* | 3.8 | 0.38 |

The Shapiro-Wilk test (1965), based on the considered sample, was used to check the assumption of normal distribution for $\varepsilon_{\log_{10}PGA}$, $\varepsilon_{\log_{10}PGV}$ and $\varepsilon_{\log_{10}I_A}$. Results of the tests, not reported here for the sake of brevity, indicate that the null hypothesis of normality cannot be rejected, assuming a 0.05 significance level, for the logarithms of all the parameters considered.

The results of the regression are slightly different from those obtained by Sabetta and Pugliese (1996), but these discrepancies are expected. Despite the work of Sabetta and Pugliese (1996), it was decided to not constrain c to the *geometrical spreading* theoretical value in any of the regressions, because data

²¹ These, still consistent with Sabetta and Pugliese (1996), may be considered small with respect to more recent GMPs. In fact, Bindi et al. (2009) calibrated a new model for Italy with the same functional form, on the new Italian Accelerometric Archive (ITACA) in which estimated standard deviations are larger. However, this does not affect scope of this study, that is, illustrating the concept of conditional hazard maps.

seem to not support such a choice (see also Stafford et al., 2009). Moreover, moment magnitude was used herein, while local magnitude and surface-wave magnitude were used by the mentioned researchers. In addition to that, the records used come from different databases and therefore may have been subjected to different processing. Finally, Sabetta and Pugliese (1996) used the component featuring the largest value of the parameter of interest separately for each regression, while in this study all the regression analyses were performed, arbitrarily, using the horizontal component featuring the largest PGA. To fit all GMPEs for PGA, PGV and I_A on the same ground motion component is useful for deriving directly a model for I_D . In fact, in order to obtain a GMPE for the logarithms of I_D as a function of M , R and local site conditions, it is possible to derive its coefficients as linear combinations of those for $\log_{10}PGA$, $\log_{10}PGV$ and $\log_{10}I_A$ as the logarithm of I_D is given by the logarithm of I_A minus the logarithms of PGA and PGV. This leads to the expression of Equation (3), in which subscripts 1, 2 and 3 refer to PGA, PGV and I_A , respectively.

$$\log_{10}I_D = a + bM + \log_{10}\left(\frac{(R^2 + h_1^2)^{c_1}(R^2 + h_2^2)^{c_2}}{(R^2 + h_3^2)^{c_3}}\right)^{\frac{1}{2}} + dS_1 + eS_2 + \varepsilon_{\log_{10}I_D} \quad (3)$$

The coefficients of Equation (3) are listed in Table 11 and Table 12 for the two distance metrics considered. For I_D , the magnitude coefficient (b) and the soil coefficients (d) and (e) resulted close to zero²²; a statistical test could be performed to check the statistical significance of these coefficients.

²² It may sound odd that an intensity measure is insensitive to magnitude, however from Equation (1) it emerges that I_D is an integral intensity measure (numerator) normalized by peak measures (denominator); in fact, it has proven to be well correlated with the *equivalent number of cycles* of a SDOF, which is a structure response measure made of hysteretic energy divided by a quantity related to the peak response (Manfredi, 2001); i.e., an engineering demand parameter normalized by peak response. In the following, however, the dependence of I_D on M has been kept in symbols for completeness.

Table 11. Regression coefficients for I_D (R_{epi}).

| Y | a | b | c_1 | c_2 | c_3 | d | e | $\sigma_{\log_{10} Y}$ |
|-------|------|--------|-------|-------|-------|---------|---------|------------------------|
| I_D | 0.58 | 0.034* | 0.89 | 0.95 | 1.69 | -0.068* | 0.0077* | 0.19 |

Table 12. Regression coefficients for I_D (R_{jb}).

| Y | a | b | c_1 | c_2 | c_3 | d | e | $\sigma_{\log_{10} Y}$ |
|-------|------|--------|-------|-------|-------|---------|---------|------------------------|
| I_D | 0.35 | 0.039* | 0.87 | 0.91 | 1.50 | -0.039* | 0.0082* | 0.19 |

The normal distribution of I_D (i.e., of the residual of the GMPE) should follow from the normality of the logarithm of PGA, PGV and I_A . Nevertheless, normality of the above parameters was based on a hypothesis test, therefore it may be prudent to also test the normality of the logarithm of I_D . So, the normality of the residual of Equation (3) was tested and such a hypothesis could not be rejected at 0.05 significance level.

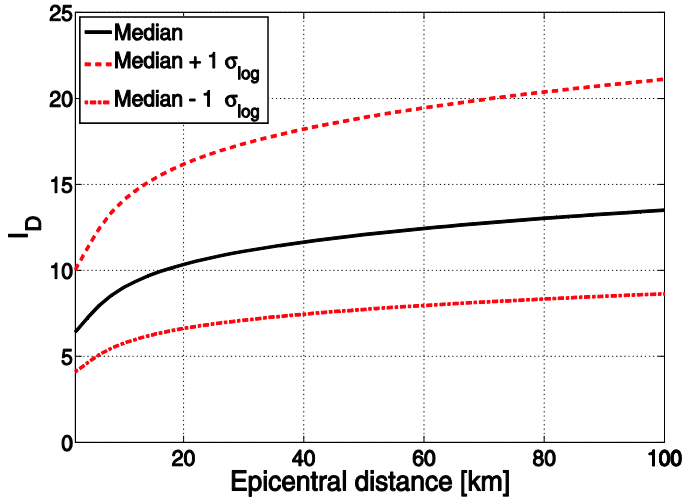


Figure 17. Plot of I_D as a function of epicentral distance.

A plot of I_D versus epicentral distance is given in Figure 17, where the typical increasing trend with distance of duration-related measures is shown (Manfredi et al., 2003).

3.3 Joint normality and conditional distributions of the logarithms of I_D and PGA

As this study aims to investigate the joint and conditional distributions of PGA and I_D , the joint normality of logarithms of the pair was tested. In fact, if the vector above can be considered normally distributed, all the possible marginal and conditional distributions obtained from the joint distribution are still Gaussian. The skewness and kurtosis' tests were used to test multivariate normality of the vector made of $\epsilon_{\log_{10}PGA}$ and $\epsilon_{\log_{10}I_D}$. Results of the Mardia's (1985) bivariate normality tests are given in Table 13 and Table 14. With a given significance level of 0.05, the multivariate skewness and kurtosis result as non-significant.

The residuals of the prediction relationships for the logarithms of PGA and I_D have been also tested for correlation in order to compute $f(\log_{10}I_D | \log_{10}PGA)$, that is, the conditional PDF of the logarithms of I_D given the logarithms of PGA. The estimated correlation coefficient (r) between $\epsilon_{\log_{10}PGA}$ and $\epsilon_{\log_{10}I_D}$ (equal to -0.25 considering R_{epi}) has been tested via a *T-test* assuming as the null hypothesis $H_0: \rho = 0$ (ρ is the "true" correlation coefficient), which has been rejected at 0.05 significance level. Then, the joint distribution of $\log_{10}I_D$ and $\log_{10}PGA$ may be defined by the bivariate normal PDF of Equation (4).

$$f(\log_{10}I_D, \log_{10}PG | M, R) = \tag{4}$$

$$= \frac{1}{2(1-\rho^2)} \left[\frac{(\log_{10}I_D - \mu_{\log_{10}I_D|M,R})^2}{\sigma_{\log_{10}I_D}^2} - \frac{2\rho(\log_{10}I_D - \mu_{\log_{10}I_D|M,R})(\log_{10}PGA - \mu_{\log_{10}PGA|M,R})}{\sigma_{\log_{10}I_D} \sigma_{\log_{10}PGA}} + \frac{(\log_{10}PGA - \mu_{\log_{10}PGA|M,R})^2}{\sigma_{\log_{10}PGA}^2} \right]$$

$$\frac{2\pi\sigma_{\log_{10}I_D} \sigma_{\log_{10}PGA} \sqrt{(1-\rho^2)}}{e}$$

In Equation (4) $\mu_{\log_{10}I_D|M,R}$ and $\sigma_{\log_{10}I_D}$ are the mean and the standard deviation of $\log_{10}I_D$ respectively; i.e., Equation (3). $\mu_{\log_{10}PGA|M,R}$ and $\sigma_{\log_{10}PGA}$ are the mean and the standard deviation of $\log_{10}PGA$ respectively; i.e., Equation (2). The covariance matrix, Σ , for $\epsilon_{\log_{10}PGA}$ and $\epsilon_{\log_{10}I_D}$ is reported in Equation (5), for R_{epi} .

$$\Sigma = \begin{pmatrix} \sigma_{\log_{10}PGA}^2 & \rho\sigma_{\log_{10}PGA}\sigma_{\log_{10}I_D} \\ \rho\sigma_{\log_{10}PGA}\sigma_{\log_{10}I_D} & \sigma_{\log_{10}I_D}^2 \end{pmatrix} = \begin{pmatrix} 0.036 & -0.009 \\ -0.009 & 0.036 \end{pmatrix} \quad (5)$$

Table 13. Tests for joint normality of the logarithms of PGA and I_D (R_{epi}).

| | <i>Mardia's test of skewness</i> | <i>Mardia's test of kurtosis</i> |
|--|----------------------------------|----------------------------------|
| <i>Test statistic</i> | 2.21 | -0.86 |
| <i>Critical value at 0.05 significance level</i> | 9.49 | ± 1.65 |

Table 14. Tests for joint normality of the logarithms of PGA and I_D (R_b).

| | <i>Mardia's test of skewness</i> | <i>Mardia's test of kurtosis</i> |
|--|----------------------------------|----------------------------------|
| <i>Test statistic</i> | 0.94 | -0.94 |
| <i>Critical value at 0.05 significance level</i> | 9.49 | ± 1.65 |

Figure 18a shows an example of joint distribution of I_D and PGA for a M 7 event and for a site characterized by an epicentral distance of 50 km. Figure 18b shows the contours of the joint distribution of I_D and PGA for different magnitude values (for a site at epicentral distance equal to 50 km). From Figure 18b, it is evident that projecting on the I_D axis the bivariate distribution contours, a similar shape of the marginal distributions is obtained regardless of the magnitude values, which reflects the fact that the marginal I_D distribution appears to be very weakly dependent on magnitude.

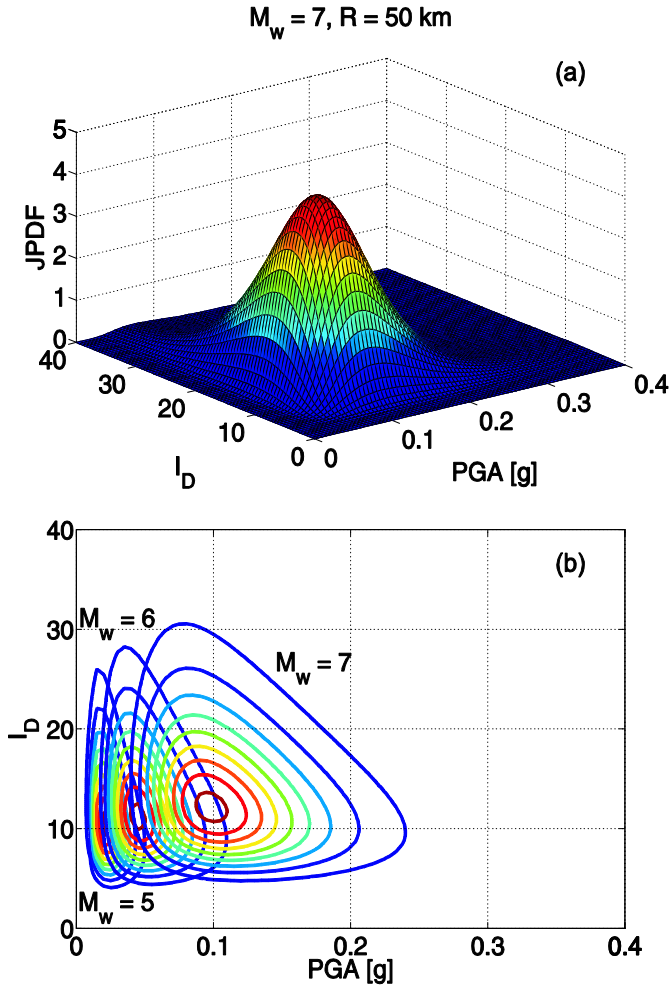


Figure 18. (a) Example of joint distribution of PGA and I_D for an M 7 event and for a site at 50 km from the source in terms of epicentral distance. (b) Contours of joint distribution of PGA and I_D for different M values (R_{epi} = 50 km).

Because of bivariate normality, the conditional PDF for one of the variables given a known value of the other, is normally distributed. The conditional mean ($\mu_{\log_{10} I_D | \log_{10} PGA, M, R}$) and standard deviation of $\log_{10} I_D$ ($\sigma_{\log_{10} I_D | \log_{10} PGA}$), given $\log_{10} PGA = z$, are reported in Equation (6).

$$\left\{ \begin{array}{l} \mu_{\log_{10}I_D | \log_{10}PGA, M, R} = \mu_{\log_{10}I_D | M, R} + \rho \sigma_{\log_{10}I_D} \frac{z - \mu_{\log_{10}PGA | M, R}}{\sigma_{\log_{10}PGA}} \\ \sigma_{\log_{10}I_D | \log_{10}PGA} = \sigma_{\log_{10}I_D} \sqrt{1 - \rho^2} \end{array} \right. \quad (6)$$

Because the joint distribution of I_D and PGA depends on the I_D and PGA GMPEs, and therefore also on magnitude and distance, to obtain the conditional distribution of the logarithms of I_D conditional on PGA only, the marginalization in Equation (7) is required.

$$\begin{aligned} f(\log_{10}I_D | \log_{10}PGA) = \\ = \iint_{M, R} f(\log_{10}I_D | \log_{10}PGA, M, R) f(M, R | \log_{10}PGA) dm dr \end{aligned} \quad (7)$$

It is easy to recognize that the $f(M, R | \log_{10}PGA)$ term in Equation (7) is the PDF of M and R given the occurrence of $\log_{10}PGA$; i.e., the result of disaggregation of seismic hazard (e.g., Bazzurro and Cornell, 1999). As an approximation of the integral in Equation 7, for example, the modal values, M^* and R^* (i.e., those corresponding to the maxima of the joint M and R distribution from disaggregation), may be plugged in Equation (6); i.e., Equation (8).

$$\mu_{\log_{10}I_D | \log_{10}PGA, M, R} \approx \mu_{\log_{10}I_D | M^*, R^*} + \rho \sigma_{\log_{10}I_D} \frac{z - \mu_{\log_{10}PGA | M^*, R^*}}{\sigma_{\log_{10}PGA}} \quad (8)$$

3.4 Illustrative application

An example of the possible use of the results obtained is given in Figure 19 and Figure 20. Figure 19b shows the PGA values on rock (expressed in fractions of g) with a 10% exceedance probability in 50 years (return period, T_R ,

equal to 475 years) in the Campania region according to the classical seismic hazard analysis procedure (see for example Convertito et al., 2009). This map was computed discretizing the region in a regular grid of nodes with spacing of about 2 km (2700 points in total).

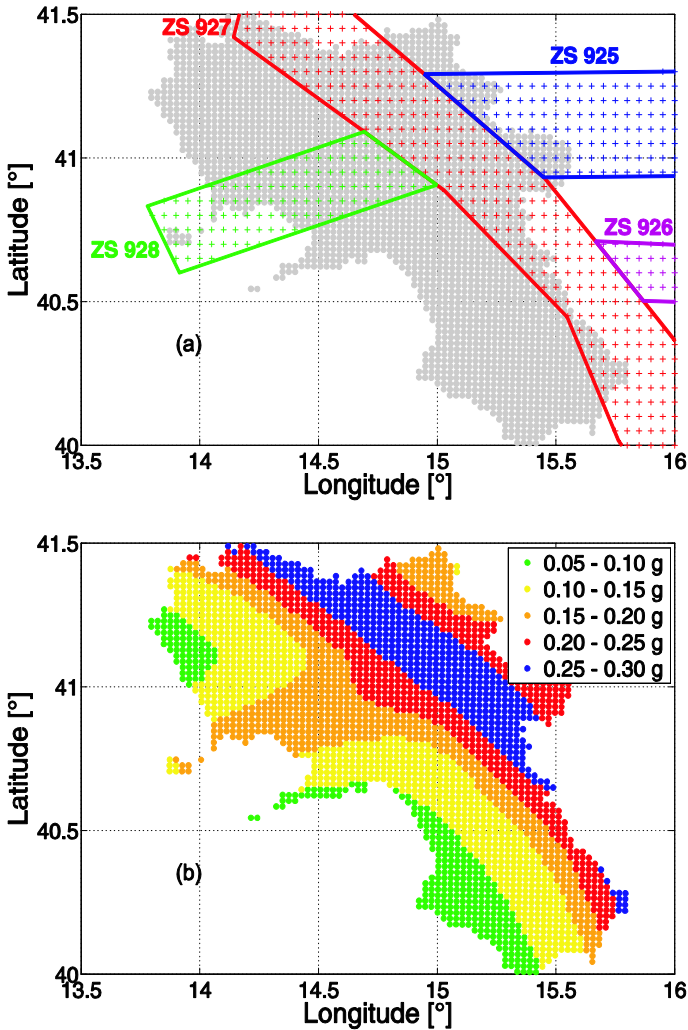


Figure 19. (a) Seismic zones considered in the analysis; (b) 475 years return period PGA on rock hazard map for the Campania region (southern Italy).

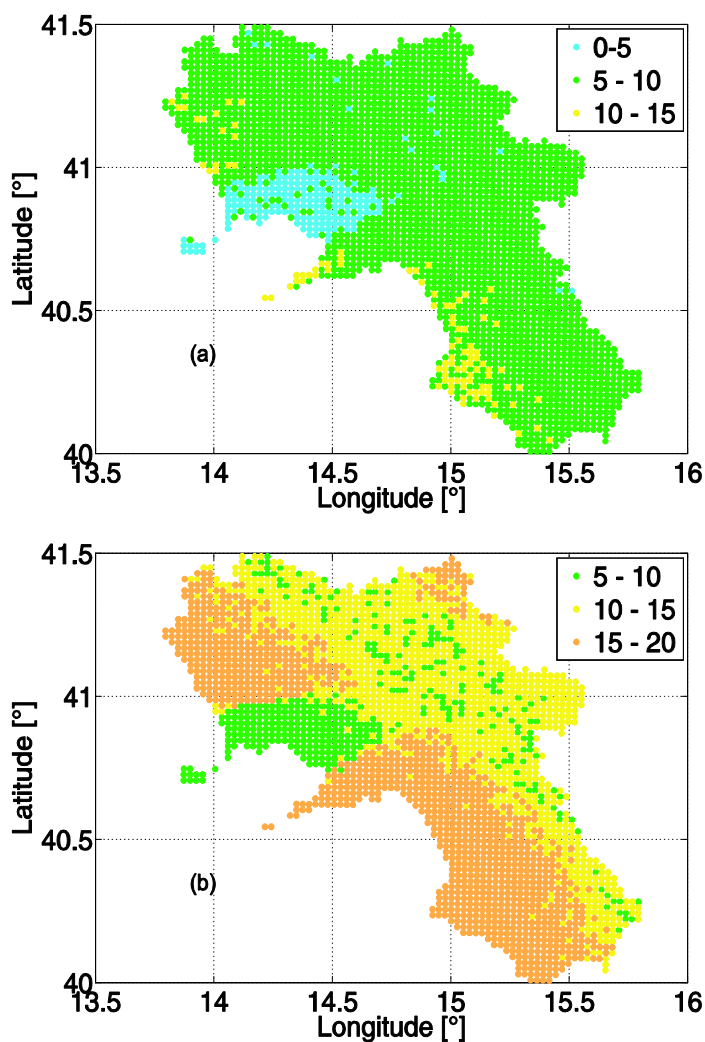


Figure 20. (a) Hazard map in term of I_D with a 50% exceedance probability given PGA of panel 19b; (d) hazard map in terms of I_D with a 10% exceedance probability given PGA of panel 19b.

Sources were modeled as the seismogenic zones of Figure 19a (Meletti et al., 2008) which have been used to compute the official Italian hazard data produced by the Istituto Nazionale di Geofisica e Vulcanologia or INGV (available at <http://esse1.mi.ingv.it/>). Because of the use of seismogenic zones, GMPEs in terms of R_{epi} were used in hazard analysis. Source features,

from Barani et al. (2009), are given in Table 15 where α is the seismicity rate, that is, the mean annual rate of occurrence of the earthquakes between M_{\min} and M_{\max} for the zone, and b is the corresponding parameter of the Gutenberg-Richter equation.

Table 15. Parameters of the selected seismogenic zones shown in Figure 4a.

| Zone | α [events/year] | b | M_{\min} | M_{\max} |
|------|------------------------|-------|------------|------------|
| 925 | 0.071 | 0.508 | 4.3 | 7.0 |
| 926 | 0.061 | 1.017 | 4.3 | 5.8 |
| 927 | 0.362 | 0.557 | 4.3 | 7.3 |
| 928 | 0.054 | 1.056 | 4.3 | 5.8 |

Figure 20a and Figure 20b show the maps of seismic hazard in terms of I_D given the PGA of Figure 19b. In particular, Figure 20a and Figure 20b are the 50th and 90th percentiles of the conditional I_D PDF, respectively. The conditional I_D maps were obtained using the distribution of parameters in Equation (6) in which z (logarithms of PGA) values are those from Figure 19b, while the values of magnitude and distance (M^* and R^*) to plug in the $\mu_{\log_{10}PGA|M,R}$ and $\mu_{\log_{10}I_D|M,R}$ terms of Equation (6) were obtained by disaggregation of hazard in terms of occurrence of design PGA values (Figure 21). The adopted disaggregation methodology is the same described in Convertito et al. (2009).

As a site-specific example, Figure 22 represent the complementary cumulative density functions of I_D conditional on PGA for the sites of S. Angelo dei Lombardi (latitude: 40.8931°, longitude: 15.1784°) and Ponticelli (latitude: 40.8516°, longitude: 14.3446°) in the Campania region. These two sites have been selected based on the fact that S. Angelo dei Lombardi is located in the epicentral area of the 23 November 1980 Irpinia earthquake, and Ponticelli is the construction site of one of the largest seismically isolated structures in Europe (Di Sarno et al, 2006). The five chosen scenarios, in terms of M and R (Table 16), refer to the mean values obtained from disaggregation of seismic hazard for PGA for different probabilities of occurrence in 50 years (corresponding to five values of T_R , from 30 to 2475 years). The curves of

Figure 22 give information on the values of I_D probabilistically consistent with respect to the hazard in terms of PGA at the site.

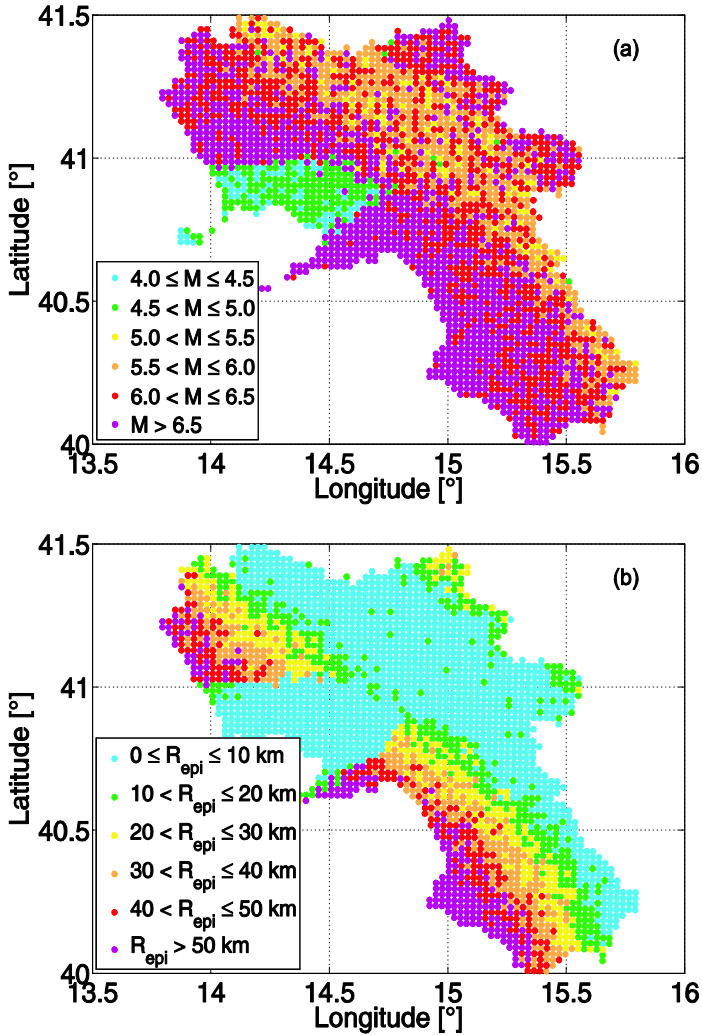


Figure 21. Modal values of magnitude and epicentral distance from disaggregation of seismic hazard in terms of PGA given in Figure 19b and used to compute the conditional distribution of I_D whose percentiles are in Figure 20a and Figure 21b.

Table 16. Considered scenarios for S. Angelo dei Lombardi and Ponticelli.

| T_R [years] | Sant' Angelo dei Lombardi | | | Ponticelli | | |
|---------------|---------------------------|------------|-----------|------------|------------|-----------|
| | M^* | R^* [km] | PGA [g] | M^* | R^* [km] | PGA [g] |
| 2475 | 6.4 | 5.8 | 0.51 | 5.0 | 5.1 | 0.28 |
| 475 | 6.0 | 8.4 | 0.26 | 5.0 | 9.9 | 0.17 |
| 140 | 5.8 | 12.5 | 0.14 | 5.2 | 18.8 | 0.10 |
| 72 | 5.7 | 16.1 | 0.10 | 5.3 | 27.3 | 0.073 |
| 30 | 5.5 | 23.7 | 0.060 | 5.4 | 42.6 | 0.046 |

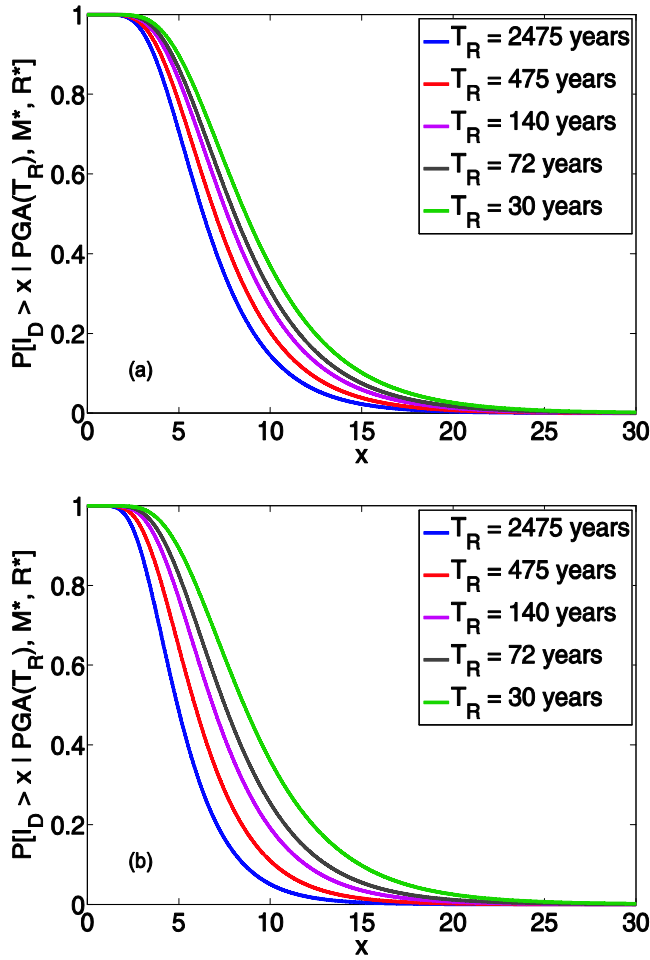


Figure 22. Probability of exceedance of I_D given PGA for five scenarios for S. Angelo dei Lombardi (a) and Ponticelli (b).

3.5 Conclusions

There are situations in which more than one ground motion parameter has to be taken into account in seismic structural assessment. For example, although it is generally believed that integral ground-motion parameters are secondary for structural demand assessment with respect to peak quantities of ground motion, sometimes the cumulative damage potential of the earthquake is also of concern. For these cases it could be useful to have a distribution of secondary intensity measures conditional on the primary parameter used to define the seismic action on structures (e.g., accelerations). Such distribution can complement the hazard curves or maps produced for the primary IM. This approach has the advantages of vector-valued seismic hazard analysis without the computational effort required by PSHA for vectors of IMs. To explore such a concept, in this chapter the distribution of a parameter which may account for the cumulative damage potential of ground-motion, conditional to peak ground acceleration (PGA), was investigated. The chosen secondary measure is the so called Cosenza and Manfredi index (I_D). A ground motion prediction relationship has been derived for the logarithm of I_D on the basis of an empirical dataset of Italian records already used for well known prediction equations proposed in the past by other researchers. Subsequently, the residuals of prediction relationships have been tested for correlation and for joint normality. The study allowed the obtaining of analytical distributions of I_D conditional on PGA and the corresponding design earthquake in terms of magnitude and distance from hazard disaggregation. Results of the study have been used to compute the distribution of I_D conditional on PGA with a return period of 475 years for each node of a regular grid having about 2 km spacing and covering the territory of the Campania region in southern Italy. The presented conditional hazard maps provide information on the values of I_D which, for example, should be taken into account along with the hazard in terms of PGA at the site, for ground motion record selection for nonlinear dynamic analysis of structures.

Data and resources

For the purposes of the present study, the ground motions and related information were obtained by the *European Strong-motion Database* (ESD), whose URL is <http://www.isesd.cv.ic.ac.uk> (Ambraseys et al., 2000; Ambraseys et al., 2004).

References

Ambraseys, N., Smit, P., Berardi, R., Rinaldis, D., Cotton, F., Berge C. (2000). Dissemination of European Strong-motion Data (Cd-Rom Collection). European Commission, DGXII, Science, Research and Development, Bruxelles.

Ambraseys, N.N., Douglas, J., Rinaldis, D., Berge-Thierry, C., Suhadolc, P., Costa, G., Sigbjornsson, R., Smit, P. (2004). Dissemination of European Strong-motion Data. Vol. 2, Cd-Rom Collection, Engineering and Physical Sciences Research Council, United Kingdom.

Baker, J.W. (2007). Probabilistic structural response assessment using vector-valued intensity measures. *Earthquake Engineering and Structural Dynamics*, 363, 1861-1883.

Barani, S., Spallarossa, D., Bazzurro, P. (2009). Disaggregation of Probabilistic Ground-Motion Hazard in Italy. *Bulletin of the Seismological Society of America*, 99, 2638-2661.

Bazzurro, P., and Cornell, C.A. (1999). Disaggregation of seismic hazard. *Bulletin of the Seismological Society of America*. 89, 501-520.

Bindi, D., Luzi, L., Pacor, F., Sabetta, F., Massa, M. (2009). Towards a new reference ground motion prediction equation for Italy: update of the Sabetta-Pugliese (1996). *Bulletin of Earthquake Engineering*, 7, 591-608.

Convertito, V., Iervolino, I., Herrero, A. (2009). The importance of mapping the design earthquake: insights for southern Italy. *Bulletin of the Seismological Society of America*, 99, 2979–2991.

Di Sarno, L., Cosenza, E., De Risi, B., Mascolo, C. (2006). Application of base isolation to a new building of Naples. *Proc. of 4th WCSCM - World Conference on Structural Control and Monitoring*, San Diego, Paper no. 173.

Hancock, J., Bommer, J.J. (2006). A state-of-knowledge review of the influence of strong-motion duration on structural damage. *Earthquake Spectra* 22, 827–845.

Iervolino, I., and Cornell, C.A. (2005). Record selection for nonlinear seismic analysis of structures. *Earthquake Spectra*, 21, 685-713.

Iervolino, I., Maddaloni, G., Cosenza, E. (2008a). Eurocode 8 compliant real record sets for seismic analysis of structures. *Journal of Earthquake Engineering*, 12, 54-90.

Iervolino, I., Giorgio, M., Galasso, C., Manfredi, G. (2008b). Prediction relationships for a vector-valued ground motion intensity measure accounting for cumulative damage potential, *Proc. of 14th WCEE - World Conference on Earthquake Engineering*, Beijing, China.

Iervolino, I., Manfredi G., Cosenza, E. (2006) Ground-motion duration effects on nonlinear seismic response. *Earthquake Engineering and Structural Dynamics*, 35, 21-38.

Joyner, W.B., Boore, D.M. (1993). Methods for regression analysis of strong-motion data. *Bulletin of the Seismological Society of America*, 83, 469-487.

Manfredi, G., Polese, M., Cosenza, E. (2003). Cumulative demand of the earthquake ground motions in the near source. *Earthquake Engineering and Structural Dynamics*, 32, 1853-1865.

Manfredi, G. (2001), Evaluation of seismic energy demand. *Earthquake Engineering and Structural Dynamics*, 30, 485-499.

Mardia, K.V. (1985). Mardia's test of multinormality. In *Encyclopedia of Statistical Sciences*, S. Kotz and N.L. Johnson eds., 5, 217-221.

Meletti, C., Galadini F., Valensise, G., Stucchi, M., Basili, R., Barba, S., Vannucci, G., Boschi, E. (2008). A seismic source zone model for the seismic hazard assessment of the Italian territory. *Tectonophysics*, 450, 85-108.

Mood, M.A., Graybill, F.A., Boes, D.C. (1974). *Introduction to the Theory of Statistics* (3rd edition). McGraw-Hill Companies, New York.

Sabetta, F., Pugliese, A. (1996). Estimation of response spectra and simulation of nonstationarity earthquake ground-motion. *Bulletin of the Seismological Society of America*, 86, 337-352.

Sabetta, F., Pugliese, A. (1987). Attenuation of peak horizontal acceleration and velocity from Italian strong-motion records. *Bulletin of the Seismological Society of America*, 77, 1491-1513.

Shapiro, S.S., Wilk, M.B. (1965). An analysis of variance test for normality (complete samples). *Biometrika*, 52, 591-611.

Stafford, P.J., Berrill, J.B., Pettinga, J.R. (2009). New predictive equations for Arias intensity from crustal earthquakes in New Zealand. *Journal of Seismology*, 13, 31-52.

Chapter 4

Including research advances into practice: REXEL

ABSTRACT

In code-based seismic design and assessment it is often allowed the use of real records as an input for nonlinear dynamic analysis. On the other hand, international seismic guidelines, concerning this issue, have been found hardly applicable by practitioners. This is related to both the difficulty in rationally relating the ground motions to the hazard at the site and the required selection criteria, which do not favor the use of real records, but rather various types of spectrum matching signals. To overcome some of these obstacles a software tool for code-based real records selection was developed. REXEL, freely available at the website of the Italian network of earthquake engineering university labs (<http://www.reluis.it>), allows to search for suites of waveforms, currently from the European Strong-motion Database and the Italian ACcelerometric Archive, compatible to target spectra being either user-defined or automatically generated according to Eurocode 8 and the recently released new Italian seismic code. The selection reflects the provisions of the considered codes and others found to be important by recent research on the topic. In the chapter, record selection criteria are briefly reviewed first, and then the algorithms implemented in the software are discussed. Finally, via some examples, it is shown how REXEL can effectively be a contribution to code-based real records selection for seismic structural analysis.

4.1 Introduction

As widely discussed in the previous chapters, one of the key issues in nonlinear dynamic analysis of structures is the selection of appropriate seismic input, which should allow for an accurate estimation of the seismic

performance based on the seismic hazard at the site where the structures is located.

If the probabilistic risk assessment of structures is concerned, procedures have been recently developed to properly select the seismic input. The basic steps are: (i) choosing a ground motion (GM) parameter which is considered to be representative of the earthquake potential with respect to the specific structure (i.e., a GM intensity measure, or IM²³); (ii) to obtain the probabilistic seismic hazard analysis (PSHA) at the site, and disaggregation, for the chosen IM; (iii) to determine probability of collapse in terms of one or more engineering (structural) demand parameters, or EDPs, as a function of the IM (i.e., the fragility function); (iv) to average the fragility over the hazard to obtain the overall failure probability; i.e., the seismic risk (Cornell, 2004).

Consistently with the load-resistance factor design (LRFD), code-based procedures apparently approximate this procedure in a semi-deterministic fashion (Iervolino and Manfredi, 2008). They often require to define a design (target) spectrum whose ordinates have a small probability of exceedance²⁴. Secondly, a scenario event or design earthquake has to be defined referring to the local seismicity (although the link of the design spectrum with the hazard at the site may be very weak). Then, in the case of nonlinear dynamic analysis, codes basically require a certain number of records to be chosen consistently with the design earthquake and the code spectrum in a broad range of periods. Finally, the performance of the structure is assessed verifying whether the maximum or average response of the structure to the records exceeds the seismic capacity.

Studies show how the most of practitioners may experience difficulties in handling code-based record selection, first of all because determining the design earthquakes may require hazard data often not readily available to

²³ For various reasons, one of the main being that hazard is easily computable, the IM is often related to the response spectrum of the record; e.g., the peak ground acceleration or PGA, and the spectral acceleration at the first mode, or some function of the spectral shape in a range of period of interest.

²⁴ This is, in principle, analogous to choosing a conservative value of the action in the LRFD in which actions are amplified and the capacity is reduced on a probabilistic basis.

engineers, or, when these are provided by authorities (e.g., in Italy), it may still require seismological skills beyond their education (see sections 2 and 3). Furthermore, if real records are concerned, to find a suite matching a design spectrum in a broad sense, may be hard or practically unfeasible if appropriate tools are not available (Beyer and Bommer, 2007; Iervolino et al., 2008; Iervolino et al., 2009). These issues traditionally favored the use of spectrum matching accelerograms, either artificial or obtained through manipulation of real records. On the other hand, real records are the best representation of seismic loading for structural assessment and design, motivating attempts to develop tools for computer aided code-based record selection, one of which being that of Naeim et al. (2004).

In this direction, a computer software, REXEL, was developed and freely distributed over the internet. REXEL allows to build design spectra according to Eurocode 8 (EC8) (CEN, 2003), the new Italian seismic code (NIBC) (CS.LL.PP., 2008), or completely user-defined, and to search for sets of 7 or 30 groups²⁵ of records, from the European Strong-motion Database (or ESD) or the Italian ACcelerometric Archive (or ITACA). These sets are compatible to the reference (i.e., target) spectra with respect to codes' provisions, but reflect also some research-based criteria considered relevant for seismic structural assessment. Automatic tools for seismic hazard disaggregation (for PGA and 1s spectral acceleration) and conditional hazard computation for earthquake's cumulative damage potential expressed in terms of *Cosenza and Manfredi index* (Chapter 3) are also developed and embedded in REXEL.

REXEL searches for sets of records for a various range of structural applications (building-like and non-building-like structures, isolated buildings, bridges, tall structures, industrial facilities, etc.) and seems to actually make the selection fast and effective in the most of cases. In the following, the procedures concerning determination of seismic action and record selection, according to EC8 and the NIBC, are briefly reviewed along with the findings of

²⁵ In the case of set of 7, each group may be made of 1, 2 or 3 component GMs; in the case of set of 30, each group may be made of 1 or 2 horizontal component GMs. Individual record search may also be performed.

other studies on the topic. Then, the software's algorithms are described; the use of REXEL is illustrated via some examples which show how it can effectively aid code-based record selection for seismic structural analysis.

4.2 Record selection in EC8

4.2.1 EC8 Part 1 - Buildings

In EC8 - Part 1 (CEN, 2003) the seismic action on structures is defined after the elastic acceleration response spectrum. In Part 1, which applies to buildings, the spectral shapes are given for both horizontal and vertical components of motion. In *section*²⁶ 3.2.2 of the code two spectral shapes, *Type 1* and *Type 2*, are defined, the latter applying if the earthquake contributing most to the seismic hazard has surface wave magnitude not greater than 5.5, otherwise the former should be used. All shapes have a functional form which depends, apart from the soil class, on a single value, a_g , anchoring the spectrum to the seismicity of the site. a_g refers to the seismic classification of the territory in each country; it is basically related to the hazard in terms of peak ground acceleration (PGA) on rock for the site (see section A.1 in the Appendix A).

Once the target spectrum has been defined, EC8 - Part 1 allows the use of any form of accelerograms for structural assessment; i.e., real, artificial or obtained by simulation of seismic source, propagation and site effects. To comply with Part 1 the set of accelerograms, regardless its type, should basically match the following criteria:

- a) a minimum of 3 accelerograms should be used;*

²⁶ References to sections and verbatim quotations of codes are given in *Italic* hereinafter.

- b) *the mean of the zero period spectral response acceleration values (calculated from the individual time histories) should not be smaller than the value of $a_g S$ for the site in question (S is the soil factor);*

- c) *in the range of periods between $0.2T_1$ and $2T_1$, where T_1 is the fundamental period of the structure in the direction where the accelerogram will be applied, no value of the mean 5% damping elastic spectrum, calculated from all time histories, should be less than 90% of the corresponding value of the 5% damping elastic response spectrum.*

According to the code, in the case of spatial structures, the seismic motion shall consist of three simultaneously acting accelerograms representing the three spatial components of the shaking, then 3 of condition (a) means 3 times the number of translational components of motion to be used (e.g., 3 groups of motion each of those includes the two horizontal and the vertical recordings).

In *section 4.3.3.4.3*, the code allows the consideration of the mean effects on the structure, rather than the maxima, if at least seven nonlinear time-history analyses are performed. Moreover, the vertical component of the seismic action should be taken into account only for base-isolated structures, and for some special cases in regular buildings, if the design vertical acceleration for the A-type site class (a_{vg}) is greater than 0.25g. Finally, some provisions regarding duration are given for artificial accelerograms, while real or simulated records should be *adequately qualified with regard to the seismogenetic features of the sources and to the soil conditions appropriate to the site.*

4.2.2 EC8 Part 2 – Bridges

EC8 – Part 2 (CEN, 2005) refers to the same spectral shapes of Part 1 in order to define the seismic input for time-history analysis of bridges. The requirements for the horizontal components are somehow similar to those for buildings but not identical. The relevant points are:

- a) *for each earthquake consisting of a pair of horizontal motions, the SRSS spectrum shall be established by taking the square root of the sum of squares of the 5% -damped spectra of each component;*
- b) *the spectrum of the ensemble of earthquakes shall be formed by taking the average value of the SRSS spectra of the individual earthquakes of the previous step;*
- c) *the ensemble spectrum shall be scaled so that it is not lower than 1.3 times the 5% damped elastic response spectrum of the design seismic action, in the period range between $0.2T_1$ and $1.5T_1$, where T_1 is the natural period of the fundamental mode of the structure in the case of a ductile bridge.*

As Part 1, Part 2 also allows the consideration of the mean effects on the structure when non-linear dynamic analysis is performed for at least seven independent GMs and the vertical action has to be considered in special cases only. Part 2 has specific provisions for near-source conditions and cases in which the spatial variability of GM has to be considered.

4.2.3 Findings of previous investigations about record selection in EC8

In other studies the actual applicability of EC8 provisions about record selection were investigated. In particular, in Iervolino et al. (2008) it was investigated whether it is possible to find unscaled real record sets fulfilling, as much as possible, the requirements of EC8 – Part 1. The investigations were based on the former Italian classification in seismic zones now superseded by the new seismic code (see following section), but still adopted in similar forms in many countries.

Combinations were found in ESD, for sites featuring moderate-to-low seismicity, while it was not possible to find suitable results for the more severe design spectra. Moreover, the condition of having unscaled record sets strictly matching EC8 spectra resulted in a large record-to-record variability in the spectral ordinates within the same set. Both shortage of compatible sets for the

severe spectra and large individual spectra scatter, could be avoided searching for records with a spectral shape as similar as possible to that of the code (after rendering the spectra non-dimensional dividing their ordinates by the PGA). Nevertheless, this implies amplitude scaling in the time domain (amplitude scaling, or simply scaling, hereinafter) of the records, and may lead to large scaling factors.

As a general conclusion it was found that provisions do not easily allow to select suitable real record sets, factually favoring the use of records obtained either by computer techniques or manipulation of real records to have a spectral shape coincident to that of the target in a broad range of periods. This is mainly because:

1. it is almost unfeasible for practitioners to search in large databases to find suites of seven real records (eventually multi-component) whose average matches closely the design spectral shape without a specific software tool;
2. the spectra based on seismic zonation may be too severe in a way that do not exist suites of unscaled records whose average has such spectral shape;
3. it is not easy to control the variability (very large) of individual spectra in a combination, and this, in the fortunate case combinations are found, may impair the confidence in the estimation of the seismic performance using such a set;
4. the requirement of selecting records consistent with the earthquake events dominating the hazard at the site (i.e., the design earthquakes) requires PSHA/disaggregation data and skills seldom available to practitioners;

In Iervolino et al. (2009) a similar study concerning EC8 - Part 2 was carried out. It was found that, although seemingly different, the requirements of the two part of the code are substantially equivalent and lead to similar results in terms of combinations found (i.e., combinations complying with Part 2 are likely to comply also with provisions of Part 1) and limitation of applicability to real records. As discussed in the following, more advanced codes (i.e., NIBC) and/or tools as REXEL may help to overcome, in the most of cases, the issues 1 to 4 above.

4.3 Seismic input according to NIBC

EC8 has design spectra related to the seismicity via only one parameter, this is also because of the unavailability of detailed country-wide hazard analysis results in most European countries. In other fortunate cases such as Italy, the building code (CS.LL.PP., 2008) links the seismic design actions on structures directly to the PSHA. In fact, the *Istituto Nazionale di Geofisica e Vulcanologia* (INGV) evaluated probabilistic seismic hazard for each node of a regular grid having 5km spacing and covering the whole Italian territory with over 10^3 nodes. This resulted in hazard curves in terms of PGA (also disaggregation is provided for PGA) and spectral acceleration, $S_a(T)$, for 10 different periods from 0.1 to 2 seconds. Hazard curves are lumped in 9 probabilities of exceedance in 50 years (from 2% to 81%). All data can be accessed at <http://esse1-gis.mi.ingv.it> (see also Montaldo et al., 2007).

NIBC acknowledges these data defining completely site-dependent design spectra which, although given with standard (EC8-like) functional form, practically coincide with uniform hazard spectra (UHS) on rock for the site in question. The exceedance probability the UHS has to refer to depends on the limit state of interest, the type and the nominal life of the structure. In case the soil is not rock/stiff (the classification is the same as EC8) coefficients apply to amplify the spectrum accordingly, see section A.2 in the Appendix A.

As per EC8, the signals can be artificial, simulated and natural accelerograms. Three is still the minimum number of records to use, and seven allows the consideration of the mean effects on the structure as design value (rather than the maxima).

For the artificial records also the main condition the set of records should satisfy is the same as per EC8. The average elastic spectrum has not to underestimate the 5% damping elastic code spectrum, with a 10% tolerance, in the larger range of period between $[0.15s, 2s]$ and $[0.15s, 2T_1]$. This condition applies to ultimate limit states, while for serviceability limit states the largest of the two ranges $[0.15s, 2s]$ and $[0.15s, 1.5T_1]$ has to be considered. For seismically isolated structures the code provides, reasonably, a narrower range for the average matching, i.e., $[0.15s, 1.2T_{is}]$, where T_{is} is the equivalent period of the isolated structure.

Real records or accelerograms generated through a physical simulation of earthquake process, may be used, provided that, again as in EC8, *the samples used are adequately qualified with regard to the seismogenetic features of the source and the soil conditions appropriate to the site*. Selected real records have to be scaled to approximate somehow the elastic response spectrum in a range of period of interest for the structure.

These statements allow for some arbitrariness in record selection, which may be considered positive as they enable, in principle, to determine the source parameters dominating the hazard at the site (i.e., the design earthquakes) by, for example, disaggregation of seismic hazard; then, the records may be scaled to match the target spectrum at the period corresponding to the first mode of the structure, which is the current best practice in record selection and manipulation (Iervolino and Manfredi, 2008). However, even in the fortunate Italian case, where the hazard data are available for any given site, the features of the source and GM at the site from disaggregation (e.g., magnitude, distance, and epsilon) are not always available to practitioners. In fact, INGV provides disaggregation values for peak acceleration only, while it is now acknowledged that the disaggregation should be performed for those ranges of the response spectrum more relevant

for the behavior of the structure, for example, close to the fundamental period; see Convertito et al. (2009) for a discussion. On the other hand, some studies (e.g. Chapter 2) have shown that in most of the cases some of the variables dominating the hazard and recommended for consideration by codes (i.e., magnitude and distance) may be not particularly relevant for a correct estimation of the structural response if the spectral shape is the parameter driving record selection (Iervolino and Cornell, 2005).

NIBC accounts for these considerations about record selection and required input information. In fact, the instructions for code application allow, as an alternative, in the case of real accelerograms, record selection procedures which apply to artificial record; i.e., average spectral compatibility in a period range. As an additional feature it is recommended to choose, if possible, records having spectral shape similar to that of the code. In this case one can avoid to reflect explicitly specific source parameters in selection (i.e., to not reflect specific design earthquakes). If this implies amplitude scaling of the records, it is also specified that the scale factor is to be limited in the case of signals from events of small magnitude (CS.LL.PP., 2009).

4.4 REXEL

To enable record selection according to both approaches of EC8 and NIBC, a specific software tool was developed (Figure 23). It features a MATHWORKS-MATLAB® graphic user interface (GUI) and a FORTRAN engine, based on the software developed for the studies of Iervolino et al. (2008 and 2009). In particular, the computer program was developed to search for individual record or combinations of seven²⁷ or thirty accelerograms compatible in the average with the target spectra according to code criteria discussed above. It is also possible to reflect in selection the characteristics of

²⁷ Seven has to be intended as the size of the set which may include 1-component, 2-components, or 3-components records, which means 7, 14 or 21 waveforms respectively. In the case of 30-records search, sets may include only 1- or 2-horizontal components.

the source (if available) and site, in terms of magnitude (M), epicentral distance (R), and EC8 soil site classification or other ground motion IMs, i.e., horizontal PGA, horizontal peak ground velocity (PGV), horizontal-components *Arias intensity* (I_A) or horizontal-components *Cosenza and Manfredi index* (I_D). REXEL (now at version 3.1 beta), freely available on the internet at the website of the Italian consortium of earthquake engineering laboratories (*Rete dei Laboratori Universitari di Ingegneria Sismica - ReLUIS*; <http://www.reluis.it>), currently contains the accelerograms belonging to the ESD (<http://www.isesd.cv.ic.ac.uk/>; last accessed July 2007) (Ambraseys et al., 2000 and 2004) and to ITACA (<http://itaca.mi.ingv.it>; last accessed October 2010).

The procedure implemented for record selection deploys in 4 basic steps:

1. definition of the design (target) horizontal and/or vertical spectra the set of records has to match on average; the spectra can be built according to EC8, NIBC, or user-defined;
2. list and plot of the records contained in the chosen database (ESD or ITACA) and embedded in REXEL which fall into the magnitude and distance bins specified by the user (or into the specified range for another chosen ground motion parameter) for a specific site class or for any site class;
3. assigning the period range where the average spectrum of the set has to be compatible with the target spectrum, and specification of tolerances in compatibility;
4. running the search for individual record or combinations of seven or thirty records which include one, two or, only in the case of seven records search, all three components of motion and that, on average, match the design spectrum with parameters specified in step 3.

Other functions are related to visualization of results, return of selected waveforms to the user, and secondary options. In the following descriptions of fundamental phases 1 to 4 are given, although for a more complete user guide one should refer to the REXEL tutorial (Iervolino and Galasso, 2009).

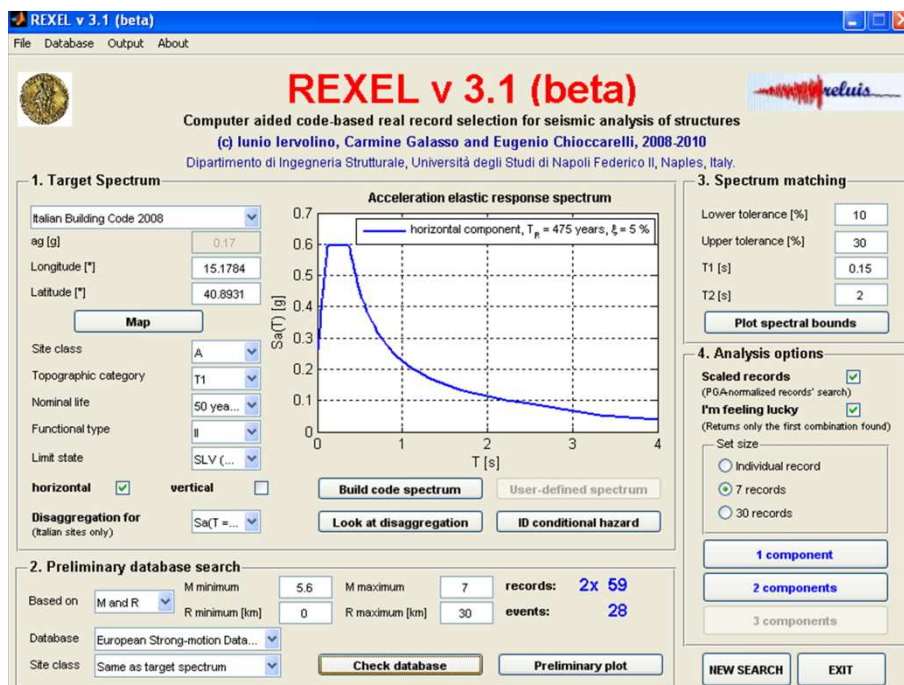


Figure 23. Image of the software GUI.

4.4.1 Target (design) spectrum

To build the elastic acceleration response spectrum for the site of interest three options are available in REXEL: (1) NIBC; (2) EC8 (*Type 1* or *Type 2* spectra); and (3) user-defined spectral shape.

In case (1) it is necessary to enter the geographical coordinates of the site (applicable to Italy only), *longitude* and *latitude* in decimal degrees, and to specify the *Site Class* (A, B, C, D or E of EC8), the *Topographic Category*, *Nominal Life* of the structure, *Functional Type* of the structure and the *Limit State* of interest (these are required by the code to define the return period of the

seismic action, see Appendix A again). Then the software automatically generates the spectrum accordingly.

In case (2), it is necessary to specify only the anchoring value of the spectrum, a_g , and the site class. The value of a_g can be defined manually by the user or, in the case of sites on the Italian territory, can be obtained automatically from the geographical coordinates of the site.

In both cases (1) and (2), if the spectrum is to be obtained automatically after geographical coordinates, the software has built-in the official hazard data of the NIBC (derived from the INGV study).

In case (3) the spectral acceleration ordinates corresponding to 122 periods between 0s and 4s (i.e., the same format of ESD spectra) have to be entered by the user.

Finally, it is necessary to specify the component of the spectrum to consider; i.e., horizontal and/or vertical. The two orthogonal independent components that describe the horizontal motion (X and Y) are characterized by the same elastic response spectrum as per the considered codes, while the component that describes the vertical motion (Z) is characterized by a specific spectrum. It is possible to select X/Y and Z separately or contemporarily, depending on the number of components of GM (1, 2 or 3) desired to be included in the set.

Looking at disaggregation

As discussed in the Chapter 1, disaggregation is a procedure which allows to identify, from a probabilistic point of view, the contribution to the hazard of each couple of magnitude M and R . As discussed, these contributions are dependent on hazard assessment of the site, spectral ordinates and return period. REXEL provides disaggregation results for each Italian site for two spectral ordinates, i.e. 0 second (PGA) and 1.0 second (the latter is chosen thinking to medium-long period structures) and for four return periods, i.e. 50 years, 475 years, 975 years and 2475 years. For all different return periods, REXEL provides automatically results corresponding to the

closer return period. Using disaggregation results provided by REXEL, the following points have to be considered:

1. Official Italian hazard data and disaggregation results (only for PGA) are provided by INGV and are available at the web site <http://esse1-gis.mi.ingv.it>. Disaggregation results provided by REXEL refer to a specific independent study.
2. Parameters of disaggregation analyses have been fitted for the whole Italian region and results have been considered generally reliable even if in site with low seismicity, hazard evaluation (a preliminary step for disaggregation analysis) can be wrong because the software is not able to capture hazard differences with return period. As consequence, also disaggregation results do not vary with return period and a particular attention has to be used. REXEL shows a warning for all these cases.
3. Disaggregation plots provide by REXEL suggest the best intervals of magnitude and distance for record selection but records' availability is not insured. Moreover the choice of the right intervals is up to users.

For further details and any technical aspect about disaggregation analysis refer to Chioccarelli et al., 2010 and Convertito et al., 2009.

Looking at I_D conditional hazard

As widely discussed in the Chapters 2 and 3, acceleration-based IMs, e.g., spectral ordinates, have been shown to be important and useful in the assessment of structural response of buildings. However, there are cases in which it is desirable to account for other ground motion IMs, while selecting records. For example, although it is generally believed that, under some hypotheses, integral IMs associated to duration are less important for structural demand assessment with respect to peak quantities of ground

motion, there are cases in which the cumulative damage potential of the earthquake is also of concern.

An easy yet hazard-consistent way of including secondary IMs in record selection is represented by the *conditional hazard curves* (or maps, see Chapter 3); i.e., curves of secondary ground motion intensity measures conditional, in a probabilistic sense, to the design hazard for the primary parameter.

REXEL includes the *Cosenza and Manfredi index* (I_D) conditional hazard results (see Chapter 3 again), suggesting to the user the distribution (in terms of complementary cumulative density functions) of I_D value (for Italian sites only) given the design PGA (i.e. the anchoring value of the target spectrum). This should allow for improving record input selection for earthquake engineering applications in a hazard consistent manner yet easily viable for practitioners.

4.4.2 Preliminary database search

REXEL, has built in the records (in terms of three components corrected acceleration waveforms and 5% damping spectra) belonging to ESD and ITACA. All the records contained in REXEL satisfies the free-field conditions and were produced by earthquakes of magnitude larger than 4²⁸ (any faulting style). No restrictions were applied with respect to the processing of the records, the effect of which at least on spectral displacements, was investigated by Akkar and Bommer (2006). REXEL provides distributions of the embedded records (Figure 24).

ESD and ITACA have records in common although with different seismological processing. There was no attempt to homogenize/combine the two databases, which are separated in the software. Moreover, the two databases cover different magnitude and distance ranges, therefore the

²⁸ The EC8 *Type 1* spectra apply if the event of interest has surface wave magnitude larger than 5.5 (see APPENDIX A). Therefore, in the case of selection according to EC8 *Type 1* spectrum, the user can limit the magnitude to be above the threshold (see following section); alternatively he can include records from lower magnitude events.

appropriate database to use in searches may also depend on which range of magnitude and distance one is interested in.

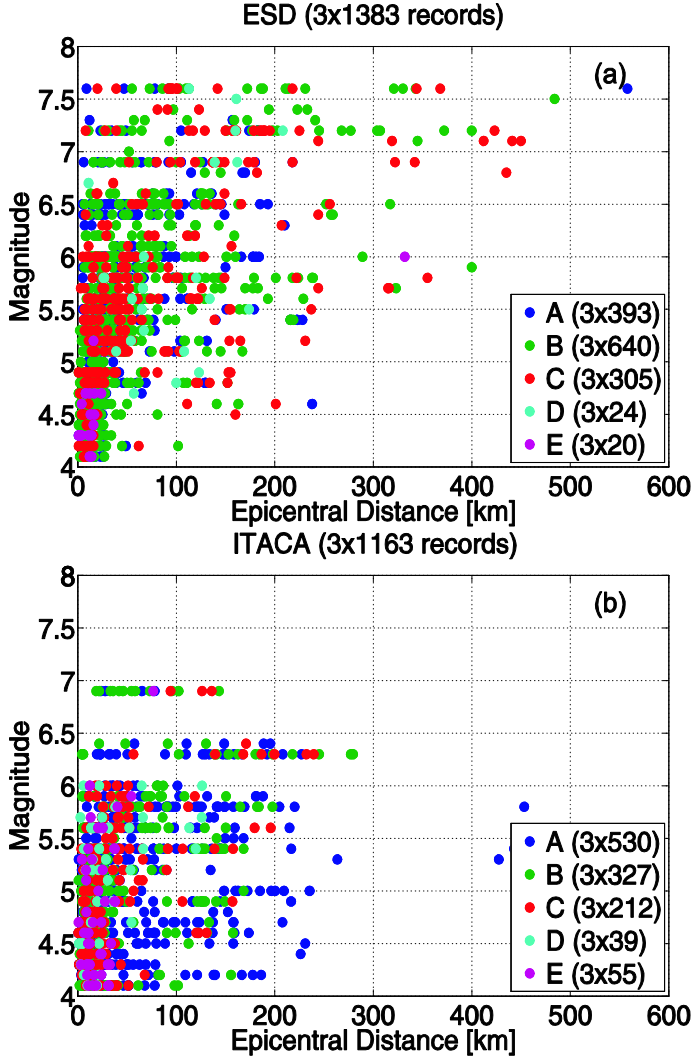


Figure 24. Magnitude (M_W only for ESD, M_W or M_L for ITACA) vs epicentral distance distribution for the ESD (a) and ITACA (b) records featured in REXEL. The records are grouped by site class according to EC8 classification²⁹.

²⁹ ITACA stations soil classification (according to Eurocode 8) refers to the results of the S4 project (<http://esse4.mi.ingv.it>), task 2 "Catalogazione geologico-geotecnica dei siti di ITACA".

A parameter that is desirable to include in record selection is the site classification, affecting both the amplitude and shape of response spectra. However, specifying a close match for this parameter in record selection may not always be feasible, because for some soft soils, only a few records are usually available. Moreover, if the spectral shape is assigned by the code, the site class of real records may be of secondary importance (see for example Chapter 2) and there may be cases in which it may be useful to relax the matching criteria for site classification.

In light of these considerations, in REXEL it is possible to select records from *same as target spectrum* soil (i.e., the soil type is decided in step 1 while defining the spectrum, and this choice automatically limits the search of the combinations to the records belonging to this specific site class) or from *any site class*. This, should help to overcome some of the problems when for specific site conditions it is hard to find spectrum matching sets.

Moreover, the user can choose to search for combinations coming from specific M and R ranges³⁰ or, alternatively, from a specific range of a selected ground motion parameters. More specifically, the user may select the records of database corresponding to a given range of PGA of horizontal components of motion, in fraction of g (the acceleration of gravity), peak ground velocity (PGV) of horizontal components of motion, in m/s, *Cosenza and Manfredi index* (I_D) (e.g. this choice may be guided by conditional hazard tool, see step 1) of horizontal components of motion and, finally, *Arias Intensity* (I_A) of horizontal components of motion, in m/s. To this aim, the user must specify the intervals [min, max] of the ground motion parameter of interest in which he wants the accelerograms fall and the database of interest.

The classification is based on 1:100000 geological map, except for those stations where $V_{s,30}$ was available; classification maybe updated in the future.

³⁰ It is always moment magnitude (M_W) for ESD, except for soil E where M is expressed in terms of local magnitude (M_L), as M_W was not available in ESD. For ITACA, it is M_W or M_L , based on availability in the database. R is always (for both ESD and ITACA) the distance from the epicenter of the event because fault distance (the only alternative measure of distance given in the database) was available for part of the records only. However in those cases where the latter is also available it is provided by REXEL.

The selection based on M and R may prove useful if data about the events of interest are available, for example from disaggregation of seismic hazard (provided by REXEL for Italian sites only), and it is consistent with code criteria which require to select records taking care of the seismogenetic features of the source of the design earthquake. In this case, the user can specify the magnitude and distance intervals, $[M_{\min}, M_{\max}]$ and $[R_{\min}, R_{\max}]$, in which the records to be searched have to fall.

After these bounds are defined, the software returns the number of records (and the corresponding number of originating events) available in the intervals. This list constitutes the inventory of records in which to search for suites of seven which are in the average compatible with the code spectra of step 1. These spectra may also be plotted along with the target spectrum to have a picture of the spectra REXEL will search among.

4.4.3 Spectrum matching parameters and analysis options

In this step the parameters related to the spectral compatibility are defined. In which period range, $[T_1, T_2]$, the target spectrum has to be matched has to be defined first. T_1 and T_2 can be any pair in the 0s - 4s range. Secondly, the tolerances allowed in spectral matching are required. This means the user has to specify the tolerated deviations (*lower* and *upper* limits) in percentage terms, the average spectrum of the combination can have with respect to the target in the specified period range. EC8, for example, explicitly states that the average elastic spectrum must not underestimate the code spectrum, with a 10% tolerance (lower limit) but does not provide any indication about the upper limit. It is economically viable to reduce as much as possible the overestimation of the spectrum, and this is why also an upper limit was introduced in REXEL.

In this phase it is also possible to select the *Scaled records* option, which corresponds to choose whether to search for *unscaled* or *scaled* record sets. In fact, REXEL allows to obtain combinations of accelerograms whose average is, in the desired period range, above the target spectrum times the lower bound

tolerance and below the target spectrum times the upper bound tolerance, being not manipulated (original records), but it also allows choosing sets of accelerograms compatible with the target spectrum if linearly scaled in amplitude. If this second option is chosen, the user has to check the *Scaled records* box, which means the spectra of the list defined in step 2 are preliminarily normalized dividing the spectral ordinates by their PGA. Combinations of these spectra are compared to the non-dimensional target spectrum³¹. If this option is selected, it is also possible to specify the maximum mean scale factor (SF) allowed; REXEL will discard combinations with an average SF larger than what desired by the user.

The user can also select the option *I'm feeling lucky* in order to stop the analysis after the first compatible combination is found. This option, in the most of cases, allows to immediately get a single combination compatible with the target spectrum, otherwise, the search may take a very long time (as warned by the software, which computes the number of combinations of 7 or 30 to be investigated if a certain number of records preliminarily is selected in the database³²). Alternatively, the *maximum number of compatible combinations to find* after which the search has to stop, can be specified.

4.4.4 Combinations search

At this point the initial list of records and the analysis parameters are set and it is possible to decide which kind of search to perform. The software searches for

- individual records, matching the target spectrum in the specified range of periods and with the provided upper- and lower-bound tolerances;

³¹ This, as already demonstrated in Iervolino et al. (2008 and 2009) allows to have combinations whose spectra are similar to target spectrum, then reducing the record-to-record spectral variability within a set, which is a desirable feature if one has to estimate the seismic demand on the basis of 7 analyses only.

³² This is given by the binomial coefficient; for example if 100 records are selected, the maximum number of combinations of 7 which have to be checked for spectral compatibility are about 16 billions.

or combinations of:

- 7 or 30 1-component accelerograms whose average matches the target spectrum in the specified range of periods and with the provided upper- and lower-bound tolerances. The found combinations can be applied in one direction for plane analysis of structures³³;
- 7 or 30 pairs of accelerograms. This option allows to search for 14 (60) records which are 7 (30) 2-components recordings [both X and Y components of 7 (30) recording stations only], which on average³⁴ are compatible with the target spectrum; this kind of search is for cases in which horizontal motion has to be applied in both directions of a 3D structure;
- 7 groups of accelerograms which include the two horizontal and the vertical component of seven recordings (i.e., 21 records which are the X, Y and Z components of 7 recording stations only) for full 3D analysis. In this case, the selection proceeds in two sub-steps: first, the combinations compatible with the horizontal component of the code spectrum are found, exactly as in the previous case (7 2-components search); then, the software analyzes the vertical components of only those horizontal combinations which have been found to be compatible with the code spectrum, and verifies if the set of their seven vertical components is also compatible with the vertical code spectrum. The tolerances and period ranges for average vertical spectral matching may be different from those

³³ Note that this option applies alternatively to horizontal or vertical components of motion, although it is unlikely one is looking for a suites of seven vertical accelerograms only.

³⁴ The average is taken on the 14 (or 60) records all together as found appropriate in Iervolino et al. (2008) for EC8 – Part 1. This is not perfectly consistent with provisions of EC8 – Part 2, which require the average to be taken to the seven SRSS spectra; nevertheless, the two procedures were found to be equivalent to some extent in Iervolino et al. (2009).

regarding horizontal components and may be defined by the user after the horizontal analysis has finished.

An important feature of REXEL is that the list of records out of step 2, which is an input for this phase, are ordered, when the analysis is launched, in ascending order of the parameter defined in Equation (1), which gives a measure of how much the spectrum of an individual record deviates from the target spectrum. In Equation (1), $Sa_j(T_i)$ is the pseudo-acceleration ordinate of the real spectrum j corresponding to the period T_i , while $Sa_{target}(T_i)$ is the value of the spectral ordinate of the target spectrum at the same period, and N is the number of spectral ordinates within the considered range of periods.

$$\delta = \sqrt{\frac{1}{N} \sum_{i=1}^N \frac{Sa_j(T_i) - Sa_{target}(T_i)}{Sa_{target}(T_i)}} \quad (1)$$

Preliminary ordering allows to analyze first the records which have a similar spectral shape with respect to the target. This ensures the first combinations (e.g., the one found with the *I'm feeling lucky* option) to be those with the smallest individual scattering in respect to the target spectrum, as shown in the following examples. This is an important point although codes, generally, don't ask to control this individual spectral variability, only requiring to control the average spectrum of the combination. On the other hand, large individual variability may affect the accuracy of the estimation of the structural performance if a limited number of records (e.g., 7) is employed (Cornell, 2004). Moreover, this also enables to have individual records in the combination with a spectral shape as much as possible similar to that of the target spectrum. This is consistent with the current research on the topic, which considers the spectral shape as the most important proxy for earthquake damage potential on structures, more than event parameters as M and R .

4.4.5 Post-analysis

After the analysis has finished, REXEL returns a list of combinations whose average spectrum respects compatibility with the target in the chosen range of periods and with the assigned tolerances. The results of the analysis are sorted so that the combinations with the smallest deviation from the spectrum of the code are at the beginning of the output list, due to the preliminary ordering of records according to δ . Combinations returned are uniquely identified by a serial number; this code can be used to display the spectra of a specific combination of interest and obtain the acceleration time-histories (and the corresponding elastic spectra with a text file summarizing the selection criteria) grouped in a compressed file. Each record is identified by the 8 characters filename whose initial 6 digits are the waveform ID associated to records in the ESD or in ITACA³⁵, while the last two may correspond to *xa*, *ya*, and *za* indicating the component of the recording: X, Y and Z respectively.

If a specific combination is chosen REXEL also returns the mean value of M and R and the other ground motion parameters of the combination and the information about the individual records as retrieved by the databases that is, recording station, event (time, date and country), M, R, fault mechanism, etc. In the case of scaled records sets, the scale factors of the individual records and the mean scale factor of the combination are given. For all the combinations found, it is possible to calculate the deviation of each accelerogram, and the deviation of the average spectrum from the target elastic response spectrum. In this latter case Equation (1) is still used, replacing $Sa_j(T_i)$ with the average spectral acceleration of the combination.

Different 2 and Different 3 options

Although both considered codes only require a minimum size for GM suites of 7 in order to consider mean effects on the structure, it is known how

³⁵ Actual ITACA waveforms codes have a total length of 33 characters, containing several information (see Chapter 4); nevertheless, in REXEL simplified codes were used (see RELUIS website for a table of matching between ITACA records and the accelerograms IDs in REXEL).

this number may affect the confidence (i.e., the standard error) in the estimation of the structural response, which increases as the variability of individual records with respect to the target increases. Therefore, in the case one wants to run the analyses with a larger number of records, REXEL has two further options (beyond the 30-records search) which both are applicable to the list of results of the analyses discussed in the previous section:

Different 2 allows to search within the list of output, pairs of combinations (i.e., 2 sets of 7 records) which have accelerograms from earthquake events which do not overlap. This allows to have a larger set of 14 one- or multi-component records, spectrum matching in the average, in which there are no dominating events. For each found pair of sets the software also computes the maximum deviation δ_i of the individual records in the two original combinations and this may be a parameter for choosing one pair with respect to another;

Different 3 allows to search within the list of output, triplets of combinations (3 of 7 one- or multi-component records) having no accelerograms in common although may have common events. This analysis provides sets of 21 records which, still, fulfill the code-required average spectral compatibility with the given tolerances.

Repeat search excluding a station.

In some cases, the analyst may want to exclude a particular record appearing in a found combination. To this aim, REXEL includes the option *Repeat search excluding a station*, which allows to repeat the performed analysis by excluding from the list of records created in the *Preliminary database search* (i.e. from the list of accelerograms returned in step 2) one or more waveforms, in an iterative way.

Displacement spectra compatibility.

REXEL allows to check the displacement spectra compatibility for a combination selected to match a pseudo-acceleration spectrum. For each period T , the elastic spectral displacement is computed as inverse transformation of elastic pseudo-spectral acceleration.

The examples below illustrate the developed tool capabilities and how it, in many cases, allows for a rational and fast selection of seismic input for code-based nonlinear dynamic analysis of structures. For the sake of brevity, all the examples refers to search in ESD database.

A simplified version of REXEL, named REXELite was also developed and it operates online on ITACA since January 2010. In Chapter 5, via some illustrative examples it is shown how factually REXELite easily allow for a rational record selection in ITACA for earthquake engineering applications.

4.5 Illustrative applications

4.5.1 Selection according to NIBC

As an example let's consider selection of 7-horizontal accelerograms according to NIBC for the life safety limit state of an ordinary structure (Functional class II, see section A.1 in the Appendix A) on soil type A with a nominal life of 50 years (which corresponds to design for a 475 years return period according to the code) and located in Sant'Angelo dei Lombardi (15.1784° longitude, 40.8931° latitude). Setting the coordinates of the site and the other parameters to define the seismic action according to NIBC, the software automatically builds the elastic design spectrum. Consider also that selection should reflect disaggregation of $S_a(T=1s)$ hazard³⁶ on rock with a 10%

³⁶ Note that it is often recommended to consider as design earthquakes the results of hazard disaggregation for the spectral ordinates in the range of interest for the nonlinear structural behavior. This may differ from disaggregation of PGA hazard, especially when M and R joint distribution has multiple modal values (Convertito et al., 2009).

probability of exceedance in 50 years Figure 25) at the site, which may be easily obtained by REXEL tools for disaggregation. Specifying the M and R intervals to [5.6, 7] and [0km, 30km] respectively, REXEL finds 177 records (59×3 components of motion) from 28 earthquakes, whose horizontal spectra, unscaled and scaled, are given in Figure 26, which the software automatically returns. REXEL will search among these spectra.

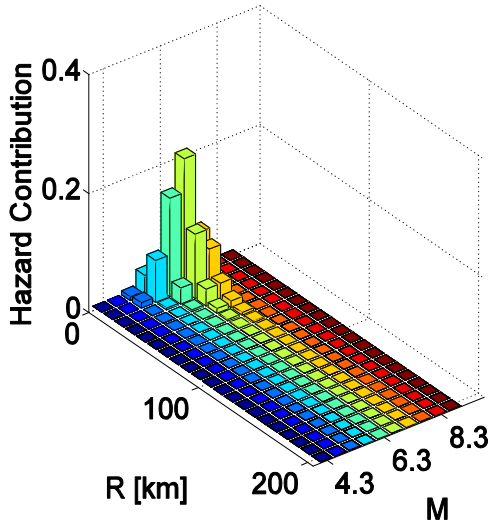


Figure 25. Disaggregation of the $S_a(T=1s)$ with 475 years return period on rock for Sant'Angelo dei Lombardi.

Assigning, as tolerances for the average spectral matching, 10% lower and 20% upper in the period range $0.15s \div 2s$ and selecting the option to stop the search after the first combination is found (i.e., *I'm feeling lucky*), REXEL immediately returns the combinations of 7-accelerograms in Figure 27a if the 1-component search is performed. In the figure, which the software automatically plots, thick solid lines are the average of the set and the code spectrum, while the dashed are the tolerance and period range bounds where compatibility is ensured. Solid thin lines are the seven individual spectra of the combination. In the legend the ESD station and component IDs, along with the earthquake IDs, are given. Selecting the search for set of seven pairs of

horizontal components (e.g., for the analysis of spatial structures), instead, the software returns the 14 records of Figure 27b. Note that in this case the records are 7 pairs of X and Y components of 7 stations only. In Table 17 and Table 18 the data about the two combinations³⁷ are given as they are returned by REXEL.

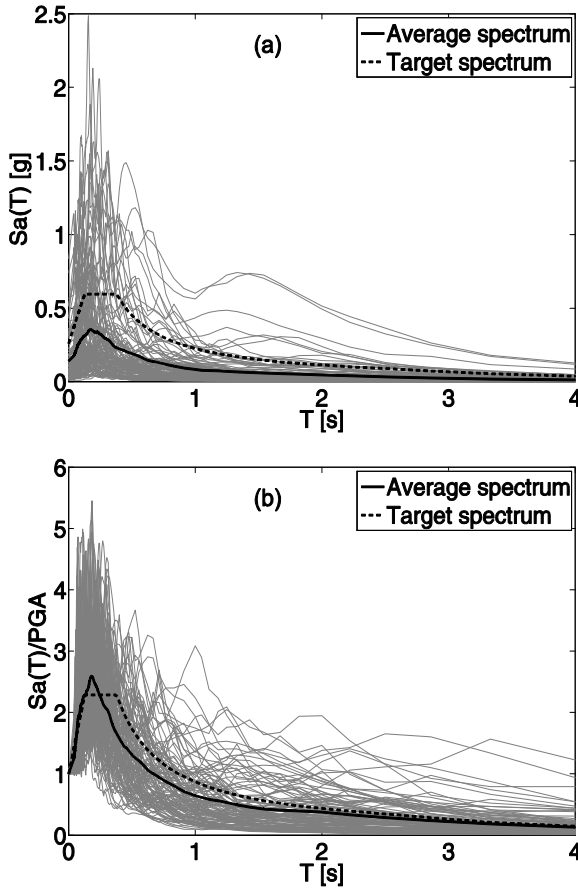


Figure 26. Plot of the spectra found in the ESD for the selected M and R bins in the case of site class A.

³⁷ Data about combinations are not given for the subsequent examples for the sake of brevity, nevertheless they can be easily obtained by the reader from the information in the legend of the figures.

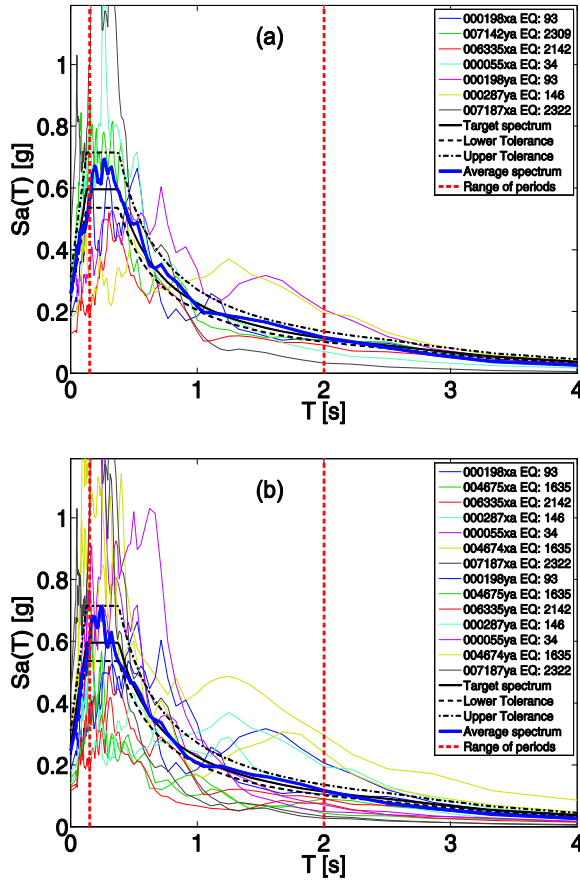


Figure 27. Unscaled combinations found for the assigned example in Sant'Angelo dei Lombardi using the *I'm feeling lucky* option in the case of horizontal 1-component (a) and 2-components (b) GMs.

It is claimed in the description of the software that the first combination has a low scatter with respect to subsequent combinations eventually found. This may be shown, for example, not selecting the *I'm feeling lucky* option and limiting the maximum number of combinations to 1000 and repeating the same two searches above. Then, REXEL returns, in about one minute with a standard personal computer, 1000 1-component compatible combinations, and in a few minutes, 520 combinations featuring both the two horizontal components of motion. Figure 28a and Figure 28b show the last

Chapter 4

Including research advances into practice: REXEL

combination (no. 1000 and no. 520 respectively) of the output list in the two cases.

Table 17. Essential record data returned by REXEL for the combination of Figure 27a.

| <i>Record ID</i> | <i>Event ID</i> | <i>Earthquake Name</i> | <i>Date</i> | <i>M</i> | <i>Fault Mechanism</i> | <i>R [km]</i> |
|------------------|-----------------|------------------------|-------------|----------|------------------------|---------------|
| 000198xa | 93 | Montenegro | 15/04/1979 | 6.9 | thrust | 21 |
| 007142ya | 2309 | Bingol | 01/05/2003 | 6.3 | strike slip | 14 |
| 006335xa | 2142 | South Iceland (aft.) | 21/06/2000 | 6.4 | strike slip | 15 |
| 000055xa | 34 | Friuli | 06/05/1976 | 6.5 | thrust | 23 |
| 000198ya | 93 | Montenegro | 15/04/1979 | 6.9 | thrust | 21 |
| 000287ya | 146 | Campano Lucano | 23/11/1980 | 6.9 | normal | 23 |
| 007187xa | 2322 | Avej | 22/06/2002 | 6.5 | thrust | 28 |

Table 18. Essential record data returned by REXEL for the combination of Figure 27b.

| <i>Station ID</i> | <i>Event ID</i> | <i>Earthquake Name</i> | <i>Date</i> | <i>M</i> | <i>Fault Mechanism</i> | <i>R [km]</i> |
|-------------------|-----------------|------------------------|-------------|----------|------------------------|---------------|
| 000198 | 93 | Montenegro | 15/04/1979 | 6.9 | thrust | 21 |
| 004675 | 1635 | South Iceland | 17/06/2000 | 6.5 | strike slip | 13 |
| 006335 | 2142 | South Iceland (aft.) | 21/06/2000 | 6.4 | strike slip | 15 |
| 000287 | 146 | Campano Lucano | 23/11/1980 | 6.9 | normal | 23 |
| 000055 | 34 | Friuli | 06/05/1976 | 6.5 | thrust | 23 |
| 004674 | 1635 | South Iceland | 17/06/2000 | 6.5 | strike slip | 5 |
| 007187 | 2322 | Avej | 22/06/2002 | 6.5 | thrust | 28 |

Although all average spectra of Figure 27 and Figure 28 match with similar good approximation the code spectrum, it is evident that the preliminary ordering of accelerograms according to δ enables the high ranking combinations to have individual spectra with a smaller dispersion with respect to the target spectrum.

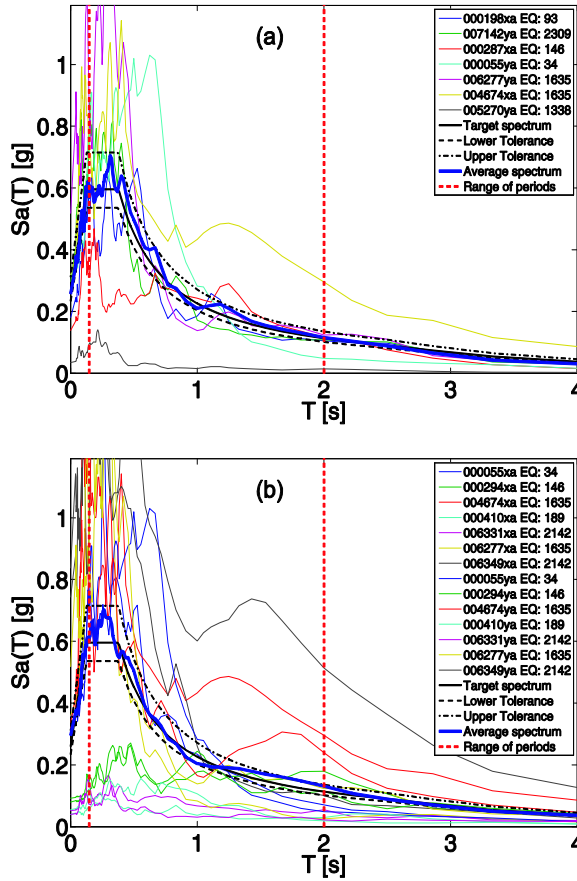


Figure 28. Last of 1000 and 520 unscaled combinations found for the assigned example in Sant’Angelo dei Lombardi in the case of horizontal 1-component (a) and 2-components (b) GMs.

Nevertheless, the presented results show that the deviation of the individual spectra compared with the target can still be large (e.g., Figure 27b). To reduce the scatter of individual records further, the *Scaled records* option can be used, which means that records found have to be linearly scaled to be spectrum matching in the average. In this case, repeating the search for Sant’Angelo dei Lombardi simply considering accelerograms with $M \geq 6$ and R within $0\text{km} \div 25\text{km}$, with the same compatibility criteria as per the previous case and using the option *I’m feeling lucky*, REXEL returns immediately

combinations shown in Figure 29a and Figure 29b, which feature records less scattering with respect to those unscaled of Figure 27. In this case, the individual scale factors are given in the legend. Note also that the code asks for the maximum value the average scale factor (SF_{mean}) can assume, which in this case was limited to 2.

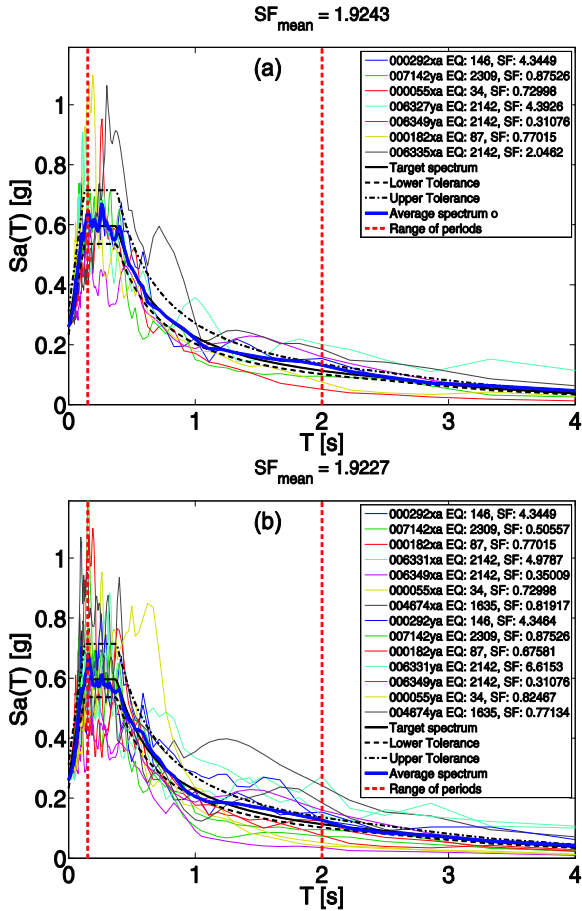


Figure 29. Scaled combinations found for the assigned example in Sant'Angelo dei Lombardi using the *I'm feeling lucky* option in the case of horizontal 1-component (a) and 2-components (b) GMs.

Search that includes the vertical component of seismic motion

REXEL allows selecting combinations of 7-accelerograms that include the vertical component of the records, although NIBC and EC8 require to account for it only in peculiar cases. Considering again the same example in Sant'Angelo Lombardi, and specifying as the M and R intervals as [6, 7.8] and [0km, 50km] respectively, REXEL founds 58 groups of accelerograms from 23 events.

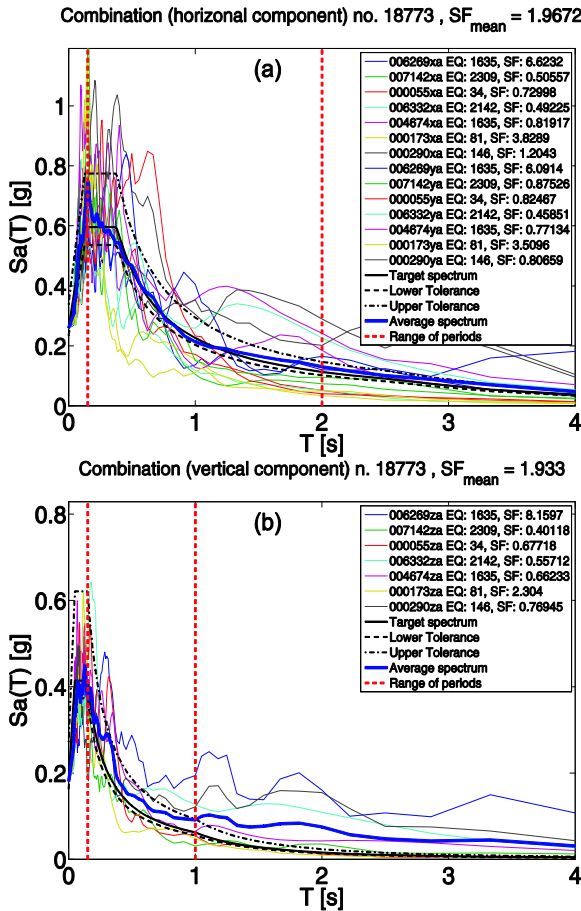


Figure 30. First scaled combination found for the assigned example in Sant'Angelo dei Lombardi which includes the two horizontal (a) and the third vertical (b) components of GM matching the respective target spectra.

Assigning a tolerance compatibility of the average of 10% lower and 30% upper for the horizontal component, and 10% lower and 50% upper for the vertical component, in the range of periods 0.15s ÷ 2s (for the horizontal components) and 0.15s ÷ 1s (for the vertical component), the software returns 100000 scaled combinations compatible with the horizontal target spectrum (the maximum number of combinations was limited to 100000, for simplicity), 160 of which are also compatible with the vertical target spectrum. The maximum value of the average scale factor was limited to 2.

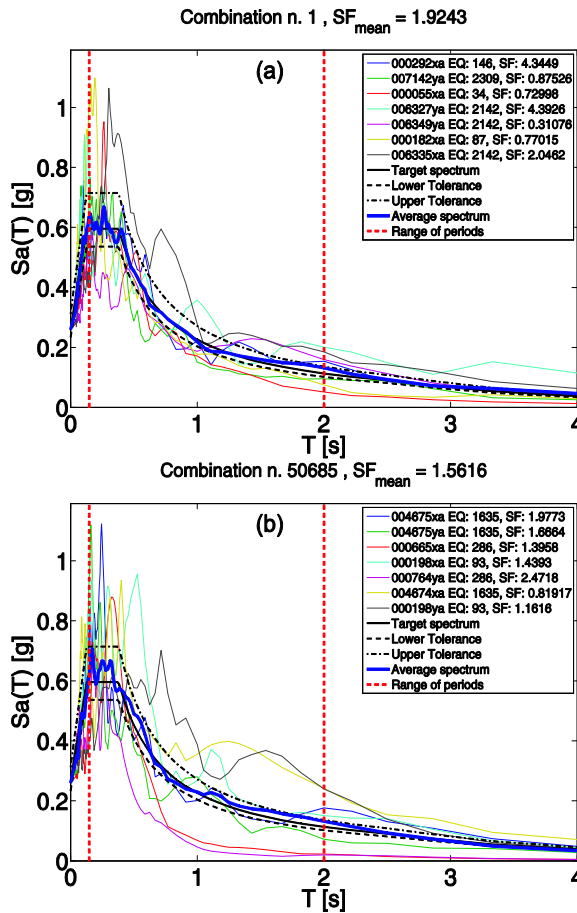


Figure 31. Scaled pair of combinations without overlapping events, (a) and (b).

Finally, note that when searching for combinations that include the vertical component, it may not be appropriate to use the *I'm feeling lucky* option. In fact, the first combination compatible with the horizontal code spectrum (returned by the software) may not necessarily satisfy the compatibility criteria with the vertical spectrum. For example, in the considered case of Figure 30 the first combination, which has all the three components matching the target spectra, only comes after 18772 combinations found which match the horizontal spectrum.

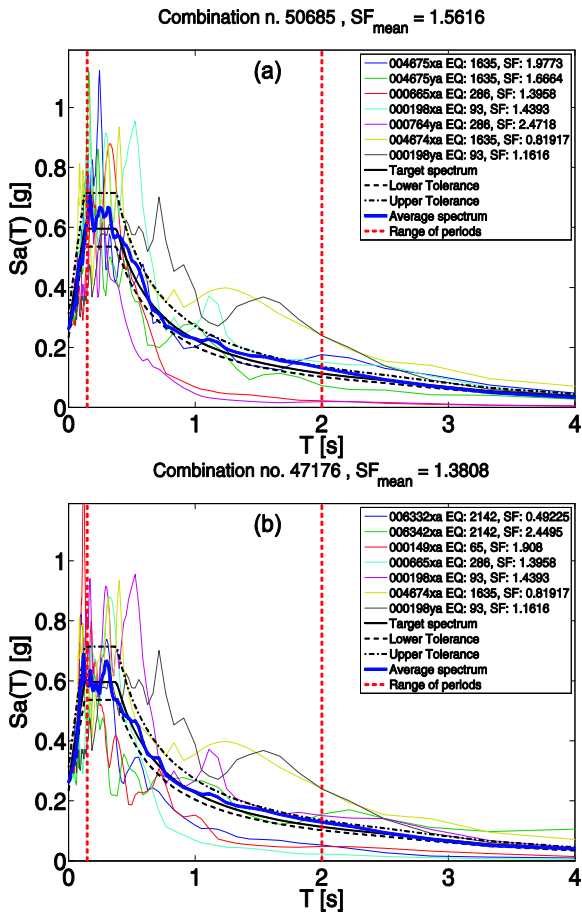


Figure 32. Scaled triplet without overlapping records 31a, 32a and 32b, for the considered example.

Different 2 and Different 3

After having performed a search to find 100000 1-component combinations for the site in question (with same constraints of the scaled search in the first example) it is possible to use the option *Different 2* limiting, for the sake of simplicity, to 100 the maximum number of pairs of combinations to find. Then, REXEL returns 100 pairs of combinations comprised of accelerograms all coming from different events. An example of these pairs found is given by the two combinations of Figure 31a and Figure 31b (see legends to check that earthquake IDs are not overlapping between the figures). Using the option *Different 3*, and limiting for simplicity to 100 the maximum number of triplets of combinations to find, REXEL returns 100 triple combinations having no accelerograms in common. An example of the triplets found with *Different 3* is given by the combinations of Figure 31a, Figure 32a and Figure 32b (see legends to check that stations codes are not overlapping among the figures).

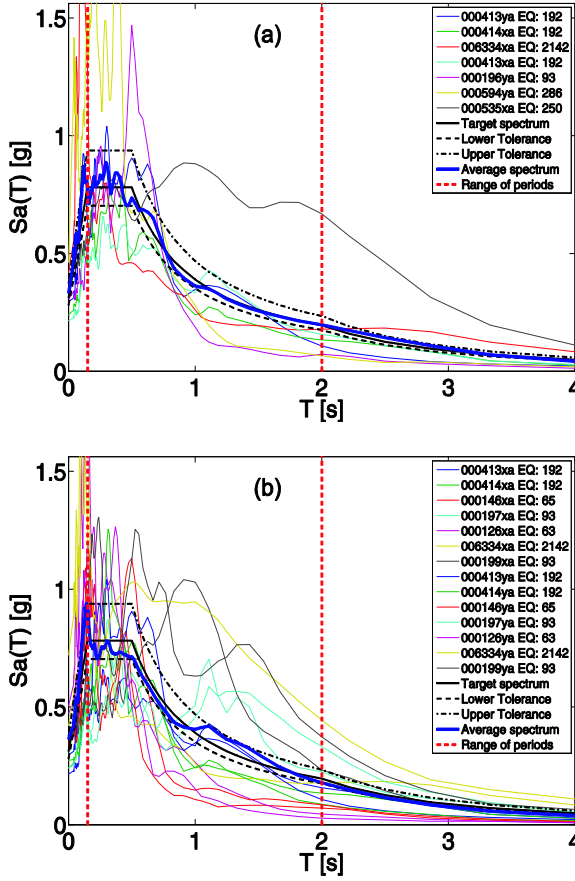


Figure 33. Unscaled combinations found for the assigned example in case of EC8 selection using the *I'm feeling lucky* option in the case of horizontal 1- (a) and 2- components (b) GMs.

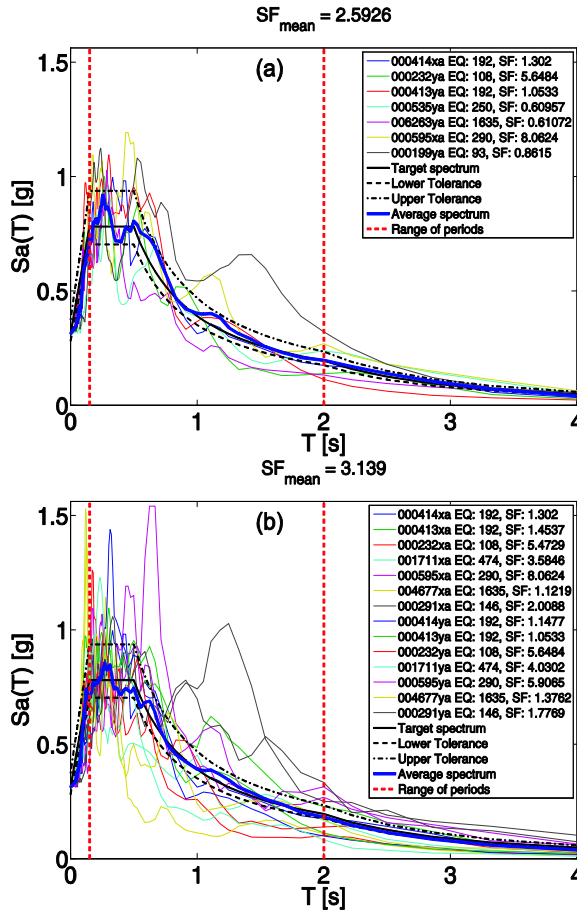


Figure 34. Scaled combinations found for the assigned example in case of EC8 selection using the *I'm feeling lucky* option in the case of horizontal 1-component (a) and 2-components (b) GMs.

4.5.2 Selection according to EC8

Suppose now one needs to select 30-horizontal accelerograms according to Eurocode 8 provisions with target to the ultimate limit state for the same structure still located in Sant'Angelo dei Lombardi, but considering soil type B. In this case the software returns automatically the code spectrum because it is able to determine the a_g value for the site (0.27g). In the case the site is not Italian the user has to input the a_g value of interest.

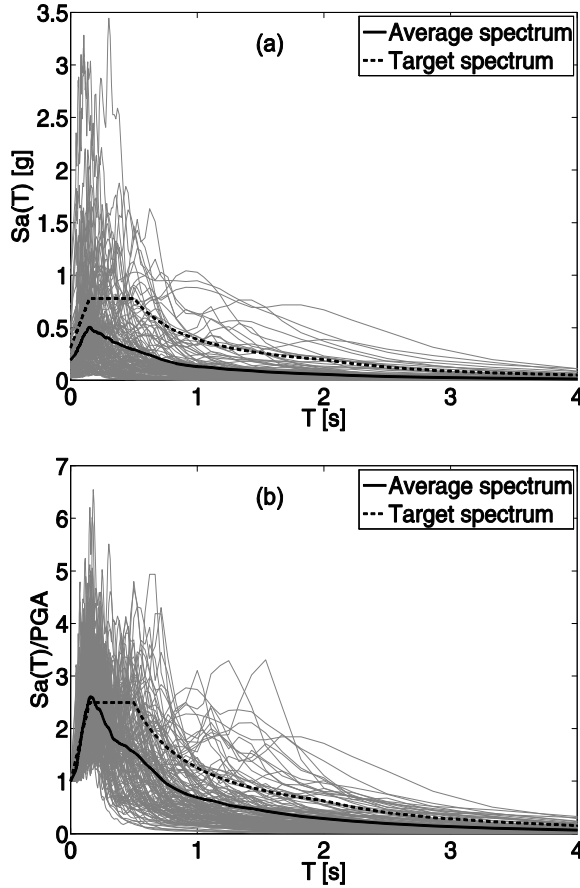


Figure 35. Plot of the spectra found in the ESD for the selected M and R bins in the case of site class B.

Specifying the M and R intervals equal to [5.6, 7] and [0km, 30km] respectively, assigning a compatibility tolerance with respect to the average spectrum of 10% lower and 20% upper in the period range $0.15s \div 2s$ and selecting the quick search option, the software immediately returns the combinations shown in Figure 33a and Figure 33b, in the case of 1-component and 2-components search respectively. Selecting the *Scaled records* option, the software immediately returns the combinations of Figure 34a and Figure 34b. The mean scale factor was limited to 5 as it, although larger than 2 used in the previous example, allows to search among more combinations and may be still

considered acceptable. Note that in case of site class B the individual records of the scaled combination (e.g., Figure 34b) have a scatter with respect to the target spectrum which is comparable to that of the corresponding unscaled combination (i.e., Figure 33b), unlike what happens for the case of soil A (see Figure 27 and Figure 29). The records among which REXEL searched in this case are given in Figure 35.

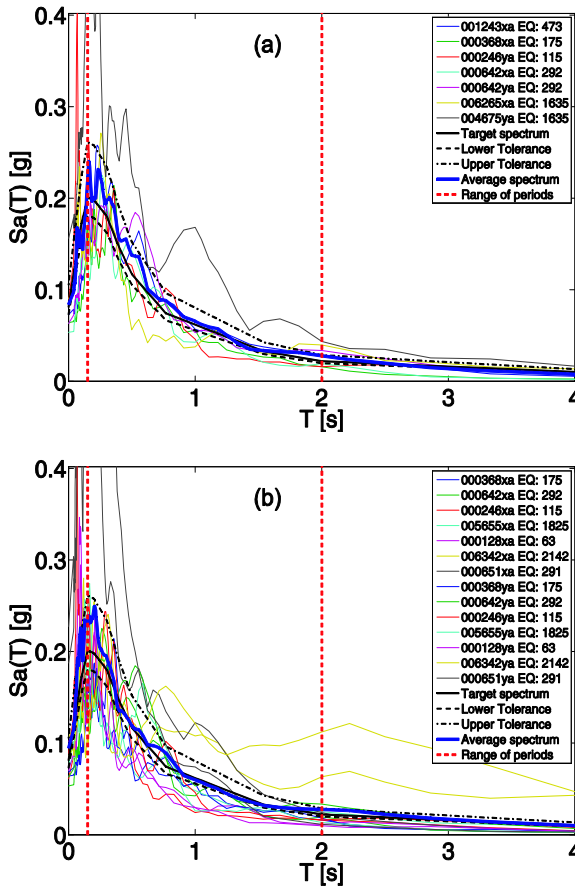


Figure 36. Unscaled combinations found for the assigned example in case of user-defined spectrum selection using the *I'm feeling lucky* option in the case of horizontal 1-component (a) and 2-components (b) GMs.

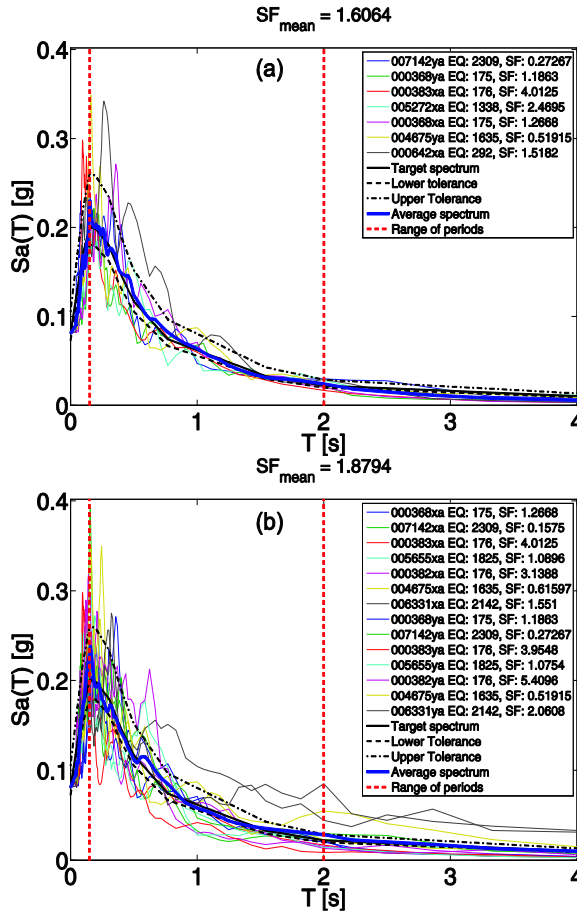


Figure 37. Scaled combinations found for the assigned example in case of user-defined spectrum selection using the *I'm feeling lucky* option in the case of horizontal 1-component (a) and 2-components (b) GMs.

4.5.3 Selection in case of user-defined spectrum

To explore the feature of REXEL allowing to search for sets of 7-records compatible with an user-defined spectrum, let's consider the UHS with a 63% probability of exceedance in 50 years for Sant'Angelo dei Lombardi (50 years return period). To this aim the spectral ordinates in the 0s – 4s range have to be input by the user, those between 0s and 2s were retrieved interpolating the

online hazard data of INGV, those from 2s to 4s were obtained by linear extrapolation (such arbitrary choice does not affect the described example).

Specifying the M and R intervals equal to [5.5, 6.5] and [0km, 30km] respectively, assigning a compatibility tolerance with respect to the average spectrum of 10% lower and 30% upper in the period range $0.15s \div 2s$ and selecting the fast search option, the software immediately returns the combinations of accelerograms shown in Figure 36a and Figure 36b.

Selecting the *Scaled records* option, the software immediately returns the combinations of Figure 37a and Figure 37b. Once again the mean scale factor was limited to 2.

4.6 Comparison with the classification in seismic zones

NIBC in defining the seismic action on structures overcomes the concept of seismic classification of the national territory in zones. In fact, previously the seismic actions of structures were defined by the OPCM 3274 (2003) and OPCM 3431 (2005) on the basis of standard shapes of the elastic response spectrum, depending on the soil type classification and anchored to a reference value of the ground acceleration (a_g). This reference value was identified on the basis of the site of interest belonging to one of four possible seismic zones. The OPCM 3519 (2006) assumed the map MPS04 (<http://zonesismiche.mi.ingv.it>), produced by INGV, as a reference for determining a_g . In particular, it was recommended to classify a specific site in Zone I, II, III or IV depending on the peak ground horizontal acceleration (PGA) on rock with a 10% probability of exceedance in 50 years (retrieved by means of probabilistic seismic hazard analysis or PSHA) falling in the intervals $]0.25g, 0.35g]$, $]0.15g, 0.25g]$, $]0.05g, 0.15g]$ and $\leq 0.05g$ respectively. To each of these zones an a_g value equal to the upper limit of the interval was conservatively assigned. This had several consequences, first of all the code spectra were only indirectly related to the seismic hazard. In fact, for a site having a PGA value close to the lower bound of the interval of interest, the corresponding a_g value overestimated the PGA

percentile derived by PSHA of about 0.1 g. Moreover, the classification of municipalities into four seismic zones only implied constant seismic hazard inside wide areas, often causing neighboring territories (with values of PGA that differ by only a few hundredths of g) to be assigned to different seismic zones (with values of a_g differing by 0.1g) as a result of the shape of administrative boundaries rather than for actual difference in the estimated seismic hazard. To mitigate this effect, both the OPCM 3274 and OPCM 3519 allowed tolerance bounds in order to enable the regions to adjust around the thresholds of the four zones, but they were rarely used.

Then, spectra defined according to the old classification were often significantly over-estimated if compared to the uniform hazard spectra with a 10% probability of exceedance in 50 years.

As an example, let's consider two neighboring sites, Nusco and Sant'Angelo dei Lombardi in the Campania region (southern Italy), whose accelerations on rock with a 10% of probability of exceedance in 50 years are 0.2416g and 0.2673g respectively. According to the old national seismic classification they would be classified in Zone II and I, respectively. Figure 38 (top) shows the location of two sites on the Campania region hazard map in terms of PGA with a return period of 475 years. Although the two sites are very close and then, obviously, have spectra calculated according to the NIBC very similar (Figure 38, bottom), the spectra determined by the OPCM 3274 were very different, and in particular that of Sant'Angelo dei Lombardi was significantly oversized with respect to the real hazard at the site. Figure 38 also shows how the spectra of the NIBC approximate well the uniform hazard spectra for the two sites. Finally, note how the maximum value of the PGA on rock in the region, corresponding to a probability of 10% in 50 years, is about 0.27g. This value is significantly lower than the anchor value of the spectrum, 0.35g, provided by the former classification for a large part of the Campania region.

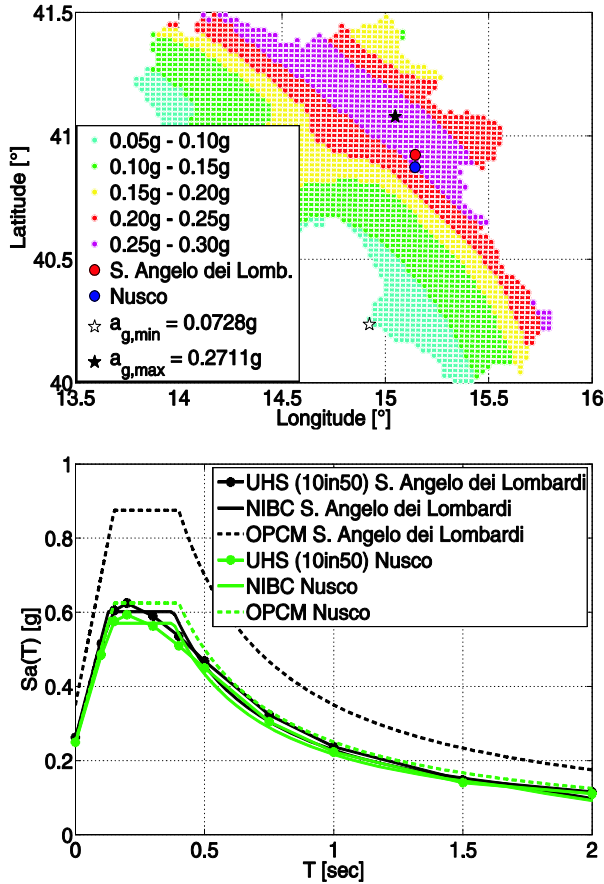


Figure 38. PGA on rock with a 475 years return period a) in Campania (southern Italy) and various spectra for two close sites in the region (b).

This lead to the difficulty of finding unscaled real records for the spectra anchored to the most severe a_g values, as shown in previous studies.

REXEL and the new classification enable a more effective selection of seismic input. For example, if one needs to select 2-components sets of unscaled accelerograms according to EC8 requirements for Sant’Angelo dei Lombardi considering as anchoring values of the spectrum: (i) the real PGA on rock with a 10% probability of exceedance in 50 years (0.27g, from INGV data); (ii) the value 0.35g (according to the old seismic classification), he gets the

number of combinations found results in Table 19³⁸. The tests were carried out assuming a [6, 7.8] M range and R varying from 0km to 40km, assigning a tolerance compatibility of the average of 10% lower and 30% upper in the range of periods 0.2s ÷ 2s.

The comparison shows that, at least in the case of soil conditions where the number of records is larger, the new seismic classification not based on hazard zonation allows, or at least simplifies, seismic input selection. Note that search for softer soil classes did not return any result mainly because the shortage of records in the ESD (Figure 24).

Table 19. Results of comparison, in terms of search for unscaled combinations, for Sant'Angelo dei Lombardi according to the new and the former seismic classifications.

| <i>Site class</i> | $a_g = 0.27g$ | $a_g = 0.35g$ |
|-------------------|---------------|---------------|
| A | 12016 | 2 |
| B | 6174 | 0 |
| C | 3 | 0 |
| D | 0 | 0 |
| E | 0 | 0 |

4.7 Conclusions

In the chapter the main issues related to code-based record selection were critically reviewed with reference to Eurocode 8 (Part 1 and Part 2) and the new Italian building code. Based on previous studies, it is shown how record selection provisions may be not easily applicable to real records. To overcome the most of the obstacles the practitioner may face when determining the seismic input for structural analysis a software tool for automatic selection of one, seven or thirty real recordings, including 1, 2 or 3 components of ground motion, was developed and presented. The main

³⁸ In the investigation of Iervolino et al. (2008) no combinations were found also for A type site class, this result here are not perfectly the same because the initial database and search conditions do not coincide precisely.

selection criterion, for unscaled or scaled sets, is the compatibility, in broad period ranges, of the average spectrum with respect to the reference spectra (which the program automatically builds) of the new Italian building code, of Eurocode 8, or user-defined. REXEL, freely available on the internet, also ensures that individual records in the combinations returned have a spectral shape like that of the target as much as possible, which is important as spectral shape is currently seen as the best proxy for earthquake damage potential on structures. The current version of the software relies on records from the European Strong-motion Database (ESD) and the ITalian ACcelerometric Archive (ITACA); nevertheless, in future developments data from other repositories could be implemented.

The capabilities of REXEL were tested and illustrated via several illustrative applications regarding selection of multi-component ground motion suites according to code- and hazard-based spectra, for different site classes and limit states or return periods. In this way it was demonstrated how the finding of spectrum-compatible sets of records, whose average is compatible with the target, can be significantly improved and facilitated. In fact, REXEL allows to select records controlling the tolerance according to which the average matches the reference spectrum. It also allows to account, beside the site class, for earthquake source characteristics (i.e., magnitude and distance) and some other ground motion parameters (e.g., I_D) which may be useful in structural assessment, as discussed above. To this aim, tools for performing disaggregation of seismic hazard for PGA and 1 sec spectral acceleration (at four different return periods) and computing the distributions of I_D conditional on design PGA, were developed and embedded in REXEL for improving record input selection for earthquake engineering applications in a hazard consistent manner yet easily viable for practitioners.

References

Akkar, S., Bommer, J.J. (2006). Influence of long-period filter cut-off on elastic spectral displacements. *Earthquake Engineering and Structural Dynamics*, 35, 1145–1165

Ambraseys, N., Smit, P., Berardi, R., Rinaldis, D., Cotton, F., Berge, C. (2000). Dissemination of European strong-motion data (Cd-Rom Collection), European Commission, DGXII, Science, Research And Development, Bruxelles.

Ambraseys, N.N., Douglas, J., Rinaldis, D., Berge-Thierry, C., Suhadolc, P., Costa, G., Sigbjornsson, R., Smit, P. (2004). Dissemination of European strong-motion data, Vol. 2, Cd-Rom Collection, Engineering and Physical Sciences Research Council, United Kingdom.

Bazzurro, P., Cornell, C.A. (1999). Disaggregation of seismic hazard. *Bulletin of the Seismological Society of America*, 89, 501-520.

Beyer, K., Bommer, J.J. (2007). Selection and scaling of real accelerograms for bi-directional loading: a review of current practice and code provisions. *Journal of Earthquake Engineering*, 11: 13–45.

CEN, European Committee For Standardisation (2003). Eurocode 8: Design provisions for earthquake resistance of structures, part 1.1: general rules, seismic actions and rules for buildings, prEN 1998-1.

CEN, European Committee For Standardisation (2005). Eurocode 8: Design of structures for earthquake resistance. Part 2: Bridges, prEN 1998-2.

Chioccarelli, E., Iervolino, I., Convertito, V. (2010) Italian Map of Design Earthquakes from Multimodal Disaggregation Distributions: Preliminary Results. *Proc. of 14th European Conference on Earthquake Engineering*, Ohrid, Republic of Macedonia.

Convertito, V., Iervolino, I., Herrero, A. (2009). The importance of mapping the design earthquake: insights for southern Italy. *Bulletin of the Seismological Society of America*, 99, 2979-2991.

Cornell, C.A. (2004). Hazard, ground-motions and probabilistic assessment for PBSO, In Performance Based Seismic Design Concepts and Implementation, PEER Report 2004/05, Pacific Earthquake Engineering Research Center University of California Berkeley.

CS.LL.PP. (2008). DM 14 Gennaio 2008. Norme tecniche per le costruzioni. *Gazzetta Ufficiale della Repubblica Italiana*, 29. (in Italian)

CS.LL.PP. (2009). Istruzioni per l'applicazione delle norme tecniche delle costruzioni. *Gazzetta Ufficiale della Repubblica Italiana*, 47. (in Italian)

Iervolino, I., and Cornell, C.A. (2005). Record selection for nonlinear seismic analysis of structures. *Earthquake Spectra*, 21, 685–713.

Iervolino, I., Galasso, C. (2009). REXEL beta - Tutorial, available at: <http://www.re Luis.it/doc/software/REXELTutorialENG.pdf>.

Iervolino, I., Maddaloni, G., Cosenza, E. (2008). Eurocode 8 compliant real record sets for seismic analysis of structures. *Journal of Earthquake Engineering*, 12, 54–90.

Iervolino, I., Maddaloni, G., Cosenza, E. (2009). A note on selection of time-histories for seismic analysis of bridges in Eurocode 8. *Journal of Earthquake Engineering*, 13, 1125-1152.

Iervolino, I., and Manfredi, G. (2008). Review of ground motion record selection strategies for dynamic structural analysis. In Modern Testing Techniques of Mechanical and Structural Systems, Oreste S. Bursi, David J. Wagg (Editors), CISM Courses and Lectures 502, Springer.

Montaldo, V., Meletti, C., Martinelli, F., Stucchi, M., Locati, M. (2007). On-Line seismic hazard data for the new Italian building code. *Journal of Earthquake Engineering*, 11, 119-132.

Naeim, F., Alimoradi, A., Pezeshk, S. (2004). Selection and scaling of ground-motion time histories for structural design using genetic algorithms. *Earthquake Spectra*, 20, 413-426.

Ordinanza del Presidente del Consiglio dei Ministri (OPCM) 3274 (2003). Norme tecniche per il progetto, la valutazione e l'adeguamento sismico degli edifici, *Gazzetta Ufficiale della Repubblica Italiana*, 105. (in Italian)

Ordinanza del Presidente del Consiglio dei Ministri (OPCM) 3431 (2005). Ulteriori modifiche ed integrazioni all'Ordinanza del presidente del Consiglio dei Ministri 3274, 2005. *Gazzetta Ufficiale della Repubblica Italiana*, 107. (in Italian)

Ordinanza del Presidente del Consiglio dei Ministri (OPCM) 3519 (2006). Criteri per l'individuazione delle zone sismiche e la formazione e l'aggiornamento degli elenchi delle medesime zone. *Gazzetta Ufficiale della Repubblica Italiana*, 108 (in Italian).

Chapter 5

Using the ITalian ACcelerometric Archive from earthquake engineering perspective

ABSTRACT

This chapter reports about REXELite, an internet version, operating on the ITalian ACcelerometric Archive (ITACA), of REXEL. REXELite was developed with the aim of integrating an advanced earthquake records' repository with a tool to define seismic input for engineering seismic analysis according to international standards (with priority to Europe). In fact, REXELite allows to define design spectra according to Eurocode 8 and the Italian building code and to searches in ITACA for the set of seven records (one or two horizontal components) matching it on average, in a user-specified period range, and with the desired tolerance. The records in the set also have, individually, the most similar spectral shape with respect to that of the code. Selection options include magnitude, source-to-site distance, soil conditions, and, if desired, linear scaling of records to reduce further record-to-record variability of spectral ordinates.

5.1 Introduction

The new ITalian Accelerometric Archive ITACA (<http://itaca.mi.ingv.it>) was developed within the S4 Project (<http://esse4.mi.ingv.it>), in the framework of the 2007-2009 research agreement between the *Istituto Nazionale di Geofisica e Vulcanologia* (INGV - Italian Institute of Geophysics and Volcanology) and *Dipartimento della Protezione Civile* (DPC - Italian Civil Defense). This project continued the activity originally developed by S6 Project (<http://esse6.mi.ingv.it>), within the previous 2004-2006 DPC-INGV agreement, in which the alpha version of ITACA was originally released (Luzi et al., 2008).

The main goal of both S6 and S4 Projects was to organize into a comprehensive, informative and reliable database (and related webtools) the wealth of strong-motion records, obtained in Italy during the seismic events occurred starting from the Ancona earthquake in 1972, up to the L'Aquila 2009 sequence.

The availability of internet strong-motion databases as ITACA is of certain interest also to earthquake engineering community as it facilitates seismic input definition for dynamic structural analysis by means of real records. However, as widely discussed in the previous chapters, seismic structural codes, regarding the ground motion selection issue, often require that the suite of records has to “match” the design spectrum for the site and the limit state of interest. This, along with other provisions, renders selection of real records hardly feasible for the practitioner if not adequately aided, as demonstrated in Iervolino et al. (2008, 2009) at least in the case of Eurocode 8, or EC8 (CEN, 2003), and the new Italian building code, or NIBC (CS.LL.PP., 2008).

To address this issue, with the aim of also translating into practice of code-based seismic analysis recent research achievements about real strong-motion record selection, a software tool, REXEL, was developed between 2008 and 2010 (Chapter 4). REXEL, freely available at the website of the Italian *Rete dei Laboratori Universitari di Ingegneria Sismica* (ReLUIS), also funded by DPC, allows to search for suites of waveforms, compatible to target spectra either user-defined or automatically generated according to EC8 and NIBC.

While REXEL is a standalone software, this chapter presents a web-based version, REXELite (<http://itaca.mi.ingv.it>), with the same record selection algorithm (yet optimized for its inclusion in the ITACA web portal) operating online on the ITACA database since January 2010. REXELite seems successful in standardizing and aiding seismic input definition in practice according to seismic codes, allowing to search for horizontal combinations of seven 1- or 2-horizontal components strong motion records, compatible on average with a specified target (code) spectrum, in a range of periods of interest and with arbitrary tolerances.

Because when selecting a set of accelerograms for structural analysis the main objective is to reflect the relevant hazard scenarios at the site (e.g., Chioccarelli et al., 2010), REXELite allows to select suites which also belong to user-defined magnitude and source-to-site distance bins and to the same site class of the location of the structure. ITACA may be searched for spectrum-matching sets of records which are original (unscaled) or ground motions linearly scaled in amplitude. Finally, REXELite not only ensures the set resulting from the search has its average matching the target spectrum, but also that it is the one with the smallest individual record-to-record variability (see section 5.4).

In the following, after an introduction to ITACA, provisions regarding record selection for dynamic structural analysis are briefly reviewed, laying emphasis on NIBC and EC8 procedures. Then, how REXELite addresses this task is discussed and examples of online code-based record selection in ITACA are shown.

5.2 The ITalian ACcelrometric Archive (ITACA)

The version 1.0 of ITACA was updated at the end of S4 Project (June, 2010), contains 2550 three-component waveforms: 2293 of them were recorded during 1002 earthquakes with a maximum moment magnitude of 6.9 (the 1980 Irpinia earthquake) between 1972 and 2004, while the rest comes from the M_w 5.4 2008 Parma (Northern Italy) and from the M_w 6.3 2009 L'Aquila (Central Italy) earthquakes and related $M_w > 4$ aftershocks.

The waveforms collected in ITACA were recorded by 665 strong-motion stations in total³⁹. The recordings mainly come from the National Accelerometric Network (RAN, *Rete Accelerometrica Nazionale*), operated by DPC. RAN presently consists of 334 free-field digital stations and 84 analogue stations, the replacement of which with digital instruments is currently in

³⁹ Among these stations, 287 are presently not in operation, since they were either part of temporary networks or equipped with old analogue instruments, which were removed.

progress. The goal is to achieve a final configuration of more than 500 digital stations installed throughout the Italian territory, with an average inter-station distance of about 20-30 km in the most seismically active regions of Italy.

Further records are provided by the Strong Motion Network of Northern Italy (*Rete Accelerometrica dell'Italia Settentrionale*, RAIS, <http://rais.mi.ingv.it/>), comprised of digital instruments, installed around the Garda lake area, and by sparse stations (analogue and digital) operated by ENEA (*Ente per le Nuove tecnologie, l'Energia e l'Ambiente*), between 1972 and 2004. In addition to these, waveforms recorded during the L'Aquila seismic sequence by the accelerometer installed in the AQU station (<http://mednet.rm.ingv.it>) are also included.

All ITACA records have been re-processed with respect to the alpha version (Massa et al., 2009), with a special care to preserve information about *late-triggered* (to follow) events and to ensure compatibility of corrected records; i.e., velocity and displacement traces obtained by the first and second integration of the corrected acceleration should not be affected by unrealistic trends. The newly adopted processing scheme is described in Paolucci et. al (2010).

Seismic stations which recorded ground motions included in ITACA are classified, with respect to soil site class, according to the EC8; i.e., on the basis of the V_{s30} (average shear wave velocity in the upper 30 meters) either determined by direct measurement or on geological maps. Figure 39 summarizes the main characteristics (magnitude and epicentral distance) of the ITACA dataset on which REXELite operates. All these records satisfy the free-field conditions and were produced by earthquakes of moment magnitude larger than 4.

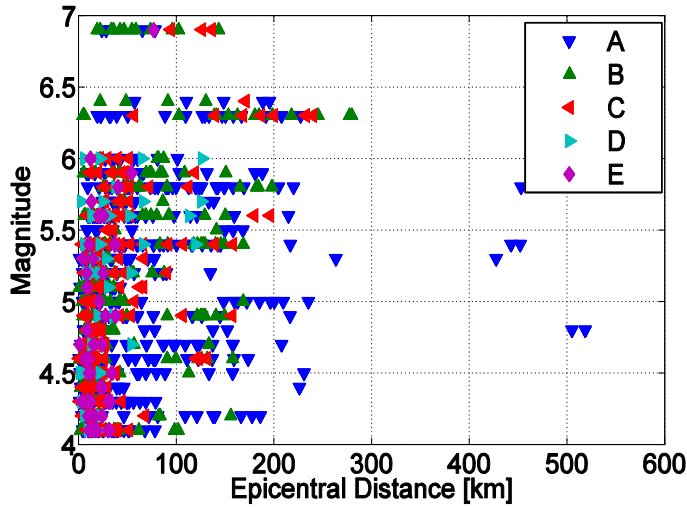


Figure 39. Magnitude (moment or local) vs epicentral distance distribution for the ITACA dataset on which REXELite operates. The records are grouped by site class according to EC8 classification.

ITACA website includes a wide range of search tools enabling the practitioner to interactively retrieve events, recording stations and waveforms, through a graphical user interface. The interface allows queries selecting waveform parameters, seismic events and stations. Each query returns a list of matching results and the single outcome can be explored allowing to get detailed and elaborated information; more details are available in Luzi et al. (2008).

5.3 European and Italian standards for record selection for dynamic structural analysis

Nonlinear dynamic analysis (NLDA) of structures implies that, given that a model for the structure is available, the seismic performance is determined by time-history response analysis to a suite of earthquake ground motions. The apparently simple procedures for selecting and scaling (or more generally manipulating) ground motions records for an engineering project,

and their implementation in state-of-the-art or next generation of seismic codes, have been the subject of much research in recent years; see Iervolino and Manfredi (2008) for a review.

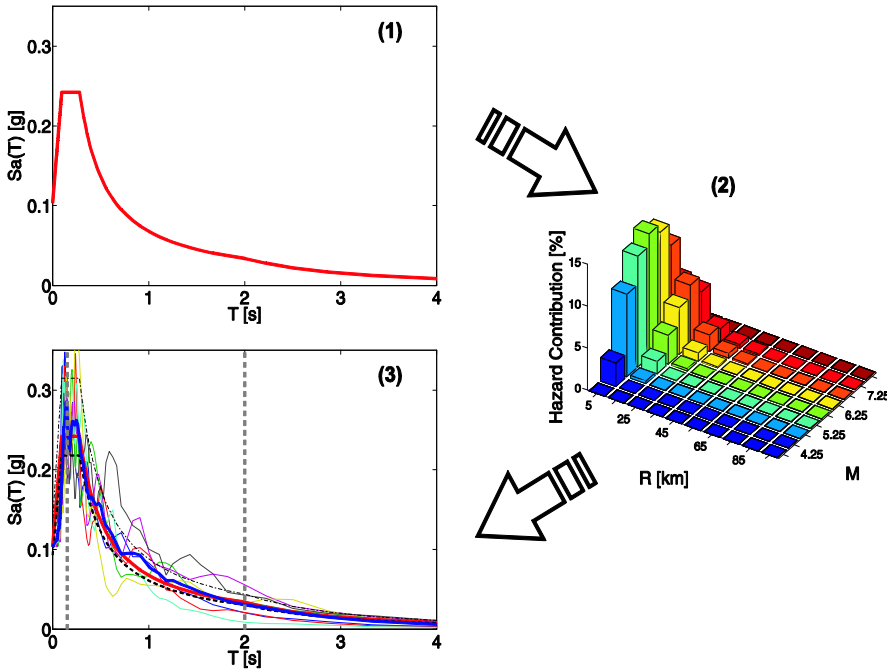


Figure 40. Steps to define seismic action according to the hazard at the site; from (1) to (3): target spectrum for the limit-state of interest, hazard disaggregation for the spectral ordinate at the period of the first mode of the structure, selection of a set of records compatible to disaggregation and matching the target spectrum in a range of periods.

Once a target spectrum (i.e., a *design* spectrum) is defined, for example an *uniform hazard spectrum* (UHS) from probabilistic seismic hazard analysis (PSHA), a relatively rational approach in record selection is to choose ground motions associated with the *design earthquakes* (i.e., one or more event scenarios in terms of magnitude, distance, and possibly other characteristics⁴⁰). This

⁴⁰ It is to note that some studies (e.g., Iervolino and Cornell, 2005) have shown that, to some extent, if the target spectrum is matched, may be not strictly necessary to also select

choice, consistently with determination of the spectrum by PSHA, should be driven by disaggregation of seismic hazard (e.g., Convertito et al., 2009; Chioccarelli et al., 2010) in order to identify the scenario giving the largest contribution to the spectral ordinates more relevant for the behaviour of the structure (e.g., close to the fundamental period, T_1). Then a waveforms' repository may be accessed and a suite of records selected compatibly with the values of source parameters defining the design earthquakes. Finally, records are rendered somehow compatible also to the target spectrum, for example by scaling each record to the design spectrum ordinate at the fundamental vibration period of the structure, $S_a(T_1)$, or in a range around it, Figure 40.

If to requiring it explicitly, modern codes allow such procedure (e.g., Chapter 4). In fact, the recently released Italian code avails of the work of the INGV concerning the seismic hazard analysis of the Italian territory in the framework of a specific project, S1 Project (<http://esse1.mi.ingv.it>); Montaldo et al. (2007). This is reflected in the definition of seismic action on structures based on site-dependent elastic acceleration spectra closely approximating UHSs for several return period of seismic action at each site.

Regarding seismic input for NLDA, there are a number of allowed options to obtain suites of acceleration time-histories, including the generation of spectrum-compatible accelerograms (i.e., artificial records), or the simulation of records (through a physical simulation of earthquake process), see Iervolino et al. (2008). Concerning real accelerograms, according to NIBC and EC8, selection should match *the seismogenetic features of the source and the soil conditions appropriate to the site*. NIBC, then requires to render the spectra of the records *similar* to that of the design spectrum. Alternatively, if information about the *seismogenetic features of the source* is not available, it is possible to only match the elastic design spectrum (Chapter 4). More specifically, if the latter approach is chosen, the main condition to be satisfied is that the average elastic spectrum (of the chosen set) does not underestimate the 5% damping elastic code spectrum, with a 10% lower bound tolerance (see next section), in the

intentionally matching design earthquakes in terms of magnitude and distance, however is always prudent to do so and often required by codes.

larger range of periods between $[0.15s, 2s]$ and $[0.15s, 2T_1]$ for safety verifications at ultimate limit state (T_1 is the fundamental period of the structure in the direction where the accelerograms will be applied) or in the larger period ranges between $[0.15s, 2s]$ and $[0.15s, 1.5T_1]$, for structural safety checks at serviceability limit states⁴¹. For seismically isolated structures, the code provides a narrower range of matching around the fundamental period, $[0.15s, 1.2T_{is}]$, where T_{is} is the equivalent period of the isolated structure. This extended range accounting for both the contributions to the response for higher modes and the correlation of nonlinear response with spectral ordinates at periods larger than T_1 .

EC8 has very similar provisions, but the design spectrum depends on hazard only by its anchoring value (i.e., a_g or peak ground acceleration, PGA, on stiff soil) and matching in the $[0.2T_1, 2T_1]$ range⁴² is mandatory. Moreover, *the mean of the zero period spectral response acceleration values (calculated from the individual time histories) should not be smaller than the value of $a_g S$ for the site in question*, where S is the soil factor amplifying the design spectrum with respect to the stiff soil (Iervolino et al., 2008). Both NIBC and EC8 specify that a minimum of 3 records should be used and that, if less than 7 records are used, then the maximum structural response must be used as the basis for design and assessment, whereas if 7 or more time-histories are employed then the average structural response can be used.

⁴¹ In NIBC, these conditions are explicitly provided for artificial records only, while in EC8, they apply to any form of accelerograms, i.e., real, artificial or simulated. The instructions for the implementation of the NIBC (CS.LL.PP., 2009) allows to use the conditions of average spectral compatibility defined for artificial signals also for the suites of real records, respecting the geological conditions of the site and choosing accelerograms whose spectrum is, if possible, generally similar to that of the target design spectrum.

⁴² This range applies for building, whereas for bridges the $[0.2T_1, 1.5T_1]$ interval should be considered (see Iervolino et al., 2009).

5.4 REXELite

In attempting to translate the provisions described in the previous section into practice, it is easy to recognize that tools aiding record selection for code-based applications, may be useful. In fact, between 2006 and 2010, to reconcile seismic code provisions with last ten years research results about record selection, specific algorithms were developed and finally embedded into a software, REXEL (Chapter 4). REXEL, available on the ReLUIIS website (<http://www.reluis.it>) from which may be downloaded, contains the accelerograms of the *European Strong-motion Database* or ESD (<http://www.isesd.cv.ic.ac.uk/>) and of ITACA, satisfying the free-field conditions and produced by earthquakes of magnitude larger than 4.

REXEL allows one to search for combinations of accelerograms whose average is compatible with the target spectrum, and in which individual records have the shape as similar as possible with that of the target in a periods range of interest. Records may also selected reflecting disaggregation of seismic hazard in terms of magnitude and source-to-site distance and specific ranges of ground motion intensity measures. Several options, related to management of REXEL output and advanced research-based tools for improving and rendering record selection hazard-consistent, are included.

In the framework of the mentioned S4 Project, an internet version of the stand-alone software REXEL was developed and named REXELite (Figure 41). While REXEL has several advanced features and two waveform databases embedded, REXELite is a simplified version, easily accessible over the web and constantly synchronized with ITACA which continuously evolves including new records and new or revised information on existing waveforms. It represents an interesting prototype for future similar tools interfacing seismology and earthquake engineering at the level of seismic input definition for structural analysis.

REXELite allows to automatically define the target spectra according to the NIBC (or to the EC8). To do this, it is necessary to enter the geographical coordinates of the site, *latitude* and *longitude* in decimal degrees, and to specify

the *Site Class* (according to EC8 classification), the *Topographic Category* (as in EC8), the *Nominal Life*, the *Functional Type*, and the *Limit State* of interest⁴³. For EC8 spectra, it is necessary to specify only the anchoring value of the spectrum and the soil class because, as mentioned, the design spectrum is only function of a_g and S . In addition, it is necessary to specify the number of horizontal components of ground motion (1 or 2) desired to be included in the set.

REXELite allows to search for records within ITACA belonging to the same site class of the defined spectrum or to *any site class* (i.e., recording referring to different site conditions may show up in the same set matching the target spectrum⁴⁴) and corresponding to magnitudes and epicentral distances of interest. In fact, the intervals $[M_{\min}, M_{\max}]$ (moment and/or local magnitude) and $[R_{\min}, R_{\max}]$ (epicentral distance, in km), in which to search for sets of accelerograms, to be defined.

Also the recording instrument features may be specified; i.e., if also *late trigger* and/or analogue⁴⁵ recordings have to be included in the search. In a late triggered record, the recording instrument started recording after the arrival of the first seismic waves of significant amplitude. The recorded signal is then characterized by large initial values if compared to the peak of the signal, In a

⁴³ The NIBC states the principle that seismic actions on buildings are defined on the basis of the seismic hazard at the site in terms of *maximum expected* horizontal acceleration on rock and the corresponding elastic response spectrum. The maximum acceleration is defined as the peak of the acceleration which has a certain probability to be exceeded - depending on the *limit state* of interest - in a reference period V_R . V_R is equal to the *Nominal Life* of the structure (V_N , in years), times the *Importance Coefficient* for the construction (C_U). The nominal life is the number of years in which the structure, subjected to scheduled maintenance, may be used for the purpose it was designed for. The value of the importance coefficient depends on the severity of losses consequent to the achievement of a defined limited state and then on the "importance" of the structure (i.e. *Functional Type*).

⁴⁴ In fact, matching a target spectral shape may render less relevant to structural response respecting specific soil site conditions of the records.

⁴⁵ If the instrument to measure strong motion acceleration is of *analogue* type, ground acceleration is reproduced by a mechanical instrument on a physical support. Modern *digital* instruments (operating from about the mid-80s) are based on electric transduction. The data quality of digital recording is generally higher with respect to analogue recordings.

normally triggered record the recording instrument triggered early enough to properly describe the first arrivals of the seismic waves.

The screenshot displays the REXELite user interface with several sections highlighted by red circles and red text annotations:

- Session title:** L'Aquila
- Target spectrum:** Definition of code spectrum
- Latitude [degrees]:** 42.3507
- Longitude:** 13.3999
- Site definition:** (Annotation)
- Site classification (EC8):** A
- Topography:** T1 - flat surfaces, isolated cliffs and slopes with average slope angle not greater than 15°
- Nominal life [years]:** 50 years - ordinary structures
- Building functional type:** 2 - ordinary structures (Cu=1.0)
- Limit state probability:** Damage (P=63%)
- Definition of return period of seismic action:** (Annotation)
- Ground motion components:** One horizontal component
- Preliminary record search:** Definition of design earthquake
- Station site classification:** Same site class as target spectrum
- Magnitude min:** 5
- max:** 6
- Type of magnitude to consider:** Mw or MI indifferently
- Epicentral distance [km] min:** 0.0
- max:** 20
- Include late trigger events:** Yes
- Instruments features:** (Annotation)
- Include analog records:** Yes
- Spectrum matching parameters and analysis options:** Definition of compatibility parameters
- Period range [s] from:** 0.15
- to:** 2
- Tolerance [%] from:** 10.0
- to:** 30.0
- Non-dimensional:** Option for scaled records
- Accept parameters...** (button)

Figure 41. REXELite user interface

Once these options have been defined, REXELite returns the number of records (and the corresponding number of events and recording stations) available in ITACA. The spectra of the records returned by this preliminary search are used by REXELite to find a combination of seven, whose average is compatible with the defined target spectrum and some tolerance (also defined by the user) in an arbitrary interval of periods $[T_1, T_2]$ between 0s and 4s (Figure 42).

As shown in Figure 42, the user has to specify the tolerated deviations, *lower* and *upper*, in percentage terms, the average spectrum of the combination

can have with respect to the target in the chosen range of periods. NIBC and EC8 provide constraint about the maximum tolerance according to which the average of the record set may underestimate the target spectrum (i.e., 10%), but do not supply any instruction about the upper limit. It is obvious that reducing as much as possible the overestimation of the average spectrum is a rational choice.

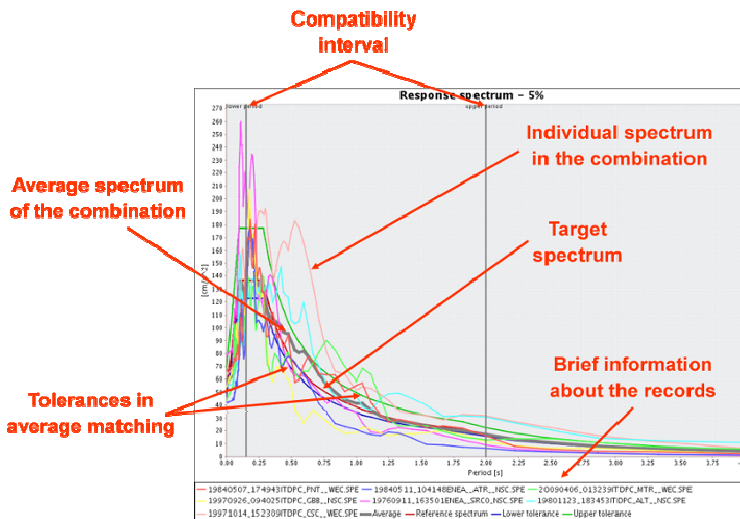


Figure 42. Definition of spectral matching parameters and illustration of REXelite output as it appears to the user.

The compatible combination can comprise 7 accelerograms to be applied in one horizontal direction for analysis of bi-dimensional (plan) structures or 7 pairs of accelerograms (i.e., two horizontal recordings of a single station) to be applied in both horizontal directions for the analysis of three-dimensional structures as provided by NIBC and EC8.

The software analyzes all the possible combinations of seven spectra that can be built from records found in the database (for the ranges of magnitude and distance chosen and which satisfied the soil and instruments options specified by the user) and checks whether each combination is compatible, in an average sense and with the assigned tolerances, with the code spectrum.

The analysis stops as soon as the first compatible combination is found. Because of a specific feature of the search algorithm, the record combination returned by REXELite is likely that better approximating the target spectrum among those that may be obtained by the preliminary search in the database (see Chapter 4 again).

REXELite allows one to obtain combinations of accelerograms compatible with the code spectrum that do not need to be scaled, but it also allows one to choose sets of accelerograms compatible with the reference spectrum, if scaled linearly (in this case, the individual records scale factors are also provided to the practitioner). In fact, given a target spectrum, allowing the records to be scaled enhances the probability of finding a matching combinations. Moreover, amplitude linear-scaling of records gives combinations whose spectra are generally more similar to the target spectrum, so reducing the record-to-record spectral variability within a set and then increasing the statistical confidence in the estimation of structural response assessed using the found set of records. The maximum mean scale factor (SF) allowed is 5, i.e., REXELite discards combinations with a mean SF (i.e., averaged scaling factors among the records in the combination) larger than 5.

When the desired combination is found, several interactive options allow users to explore selected waveforms in both time and frequency domains, to download records and/or response spectra and to retrieve detailed information on the corresponding recording station and on the corresponding earthquakes of origin.

5.5 Applications

As an example, consider the selection of 1-component horizontal accelerograms according to the NIBC for the damage state limit of an ordinary structure (*Functional Class II*) located in L'Aquila (Italy) (longitude: 13.3999°, latitude: 42.3507°) on soil type A with a nominal life of 50 years, which corresponds to the design for a 50-years return period according to the code.

When setting the coordinates of the site and the other parameters to define the seismic action according to the NIBC, the software automatically builds the elastic design spectrum. Consider also that selection should reflect disaggregation of PGA hazard⁴⁶ on rock with a 50-years return period (Figure 43) at the site, which may be easily obtained by the S1 Project website given above.

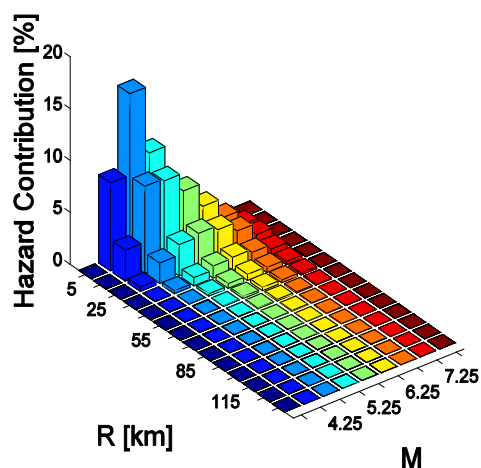


Figure 43. Disaggregation of PGA with 50 years return period on rock for L'Aquila (<http://esse1.mi.ingv.it>).

Specifying the M (moment and local magnitude indifferently) and R intervals equal to [5, 6] and [0km, 20km] respectively, including also late trigger events and analogue stations, and choosing to select records belonging to the same local geology category of the site in question (i.e., A site class), REXELite found 136 waveforms (68 x 2 components of motion) from 31 different earthquakes on 33 different recording stations.

⁴⁶ Note that it is often recommended to consider as design earthquakes the results of hazard disaggregation for the spectral ordinates in the range of interest for the nonlinear structural behavior. This may significantly differ from disaggregation of PGA hazard (e.g., Converito et al., 2009; Chioccarelli et al., 2010).

Once the sub-set of records that satisfied the selection criteria was identified, assigning as tolerance for the average spectral matching, 10% lower and 30% upper in the period range 0.15s ÷ 2s, REXELite immediately⁴⁷ returns the combination of accelerograms in Figure 44. The figure automatically plotted by the software, gives the average of the set and the code spectra, along with the seven individual spectra of the combination, the tolerances in matching and the period range bounds where compatibility is ensured. In the legend, the ITACA waveforms codes are also given⁴⁸.

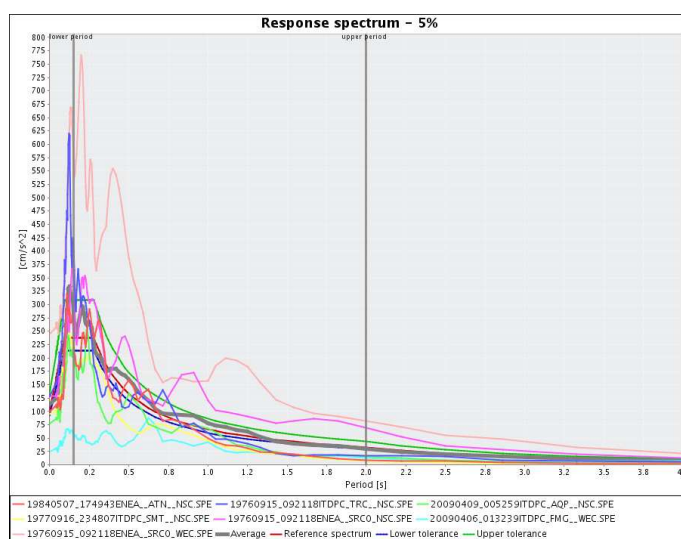


Figure 44. 1-component combination found for the assigned example in L'Aquila in the case of damage limit state.

REXELite also returns the detailed information about the individual records as retrieved by ITACA (Figure 45), e.g. recording station code and station type (analog or digital), event (date and time), etc. The selected site

⁴⁷ The software returns an error message if processing time is longer than 180 seconds.

⁴⁸ These codes include several information, i.e., origin date and time, network code, station code and component of the motion and a flag specifying whether or not the record has been processed (C means processed), for a total length of 33 characters (if network and/or station codes have less than 5 characters, the rest is replaced by one or more underscores).

(and eventually also recording stations and event) is plotted using Google Maps® interface that allow to display the site.

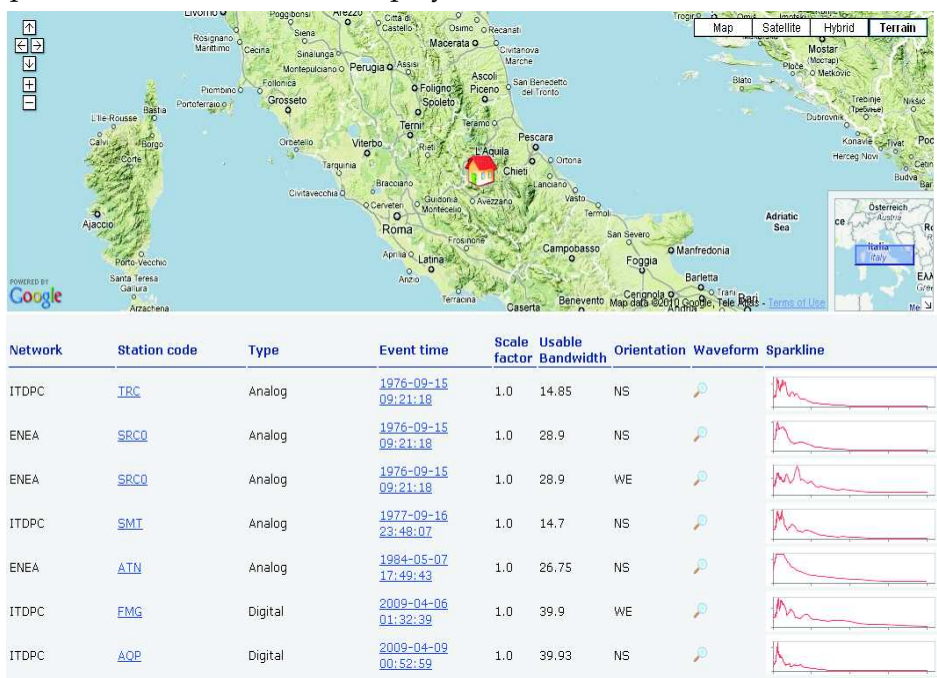


Figure 45. Essential record data returned by REXELite for the combination of Figure 44.

Other functions are related to return of selected waveforms to the user. The strong-motion data, in terms of acceleration time history, are provided in a compressed file containing the 7-corrected waveforms along with the corresponding acceleration response spectra (in ASCII format⁴⁹). The output file comprises also the target spectrum and a file, namely *data.txt*, containing the list of records obtained by preliminary search into ITACA. Finally, a file containing a summary of the performed elaboration (in terms of selected parameters and options) is provided to the users (*readme.txt*).

⁴⁹ The ASCII-format records are characterized by a header of 43 rows, containing several information in order to make the record self-consistent; see ITACA User Manual (http://itaca.mi.ingv.it/ItacaStage/doc/Manual_ITACA_beta_version.pdf) for details.

As discussed in the previous section, the records in the list in the *data.txt* file (first column) are reported in ascending order of the parameter, also reported in *data.txt* file (second column), defined in Eq. (1), which gives a measure of how much the spectrum of an individual record deviates from the target spectrum.

$$\delta = \sqrt{\frac{1}{N} \sum_{i=1}^N \frac{Sa_j(T_i) - Sa_{target}(T_i)}{Sa_{target}(T_i)}} \quad (1)$$

In Equation (1), $Sa_j(T_i)$ is the pseudo-acceleration ordinate of the real spectrum j corresponding to the period T_i , while $Sa_{target}(T_i)$ is the value of the spectral ordinate of the code spectrum at the same period, and N is the number of values within the considered range of periods. As an example, in Table 1, an extract from the *data.txt* file for the combination of Figure 44 is shown. Five of the seven records in the combination of Figure 44 are in the first ten positions in the preliminary search output sort; i.e., in the ordering of individual spectra based on the similitude with the code spectrum.

Table 20. Sample from the *data.txt* file for the combination of Figure 44.

| <i>Position in data.txt file</i> | <i>Waveform code</i> | δ |
|----------------------------------|------------------------------------|-------------|
| 1 | 19840507_174943ENEA__ATN__NSC.SPE | 0.259194157 |
| 2 | 19760915_092118ITDPC_TRC__NSC.SPE | 0.321637501 |
| 4 | 20090409_005259ITDPC_AQP__NSC.SPE | 0.322704447 |
| 5 | 19770916_234807ITDPC_SMT__NSC.SPE | 0.334124185 |
| 8 | 19760915_031518ENEA__SRC0__NSC.SPE | 0.341848254 |
| 66 | 20090406_013239ITDPC_FMG__WEC.SPE | 0.697072126 |
| 132 | 19760915_092118ENEA__SRC0__WEC.SPE | 1.615000801 |

What also emerges from Figure 44 is that to have the best average spectral compatibility, it is hard to reduce the variability of individual spectra records keeping them unscaled. Therefore, it is also possible to search for

combination of record which require to be linearly scaled to match the target spectrum. To this aim, REXElite has the *non-dimensional* option⁵⁰.

In this case, repeating the search for L'Aquila considering the same magnitude and distance ranges, with the same compatibility criteria as the previous case, the software immediately returns the combination shown in Figure 46, which features records with less scattering (maximum δ -value equal to 0.47) with respect to the un-scaled ones of Figure 44, see Table 20 and Table 21. The records in Figure 46, are multiplied by the scaling factors (SFs, automatically computed and provided by the software (Figure 47).

Table 21. Sample of data.txt file for the combination of Figure 46.

| <i>Position in data.txt file</i> | <i>Waveform code</i> | δ |
|----------------------------------|----------------------------------|-------------|
| 1 | 19840511_104148ITDPC_PSC_NSC.SPE | 0.169868902 |
| 2 | 19760915_092118ENEA_SRC0_WEC.SPE | 0.219179379 |
| 3 | 20090409_005259ITDPC_AQP_NSC.SPE | 0.239597264 |
| 6 | 19840511_104148ENEA_ATN_NSC.SPE | 0.244673986 |
| 9 | 19760915_092118ENEA_SRC0_NSC.SPE | 0.288677309 |
| 33 | 20090413_211424ITDPC_AMT_NSC.SPE | 0.379114194 |
| 61 | 19760915_031518ENEA_SRC0_NSC.SPE | 0.470464817 |

Other functions are related to visualization of waveforms using ITACA tools (Luzi et al., 2008) allowing users to view data in different contexts and extract ground motion data of interest. For example, each individual record in the found combination can be displayed (in terms of unprocessed and processed acceleration time-history, velocity and displacement time-history, Fourier spectrum and acceleration response spectrum), see Figure 48.

⁵⁰ The *Non-dimensional* option means choosing whether to search *scaled* record sets or not. In fact, if this option is chosen the spectra to be analyzed to search for compatible combinations, are preliminarily normalized dividing the spectral ordinates by their PGA. Combinations of these spectra are compared to the non-dimensional code spectrum. Combinations found in this way have to be scaled to be compatible in an average sense with the reference spectrum.

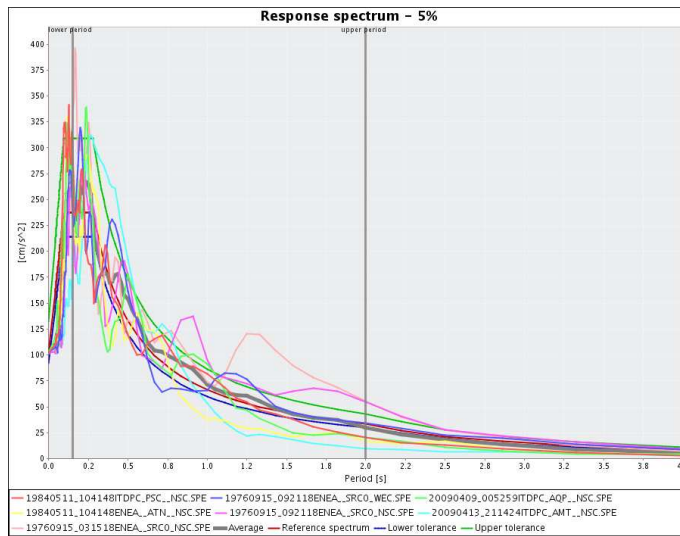


Figure 46. Scaled 1-component combination found for the assigned example in L'Aquila in the case of damage limit state.

| Network | Station code | Type | Event time | Scale factor | Usable Bandwidth | Orientation | Waveform | Sparkline |
|---------|----------------------|---------|-------------------------------------|--------------|------------------|-------------|----------|-----------|
| ENEA | SRCO | Analog | 1976-09-15 03:15:18 | 1.73636 | 28.85 | NS | | |
| ENEA | SRCO | Analog | 1976-09-15 09:21:18 | 0.793411 | 28.9 | NS | | |
| ENEA | SRCO | Analog | 1976-09-15 09:21:18 | 0.41636 | 28.9 | WE | | |
| ITDPC | PSC | Digital | 1984-05-11 10:41:48 | 5.58407 | 12.8 | NS | | |
| ENEA | ATN | Analog | 1984-05-11 10:41:48 | 4.09246 | 28.7 | NS | | |
| ITDPC | AQP | Digital | 2009-04-09 00:52:59 | 1.33814 | 39.93 | NS | | |
| ITDPC | AMT | Digital | 2009-04-13 21:14:24 | 4.832 | 39.9 | NS | | |

Figure 47. Essential record data returned by REXELite for the combination of Figure 46.

When selecting the option to search for a set of seven pairs of horizontal components, with all other conditions (i.e., magnitude and distance range, site class, instruments features, tolerances and periods range) being equal, the software doesn't find a compatible set of records for the given target spectrum within 180 seconds.

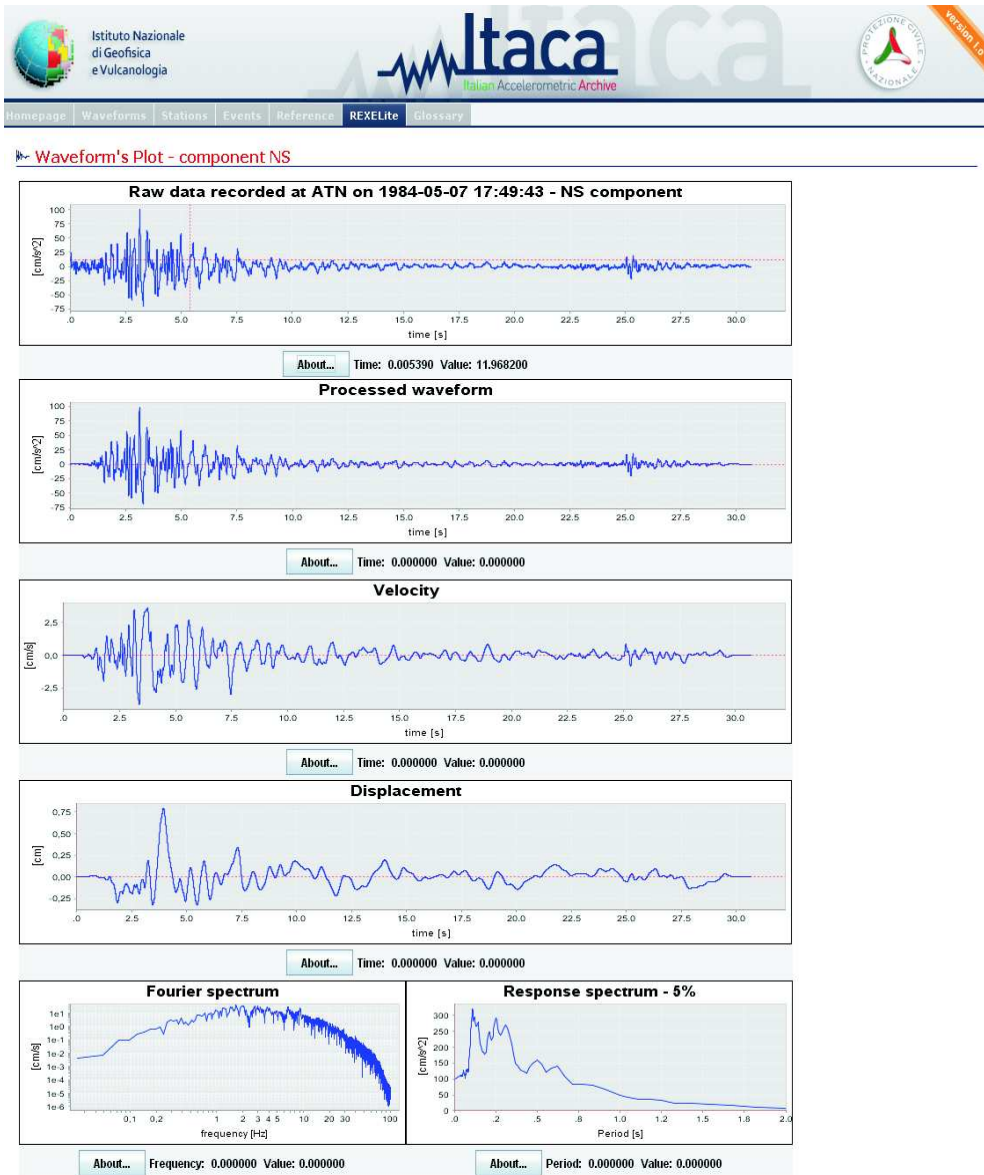


Figure 48. Screenshot of web-based waveform visualization.

To find a 2-components compatible combination, then, it was chosen to select the *Any site class* option, thus enlarging the number of records for the search for compatible sets (165 pairs of waveforms from 42 events on 77

stations); in this way, REXELite returns the combination of Figure 49 in seconds. Selecting the *non-dimensional* option, the software immediately returns the combinations of Figure 50. The mean scale factor was limited to 5 (by default) also in this case.

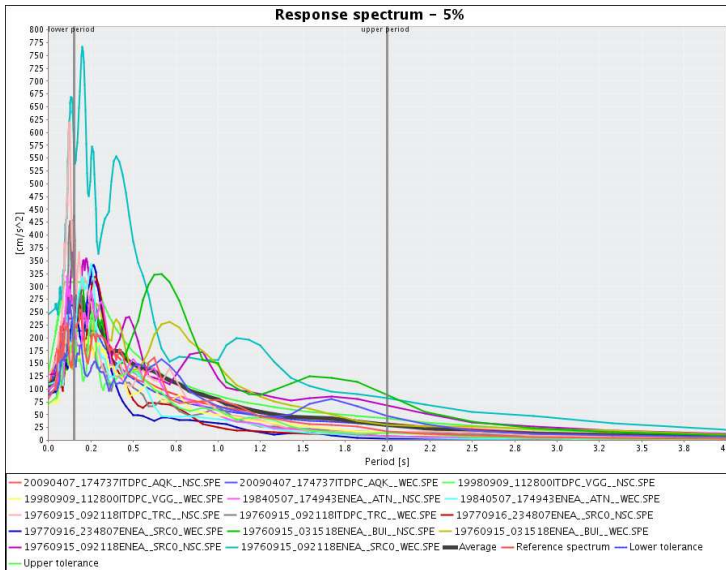


Figure 49. 2-component combination found for the assigned example in L'Aquila in the case of damage limit state.

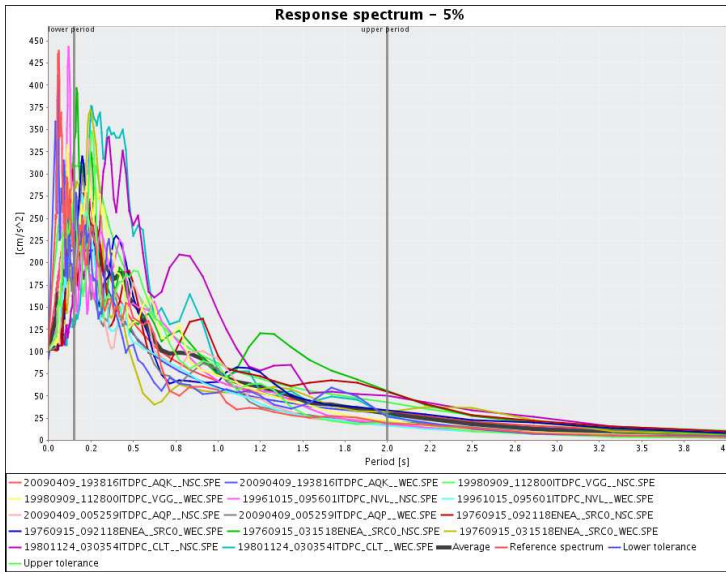


Figure 50. Scaled 2-component combination found for the assigned example in L'Aquila in the case of damage limit state.

Finally, suppose one needs to select 1-component horizontal accelerograms according to NIBC prescriptions with reference to the same target spectrum of previous examples. Moreover, suppose one is interested in only digital, normally triggered records (Figure 51).

Preliminary record search

| | | |
|-------------------------------|------------------------|----------|
| Station site classification | Any site class | |
| Magnitude min | 5.0 | max 6.0 |
| Type of magnitude to consider | Mw or MI indifferently | |
| Epicentral distance [km] min | 0.0 | max 50.0 |
| Include late trigger events | No | |
| Include analog records | No | |

Figure 51. Preliminary record search criteria.

Specifying the magnitude and distance interval equal to [5, 6] and [0km, 50km] respectively (the distance range was enlarged to balance the new constraint on data type), REXELite founds in the database 167 pairs of accelerograms (horizontal components) from 24 different earthquakes

(recorded at 56 stations on all the possible site class). Assigning a compatibility tolerance with respect to the average spectrum of 10% lower and 30% upper in the period range 0.15s ÷ 2s, the software immediately return the combinations shown in Figure 52 and Figure 53, in the case of unscaled and scaled records respectively (1-component search).

REXELite returns again the detailed information about the individual records as retrieved by ITACA (Figure 54); note that actually only accelerograms recorded by digital stations show up in the output combination.

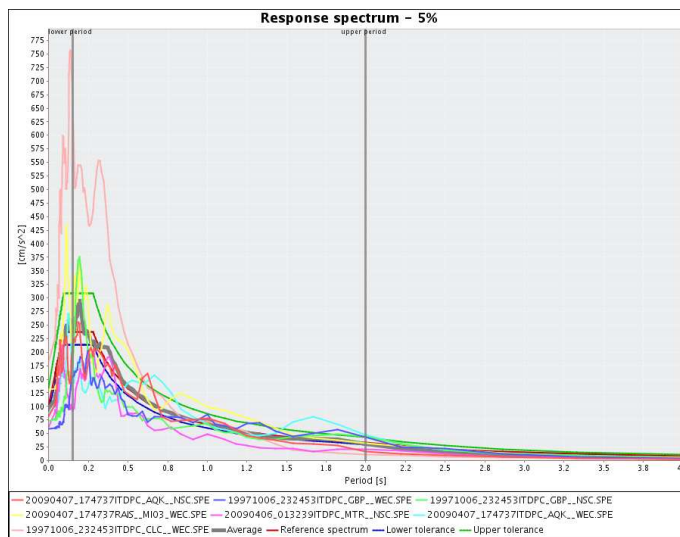


Figure 52. 1-component combination (only digital, normally triggered records) found for the assigned example in L'Aquila in the case of damage limit state.

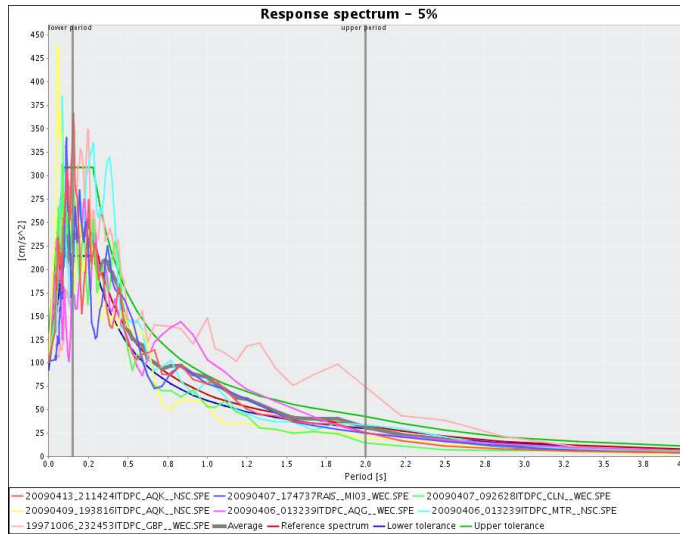


Figure 53. Scaled 1-component combination (only digital, normally triggered records) found for the assigned example in L'Aquila in the case of damage limit state.

| Network | Station code | Type | Event time | Scale factor | Usable Bandwidth | Orientation | Waveform | Sparkline |
|---------|----------------------|---------|-------------------------------------|--------------|------------------|-------------|----------|-----------|
| ITDPC | GBP | Digital | 1997-10-06 23:24:53 | 1.72015 | 29.85 | WE | | |
| ITDPC | AQK | Digital | 2009-04-06 01:32:39 | 0.233102 | 39.9 | WE | | |
| ITDPC | MTR | Digital | 2009-04-06 01:32:39 | 1.66145 | 39.92 | NS | | |
| ITDPC | CLN | Digital | 2009-04-07 09:26:28 | 19.6819 | 39.9 | WE | | |
| RAIS | MIO3 | Digital | 2009-04-07 17:47:37 | 0.780069 | 39.9 | WE | | |
| ITDPC | AQK | Digital | 2009-04-09 19:38:16 | 4.28971 | 39.9 | NS | | |
| ITDPC | AQK | Digital | 2009-04-13 21:14:24 | 5.11851 | 39.93 | NS | | |

Figure 54. Essential record data returned by REXELite for the combination of Figure 53.

5.6 CONCLUSIONS

It is widely recognized that record selection is a key issues in seismic structural analysis via nonlinear dynamics. On the other hand, practicing it,

especially with respect to code provisions, may be difficult, especially if one is looking for a suite of ground motions recorded during real earthquakes. To render practice-ready the use of strong-motion records in engineering analysis, tools implementing research-derived search algorithms may be useful, especially if these are integrated with easily accessible and constantly updated web repositories of seismic waveforms. To this aim, REXELite an internet software operating on the Italian ACcelerometric Archive, was developed for automatic selection of ground motion suites for code-based structural analysis if Eurocode 8 or the Italian seismic codes are concerned.

REXELite allows to build design spectra, according to the two codes considered, based on geographical coordinates in Italy or on the anchoring value of the spectrum and then to preliminarily select a list of records within arbitrary bounds of seismological parameters (i.e., magnitude, source-to-site distance) and recording instrument features.

Then, the program analyzes the spectra of all the combinations of seven groups (1- or 2-components) of these records and returns the set whose average spectrum is compatible with the target within the chosen period range and with the tolerances accepted; this set may be used for code-compliant engineering proposes. Moreover, the combination found by REXELite not only has the average compatible with the design spectrum, but also has the individual records with the spectral shape as similar as possible, among those preliminarily selected, to the target spectrum.

REXELite may be a successful example how integration of seismological and earthquake engineering research may effectively aid and improve seismic design and assessment practices.

References

CEN, European Committee for Standardization. (2003). Eurocode 8: Design provisions for earthquake resistance of structures, Part 1.1: general rules, seismic actions and rules for buildings, Pren1998-1.

Chioccarelli, E., Iervolino, I., Convertito, V. (2010). Italian Map of Design Earthquakes from Multimodal Disaggregation Distributions: Preliminary Results. *Proc. of 14 th European Conference on Earthquake Engineering*, Ohrid, Republic of Macedonia.

Convertito, V., Iervolino, I., Herrero, A. (2009). The importance of mapping the design earthquake: insights for southern Italy. *Bulletin of the Seismological Society of America*, 99, 2979–2991.

CS.LL.PP. (2008). DM 14 Gennaio 2008. Norme tecniche per le costruzioni. *Gazzetta Ufficiale della Repubblica Italiana*, 29. (in Italian)

CS.LL.PP. (2009). Istruzioni per l'applicazione delle norme tecniche delle costruzioni. *Gazzetta Ufficiale della Repubblica Italiana*, 47. (in Italian)

Iervolino, I., and Cornell, C.A. (2005). Record selection for nonlinear seismic analysis of structures. *Earthquake Spectra*, 21, 685-713.

Iervolino, I., Maddaloni, G., Cosenza, E. (2009). A note on selection of time-histories for seismic analysis of bridges in Eurocode 8. *Journal of Earthquake Engineering*, 13, 1125-1152.

Iervolino, I., Maddaloni, G., Cosenza, E. (2008). Eurocode 8 Compliant Real Record Sets For Seismic Analysis of Structures. *Journal of Earthquake Engineering*. 12, 54–90.

Iervolino, I., Manfredi, G. (2008). A review of ground motion record selection strategies for dynamic structural analysis. In: *Modern Testing*

Techniques of Mechanical and Structural Systems , Oreste S. Bursi, David J. Wagg (Editors), CISM Courses and Lectures 502, Springer.

Luzi, L., Hailemikael, S., Bindi, D., Pacor, F., Mele, F. (2008). ITACA (ITalian ACcelerometric Archive): a web portal for the dissemination of Italian strong motion data. *Seismological Research Letters*. 79: 716-722.

Massa, M., Pacor, F., Luzi, L., Bindi, D., Milana, G., Sabetta, F., Gorini, Marcocci, A. (2010). The Italian Accelerometric Archive (ITACA): processing of strong motion data. *Bulletin of Earthquake Engineering*. DOI 10.1007/s10518-009-9152-3. (in press)

Montaldo, V., Meletti, C., Martinelli, F., Stucchi, M., Locati, M. (2007). On-Line seismic hazard data for the new Italian building code. *Journal of Earthquake Engineering*. 11: 119-132.

Paolucci, R., Pacor, F., Puglia, R., Ameri, G., Cauzzi, C., Massa, M. (2010). Record processing in ITACA, the new Italian strong-motion database. *Proc. of 2nd Euro-Mediterranean meeting on Accelerometric Data Exchange and Archiving*. Editor: S. Akkar and P. Gulkan, Springer (in press).

Chapter 6

Conclusions

In this dissertation, record selection for non-linear dynamic analysis have been considered, focusing on consolidating the current code-based record selection procedures and on implementing research results into the practice of structural engineering.

The dissertation starts with the identification of earthquake information to be accounted for in selection once the design spectrum, which is the current basis in codes for determination of the seismic actions on structures, is given. Therefore, the developed tools for aiding the seismic input selection aim to control the spectral shape, and/or to identify other features of the signal consistent with the target spectrum and, at the same time, with the hazard (e.g., conditional hazard maps).

The final goal is to improve the estimation of structural response both in terms of *accuracy* and *efficiency*. In fact, two are the underlying critical points in the most of what discussed: (i) what ground motion parameters are relevant for structural assessment other than the spectrum (accuracy); and (ii) the “enough” number of records (small in current codes with respect to record-to-record variability of nonlinear response) to be employed in structural analysis (efficiency).

6.1 Main findings

In **Chapter 2**, different ways to obtain code-conforming real records sets were compared in terms of post elastic seismic peaks and cyclic responses. This was pursued by considering a modern code-conforming four-story RC frame building at high nonlinearity levels and a ground motion scenario (a reference

site and the corresponding code-response spectra) as case study. More specifically, maximum interstorey drift ration, roof drift and hysteretic energy were analyzed with respect to 18 sets of natural ground motion accelerograms obtained exploring all the possible options allowed by modern building codes in real record selection and modification.

Hypothesis tests were carried out with the aim of assessing quantitatively how significant these results were. Tests results shown that no particular care is required in selecting records with respect to magnitude, distance and soil condition if accelerograms match, individually or in an average sense, a target spectral shape.

Moreover, results indicated that the linearly scaled records do not show any systematic trend with respect to the unscaled record results independently of response parameters, suggesting that scaling is a legitimate technique, as many studies point out, again if the spectral shape is controlled.

Finally, it was worth noting that, as is well known, some differences in cyclic response may be observed. These differences may be predicted by some integral parameter of ground motion, which, if an appropriate hazard analysis tool is available, could be used as an additional criterion for record selection, especially in those cases when cyclic behavior has an important role in determining the seismic performances.

Starting from these consideration, **Chapter 3** presented a methodology to develop a distribution of secondary intensity measures (e.g., duration-related) conditional on the primary parameter used to define the seismic action on structures (e.g., accelerations). Such distribution can complement the hazard curves or maps produced for the primary intensity measure, especially when the cumulative damage potential of the earthquake is also of concern. This approach has the advantages of vector-valued seismic hazard analysis without the computational effort required by probabilistic seismic hazard analysis for vectors of ground motion parameters.

To explore such a concept, in this thesis the distribution of a parameter which may account for the cumulative damage potential of ground-motion,

conditional to peak ground acceleration (PGA), was investigated. The chosen secondary measure is the so called Cosenza and Manfredi index (I_D). A ground motion prediction relationship has been derived for the logarithm of I_D on the basis of an empirical dataset of Italian records already used for well known prediction equations proposed in the past by other researchers. Subsequently, the residuals of prediction relationships have been tested for correlation and for joint normality. The study allowed the obtaining of analytical distributions of I_D conditional on PGA and the corresponding design earthquake in terms of magnitude and distance from hazard disaggregation. Results of the study have been used to compute the distribution of I_D conditional on PGA with a return period of 475 years for each node of a regular grid having about 2 km spacing and covering the territory of the Campania region in southern Italy. The presented conditional hazard maps provide information on the values of I_D which, for example, should be taken into account along with the hazard in terms of PGA at the site, for ground motion record selection for nonlinear dynamic analysis of structures.

In **Chapter 4** the main issues related to code-based record selection were critically reviewed with reference to Eurocode 8 (Part 1 and Part 2) and the new Italian building code. Based on previous studies, it is shown how record selection provisions may be not easily applicable to real records. To overcome the most of the obstacles the practitioner may face when determining the seismic input for structural analysis a software tool for automatic selection of one, seven or thirty real recordings, including 1, 2 or 3 components of ground motion, was developed and presented. The main selection criterion, for unscaled or scaled sets, is the compatibility, in broad period ranges, of the average spectrum with respect to the reference spectra (which the program automatically builds) of the new Italian building code, of Eurocode 8, or user-defined. REXEL, freely available on the internet, also ensures that individual records in the combinations returned have a spectral shape like that of the target as much as possible, which is important as spectral shape is currently seen as the best proxy for earthquake damage potential on structures. The

current version of the software relies on records from the European Strong-motion Database (ESD) and the Italian ACcelerometric Archive (ITACA); nevertheless, in future developments data from other repositories could be implemented.

The capabilities of REXEL were tested and illustrated via several illustrative applications regarding selection of multi-component ground motion suites according to code- and hazard-based spectra, for different site classes and limit states or return periods. In this way it was demonstrated how the finding of spectrum-compatible sets of records, whose average is compatible with the target, can be significantly improved and facilitated. In fact, REXEL allows to select records controlling the tolerance according to which the average matches the reference spectrum. It also allows to account, beside the site class, for earthquake source characteristics (i.e., magnitude and distance) and some other ground motion parameters (e.g., I_D) which may be useful in structural assessment, as discussed above. To this aim, tools for performing disaggregation of seismic hazard for PGA and 1 sec spectral acceleration (at four different return periods) and computing the distributions of I_D conditional on design PGA, were developed and embedded in REXEL for improving record input selection for earthquake engineering applications in a hazard consistent manner yet easily viable for practitioners.

To further render practice-ready the use of strong-motion records in engineering analysis, tools, as REXEL, implementing research-derived search algorithms may be useful, especially if these are integrated with easily accessible and constantly updated web repositories of seismic waveforms. To this aim, REXELite an internet version, operating on ITACA, was developed for automatic selection of ground motion suites for code-based structural analysis if Eurocode 8 or the Italian seismic codes are concerned and presented in **Chapter 5**. REXELite allows to build design spectra based on geographical coordinates in Italy or on the anchoring value of the spectrum and then to preliminarily select a list of records within arbitrary bounds of seismological parameters (i.e., magnitude, source-to-site distance). Then the program

analyzes the spectra of all the combinations of seven groups (1- or 2-components) of these records and returns the set whose average spectrum is compatible with the target within the chosen period range and with the tolerances accepted; this set may be used for code-compliant engineering proposes. Moreover, the combination found by REXELite not only has the average compatible with the design spectrum, but also has the individual records with the spectral shape as similar as possible, among those preliminarily selected, to the target spectrum.

Via some illustrative examples it is shown how factually REXELite easily allows for a rational record selection for earthquake engineering applications.

REXEL and REXELite, therefore, may prove to be useful for practitioners to select the seismic input for code-based seismic assessment via dynamic analysis.

Finally, it is to note that the whole dissertation referred mainly to the uniform hazard spectrum as it is the current best practice to relate the design spectrum to the seismic hazard at the site; nevertheless it has some shortcomings (e.g. Chapter 1) which may impair its use as the spectrum to match in record selection, and it is likely the next generation of advanced codes will consider alternate representations of design ground motion. This could not be discussed; however, given results virtually apply to any hazard-based design spectrum.

Appendix A

Target spectra

A1. Eurocode 8 target spectra

The spectral shapes for the two horizontal orthogonal components of the seismic action, if the earthquakes that contributes most to the seismic hazard defined for the site have a surface-wave magnitude greater than 5.5 (i.e., Type 1 spectrum), is given by Equation (1):

$$\begin{aligned} 0 \leq T < T_B : S_a(T) &= a_g \cdot S \left[1 + \frac{T}{T_B} (\eta \cdot 2.5 - 1) \right] \\ T_B \leq T < T_C : S_a(T) &= a_g \cdot S \cdot \eta \cdot 2.5 \\ T_C \leq T < T_D : S_a(T) &= a_g \cdot S \cdot \eta \cdot 2.5 \left(\frac{T_C}{T} \right) \\ T_D \leq T < 4s : S_a(T) &= a_g \cdot S \cdot \eta \cdot 2.5 \left(\frac{T_C \cdot T_D}{T^2} \right) \end{aligned} \quad (1)$$

where T is the vibration period of a linear single-degree-of-freedom (SDOF) system; a_g is the design ground acceleration on type A site class; T_B and T_C are the lower and the upper limits of the constant spectral acceleration region respectively; T_D is the value defining the beginning of the constant displacement range of the spectrum; S is the soil factor and η is the damping correction factor ($\eta = 1$ for 5% viscous damping). The a_g values have to be determined by the national authorities. The values of T_B , T_C and T_D and S depend upon the ground type; the recommended values of these parameters are given in Table 22.

Appendix A

Target Spectra

Table 22. Values of the parameters describing the recommended elastic type 1 EC8 response spectra.

| <i>Ground type</i> | <i>S</i> | T_B [s] | T_C [s] | T_D [s] |
|--------------------|----------|-----------|-----------|-----------|
| A | 1.00 | 0.15 | 0.40 | 2.00 |
| B | 1.20 | 0.15 | 0.50 | 2.00 |
| C | 1.15 | 0.20 | 0.60 | 2.00 |
| D | 1.35 | 0.20 | 0.80 | 2.00 |
| E | 1.40 | 0.15 | 0.50 | 2.00 |

The vertical component of the seismic action is represented by elastic response spectrum of Equation (2). For the five ground types A, B, C, D and E, the recommended values of the parameters describing the vertical spectra are given in Table 23.

$$\begin{aligned}
 0 \leq T < T_B : S_{va}(T) &= a_{vg} \left[1 + \frac{T}{T_B} (\eta \cdot 3.0 - 1) \right] \\
 T_B \leq T < T_C : S_{va}(T) &= a_{vg} \cdot \eta \cdot 3.0 \\
 T_C \leq T < T_D : S_{va}(T) &= a_{vg} \cdot \eta \cdot 3.0 \left(\frac{T_C}{T} \right) \\
 T_D \leq T < 4s : S_{va}(T) &= a_{vg} \cdot \eta \cdot 3.0 \left(\frac{T_C \cdot T_D}{T^2} \right)
 \end{aligned} \tag{2}$$

Table 23. Recommended values of parameters describing the vertical elastic response spectra.

| <i>Ground type</i> | a_{vg}/a_g | T_B [s] | T_C [s] | T_D [s] |
|--------------------|--------------|-----------|-----------|-----------|
| A, B, C, D, E | 0.90 | 0.05 | 0.15 | 1.00 |

A.2 Italian code target spectra

The spectral shape for the two horizontal orthogonal components of the seismic action is given by Equation (3), where T is the vibration period of a linear SDOF; a_g and η have the same meaning of Eurocode 8; S is the product of the stratigraphic factor, S_s , and the topographic amplification factor, S_T ; T_B

Appendix A

Target Spectra

and T_C are the limiting periods of the spectrum's plateau; T_D is the lowest period of the constant displacement spectral portion; F_o is an amplification factor (equal to the ratio between the maximum spectral ordinate and the a_g value). The ordinates and shapes (i.e., T_B , T_C , T_D and S) depend both on the seismic hazard and site class. The same stratigraphic profiles of Eurocode 8 are considered.

$$\begin{aligned}
 0 \leq T < T_B : S_a(T) &= a_g \cdot S \cdot \eta \cdot F_o \left[\frac{T}{T_B} + \frac{1}{\eta \cdot F_o} \left(1 - \frac{T}{T_B} \right) \right] \\
 T_B \leq T < T_C : S_a(T) &= a_g \cdot S \cdot \eta \cdot F_o \\
 T_C \leq T < T_D : S_a(T) &= a_g \cdot S \cdot \eta \cdot F_o \left(\frac{T_C}{T} \right) \\
 T_D \leq T < 4s : S_a(T) &= a_g \cdot S \cdot \eta \cdot F_o \left(\frac{T_C \cdot T_D}{T^2} \right)
 \end{aligned} \tag{3}$$

The spectral shape for the vertical component of the seismic action is given by Equation (4), where T is the vertical vibration period of a linear SDOF

and F_v is the vertical amplification factor (related to F_o as $F_v = 1.35 \cdot F_o \cdot \left(\frac{a_g}{g} \right)^{0.5}$).

T_B , T_C and T_D values for the vertical response spectrum are given in Table 24.

$$\begin{aligned}
 0 \leq T < T_B : S_{va}(T) &= a_g \cdot S \cdot \eta \cdot F_v \left[\frac{T}{T_B} + \frac{1}{\eta \cdot F_o} \left(1 - \frac{T}{T_B} \right) \right] \\
 T_B \leq T < T_C : S_{va}(T) &= a_g \cdot S \cdot \eta \cdot F_v \\
 T_C \leq T < T_D : S_{va}(T) &= a_g \cdot S \cdot \eta \cdot F_v \left(\frac{T_C}{T} \right) \\
 T_D \leq T < 4s : S_{va}(T) &= a_g \cdot S \cdot \eta \cdot F_v \left(\frac{T_C \cdot T_D}{T^2} \right)
 \end{aligned} \tag{4}$$

Appendix A

Target Spectra

Table 24. Recommended values of parameters describing the vertical elastic response spectra.

| <i>Ground type</i> | S_S | T_B [s] | T_C [s] | T_D [s] |
|--------------------|-------|-----------|-----------|-----------|
| A, B, C, D, E | 1.0 | 0.05 | 0.15 | 1.00 |

The Annex B of Italian code provides a_g , F_0 and T_C^* (i.e., the T_C value for type A site class) values for the 9 return periods of seismic action (from 30 to 2500 years) and for each node of a regular grid having an about 5 km spacing and covering the whole national territory. These values are derived from the mentioned INGV seismic hazard study (Chapter 4). In particular, the F_0 and T_C^* values are obtained minimizing, for a given site and for a given return period, the deviation between the code acceleration, velocity and displacement spectra and the corresponding uniform hazard spectrum from the INGV study.

The return period to be considered depends on a (temporal) reference period (V_R , in years) and on the probability of exceedance of the a_g value in the reference period (P_{V_R}), Equation (5). P_{V_R} depends on the limit state of interest (Table 25). V_R is equal to the nominal life of the structure (V_N , in years), times the importance coefficient for the construction (C_U).

$$T_R = -\frac{V_R}{\log(1 - P_{V_R})} \quad (5)$$

Table 25. Possible values for P_{V_R} , C_U and V_N .

| P_{V_R} (Limit State) | C_U | V_N |
|-------------------------|------------------------------|---|
| 81% - Operability | 0.7 - Provisional structures | ≤ 10 years - Temporary structures |
| 63% - Damage | 1.0 - Ordinary structures | ≥ 50 years - Ordinary structures |
| 10% - Life safety | 1.5 - Important structures | ≥ 100 years - Important structures |
| 5% - Collapse | 2.0 - Strategic structures | |

For a generic return period T_R (that doesn't fall in the set of return periods for which the spectra parameters are available in the code), the value of the generic parameter may be computed by Equation (6):

Appendix A

Target Spectra

$$\log(p) = \log(p_1) + \log\left(\frac{p_2}{p_1}\right) \cdot \log\left(\frac{T_R}{T_{R1}}\right) \cdot \left[\log\left(\frac{T_{R2}}{T_{R1}}\right)\right]^{-1} \quad (6)$$

where, p is the value of the parameter of interest (a_g , F_o or T_C^*) corresponding to the required return period T_R ; T_{R1} and T_{R2} are the return periods closest to T_R and for which the p_1 and p_2 values of the p parameter are available in the code.

For the sites that don't fall in the nodes of the reference grid for which hazard was computed by INGV, the values of the parameters needed for the definition of the elastic response spectrum may be computed as a weighted averages of the values assumed by the parameters in the four vertices of the elementary (rectangular) mesh containing the point of interest. In this case, the inverse of the distances between the points of interest and the four vertices may be used as weights, as in Equation (7). In Equation (7), p is the value of the parameter of interest (a_g , F_o or T_C^*) for the site under examination, p_i is the value of the parameter of interest for the i -th vertex of the elementary mesh containing the site under examination, d_i is the distance between the site and the i -th vertex of the mesh. The code also provides relationships between a_g , F_o and T_C^* and T_B , T_C and T_D , Equation (7). The values S and C_C depend upon the site class (Table 26).

$$p = \frac{\sum_{i=1}^4 \frac{p_i}{d_i}}{\sum_{i=1}^4 \frac{1}{d_i}} \quad (7)$$

In Figure 55 the horizontal and vertical spectra for the site of the examples discussed in Chapter 4 are given. In particular Figure 55a gives the Eurocode 8 spectra, while Figure 55b provides the Italian code spectra and the uniform hazard spectrum corresponding to 63% in 50 years exceedance probability. The ordinates of the latter were retrieved from <http://esse1->

Appendix A

Target Spectra

gis.mi.ingv.it/ using the geographical coordinates of Sant'Angelo dei Lombardi.

$$T_C = C_C \cdot T_C^*$$

$$T_B = \frac{T_C}{3} \tag{8}$$

$$T_D = 4.0 \cdot \frac{a_g}{g} + 1.6$$

Table 26. Expressions defining S_S and C_C .

| <i>Site Class</i> | S_S | C_C |
|-------------------|---|------------------------------|
| A | 1.00 | 1.00 |
| B | $1.00 \leq 1.40 - 0.40 \cdot F_o \cdot \frac{a_g}{g} \leq 1.20$ | $1.10 \cdot (T_C^*)^{-0.20}$ |
| C | $1.00 \leq 1.70 - 0.60 \cdot F_o \cdot \frac{a_g}{g} \leq 1.50$ | $1.05 \cdot (T_C^*)^{-0.33}$ |
| D | $1.00 \leq 2.40 - 1.50 \cdot F_o \cdot \frac{a_g}{g} \leq 1.80$ | $1.25 \cdot (T_C^*)^{-0.50}$ |
| E | $1.00 \leq 2.00 - 1.10 \cdot F_o \cdot \frac{a_g}{g} \leq 1.60$ | $1.15 \cdot (T_C^*)^{-0.40}$ |

Appendix A
Target Spectra

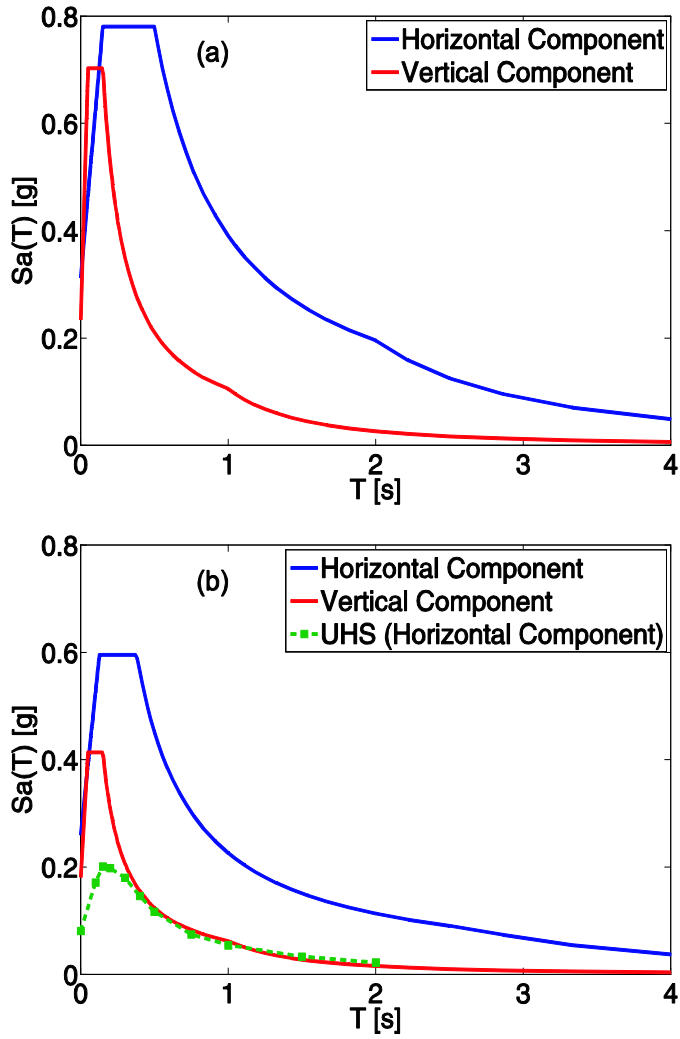


Figure 55. EC8 spectra for Sant'Angelo dei Lombardi (site class B, $a_g = 0.27g$) (a), NIBC spectra for Sant'Angelo dei Lombardi (site class A) and UHS for a 50 years return period on rock (b).

Appendix B

Earthquake ground motions used for analysis

In this appendix, essential data regarding the real record selected and used in the study (Chapter 2) are reported.

| SET | Waveform ID | Earthquake ID | Earthquake Name | Date | M | Fault Mechanism | R [km] | EC8 Site class |
|-----|-------------|---------------|----------------------------|------------|-----|-----------------|--------|----------------|
| 1 | 414 | 192 | Kalamata | 13/09/1986 | 5.9 | normal | 11 | B |
| | 413 | 192 | Kalamata | 13/09/1986 | 5.9 | normal | 10 | B |
| | 147 | 65 | Friuli (Aftershock) | 15/09/1976 | 6 | thrust | 14 | B |
| | 131 | 63 | Friuli (Aftershock) | 15/09/1976 | 6 | thrust | 14 | B |
| | 413 | 192 | Kalamata | 13/09/1986 | 5.9 | normal | 10 | B |
| | 1990 | 282 | Komilion | 25/02/1994 | 5.4 | oblique | 12 | B |
| | 230 | 108 | Montenegro (Aftershock) | 24/05/1979 | 6.2 | thrust | 8 | B |
| | mean: | | | | 5.9 | | 11 | |
| SET | Waveform ID | Earthquake ID | Earthquake Name | Date | M | Fault Mechanism | R [km] | EC8 Site class |
| 2 | 413 | 192 | Kalamata | 13/09/1986 | 5.9 | normal | 10 | B |
| | 414 | 192 | Kalamata | 13/09/1986 | 5.9 | normal | 11 | B |
| | 6334 | 2142 | South Iceland (Aftershock) | | 6.4 | strike slip | 11 | B |
| | 414 | 192 | Kalamata | 13/09/1986 | 5.9 | normal | 11 | B |
| | 413 | 192 | Kalamata | 13/09/1986 | 5.9 | normal | 10 | B |
| | 146 | 65 | Friuli (Aftershock) | 15/09/1976 | 6 | thrust | 14 | B |

Appendix B

Earthquake ground motions used for analysis

| | | | | | | | | |
|------------|--------------------|----------------------|-----------------------------|-------------|----------|------------------------|---------------|-----------------------|
| | 6334 | 2142 | South Iceland (Aftershock) | | 6.4 | strike slip | 11 | B |
| | mean: | | | | 6.1 | | 11 | |
| SET | Waveform ID | Earthquake ID | Earthquake Name | Date | M | Fault Mechanism | R [km] | EC8 Site class |
| 3 | 413 | 192 | Kalamata | 13/09/1986 | 5.9 | normal | 10 | B |
| | 6263 | 1635 | South Iceland | 17/06/2000 | 6.5 | strike slip | 7 | B |
| | 413 | 192 | Kalamata | 13/09/1986 | 5.9 | normal | 10 | B |
| | 879 | 349 | Dinar | 01/10/1995 | 6.4 | normal | 8 | C |
| | 1874 | 645 | Skydra-Edessa | 18/02/1986 | 5.3 | ? | 2 | B |
| | 322 | 153 | Campano Lucano (Aftershock) | 16/01/1981 | 5.2 | normal | 8 | B |
| | 879 | 349 | Dinar | 01/10/1995 | 6.4 | normal | 8 | C |
| | mean: | | | | 5.9 | | 8 | |
| SET | Waveform ID | Earthquake ID | Earthquake Name | Date | M | Fault Mechanism | R [km] | EC8 Site class |
| 4 | 413 | 192 | Kalamata | 13/09/1986 | 5.9 | normal | 10 | B |
| | 414 | 192 | Kalamata | 13/09/1986 | 5.9 | normal | 11 | B |
| | 879 | 349 | Dinar | 01/10/1995 | 6.4 | normal | 8 | C |
| | 7329 | 2343 | Faial | 09/07/1998 | 6.1 | strike slip | 11 | C |
| | 879 | 349 | Dinar | 01/10/1995 | 6.4 | normal | 8 | C |
| | 42 | 30 | Ionian | 04/11/1973 | 5.8 | thrust | 15 | C |
| | 7142 | 2309 | Bingol | 01/05/2003 | 6.3 | strike slip | 14 | A |
| | mean: | | | | 6.1 | | 11 | |
| SET | Waveform ID | Earthquake ID | Earthquake Name | Date | M | Fault Mechanism | R [km] | EC8 Site class |
| 5 | 104 | 28 | Friuli Earthquake 4th Shock | 15/09/1976 | 5.9 | n/a | 5 | B |
| | 232 | 59 | N/A | 16/01/1981 | 5.2 | n/a | 9 | B |
| | 467 | 114 | App. Umbro-Marchigiano | 12/10/1997 | 5.2 | n/a | 19 | B |

Appendix B

Earthquake ground motions used for analysis

| | | | | | | | | |
|------------|------------------------|--------------------------|-----------------------------------|-------------|----------|----------------------------|-------------------|-------------------------------|
| | 232 | 59 | N/A | 16/01/1981 | 5.2 | n/a | 9 | B |
| | 791 | 178 | L'aquila Mainshock | 06/04/2009 | 6.3 | n/a | 6 | B |
| | 91 | 25 | Friuli Earthquake 3rd Shock | 15/09/1976 | 5.9 | n/a | 5 | B |
| | 171 | 47 | Irpinia Earthquake | 23/11/1980 | 6.9 | n/a | 19 | B |
| | mean: | | | | 5.8 | | 10 | |
| SET | Waveform ID | Earthquake ID | Earthquake Name | Date | M | Fault Mechanism | R [km] | EC8 Site class |
| 6 | 790 | 178 | L'aquila Mainshock | 06/04/2009 | 6.3 | n/a | 4 | A |
| | 791 | 178 | L'aquila Mainshock | 06/04/2009 | 6.3 | n/a | 6 | B |
| | 791 | 178 | L'aquila Mainshock | 06/04/2009 | 6.3 | n/a | 6 | B |
| | 102 | 28 | Friuli Earthquake 4th Shock | 15/09/1976 | 5.9 | n/a | 17 | B |
| | 792 | 178 | L'aquila Mainshock | 06/04/2009 | 6.3 | n/a | 5 | B |
| | 91 | 25 | Friuli Earthquake 3rd Shock | 15/09/1976 | 5.9 | n/a | 5 | B |
| | 171 | 47 | Irpinia Earthquake | 23/11/1980 | 6.9 | n/a | 19 | B |
| | mean: | | | | 6.3 | | 9 | |
| SET | Waveform ID | Earthquake ID | Earthquake Name | Date | M | Fault Mechanism | R[km] | EC8 Site class |
| 7 | 104 | 28 | Friuli Earthquake 4th Shock | 15/09/1976 | 5.9 | n/a | 5 | B |
| | 261 | 70 | Val Comino Earthquake | 07/05/1984 | 5.9 | n/a | 20 | C |

Appendix B

Earthquake ground motions used for analysis

| | | | | | | | | |
|------------|--------------------|----------------------|-----------------------------|-------------|----------|------------------------|---------------|-----------------------|
| | 136 | 35 | Patti Gulf Earthquake | 15/04/1978 | 6 | n/a | 18 | C |
| | 88 | 25 | Friuli Earthquake 3rd Shock | 15/09/1976 | 5.9 | n/a | 12 | C |
| | 103 | 28 | Friuli Earthquake 4th Shock | 15/09/1976 | 5.9 | n/a | 16 | A |
| | 791 | 178 | L'aquila Mainshock | 06/04/2009 | 6.3 | n/a | 6 | B |
| | 171 | 47 | Irpinia Earthquake | 23/11/1980 | 6.9 | n/a | 19 | B |
| | mean: | | | | 6.1 | | 14 | |
| SET | Waveform ID | Earthquake ID | Earthquake Name | Date | M | Fault Mechanism | R [km] | EC8 Site class |
| 8 | 790 | 178 | L'aquila Mainshock | 06/04/2009 | 6.3 | n/a | 4 | A |
| | 791 | 178 | L'aquila Mainshock | 06/04/2009 | 6.3 | n/a | 6 | B |
| | 104 | 28 | Friuli Earthquake 4th Shock | 15/09/1976 | 5.9 | n/a | 5 | B |
| | 364 | 99 | Umbria-Marche 1st Shock | 26/09/1997 | 5.7 | n/a | 3 | D |
| | 791 | 178 | L'aquila Mainshock | 06/04/2009 | 6.3 | n/a | 6 | B |
| | 102 | 28 | Friuli Earthquake 4th Shock | 15/09/1976 | 5.9 | n/a | 17 | B |
| | 91 | 25 | Friuli Earthquake 3rd Shock | 15/09/1976 | 5.9 | n/a | 5 | B |
| | mean: | | | | 6.0 | | 6 | |
| SET | Waveform ID | Earthquake ID | Earthquake Name | Date | M | Fault Mechanism | R [km] | EC8 Site class |
| 9 | 1229 | 472 | Izmit | 17/08/1999 | 7.6 | strike slip | 73 | B |

Appendix B

Earthquake ground motions used for analysis

| | | | | | | | | |
|------------|--------------------|----------------------|------------------------|-------------|----------|------------------------|---------------|-----------------------|
| | 202 | 93 | Montenegro | 15/04/1979 | 6.9 | thrust | 56 | B |
| | 181 | 87 | Tabas | 16/09/1978 | 7.3 | oblique | 68 | B |
| | 289 | 146 | Campano Lucano | 23/11/1980 | 6.9 | normal | 48 | B |
| | 289 | 146 | Campano Lucano | 23/11/1980 | 6.9 | normal | 48 | B |
| | 288 | 146 | Campano Lucano | | 6.9 | normal | 43 | B |
| | 181 | 87 | Tabas | 16/09/1978 | 7.3 | oblique | 68 | B |
| | mean: | | | | 7.1 | | 58 | |
| SET | Waveform ID | Earthquake ID | Earthquake Name | Date | M | Fault Mechanism | R [km] | EC8 Site class |
| 10 | 197 | 93 | Montenegro | | 6.9 | thrust | 24 | B |
| | 4673 | 1635 | South Iceland | 17/06/2000 | 6.5 | strike slip | 15 | B |
| | 196 | 93 | Montenegro | | 6.9 | thrust | 25 | B |
| | 291 | 146 | Campano Lucano | 23/11/1980 | 6.9 | normal | 16 | B |
| | 4677 | 1635 | South Iceland | 17/06/2000 | 6.5 | strike slip | 21 | B |
| | 288 | 146 | Campano Lucano | | 6.9 | normal | 43 | B |
| | 199 | 93 | Montenegro | | 6.9 | thrust | 16 | B |
| | mean: | | | | 6.8 | | 23 | |
| SET | Waveform ID | Earthquake ID | Earthquake Name | Date | M | Fault Mechanism | R [km] | EC8 Site class |
| 11 | 1228 | 472 | Izmit | 17/08/1999 | 7.6 | strike slip | 47 | A |
| | 1229 | 472 | Izmit | 17/08/1999 | 7.6 | strike slip | 73 | B |
| | 202 | 93 | Montenegro | 15/04/1979 | 6.9 | thrust | 56 | B |
| | 6761 | 2222 | Vrancea | 30/08/1986 | 7.2 | thrust | 49 | A |
| | 181 | 87 | Tabas | 16/09/1978 | 7.3 | oblique | 68 | B |
| | 289 | 146 | Campano Lucano | 23/11/1980 | 6.9 | normal | 48 | B |
| | 181 | 87 | Tabas | 16/09/1978 | 7.3 | oblique | 68 | B |
| | mean: | | | | 7.3 | | 58 | |
| SET | Waveform ID | Earthquake ID | Earthquake Name | Date | M | Fault Mechanism | R [km] | EC8 Site class |
| 12 | 290 | 146 | Campano | 23/11/1980 | 6.9 | normal | 32 | A |

Appendix B

Earthquake ground motions used for analysis

| | | | | | | | | |
|------------|--------------------|----------------------|-----------------------------|-------------|----------|------------------------|---------------|-----------------------|
| | | | Lucano | | | | | |
| | 290 | 146 | Campano Lucano | 23/11/1980 | 6.9 | normal | 32 | A |
| | 200 | 93 | Montenegro | 15/04/1979 | 6.9 | thrust | 65 | A |
| | 196 | 93 | Montenegro | | 6.9 | thrust | 25 | B |
| | 6500 | 497 | Duzce 1 | 12/11/1999 | 7.2 | oblique | 23 | A |
| | 197 | 93 | Montenegro | | 6.9 | thrust | 24 | B |
| | 1560 | 497 | Duzce 1 | 12/11/1999 | 7.2 | oblique | 39 | C |
| | mean: | | | | 7.0 | | 34 | |
| SET | Waveform ID | Earthquake ID | Earthquake Name | Date | M | Fault Mechanism | R [km] | EC8 Site class |
| 13 | 178 | 47 | Irpinia Earthquake | 23/11/1980 | 6.9 | n/a | 36 | B |
| | 170 | 47 | Irpinia Earthquake | 23/11/1980 | 6.9 | n/a | 54 | B |
| | 375 | 100 | Umbria-Marche 2nd Shock | 26/09/1997 | 6 | n/a | 81 | A |
| | 8 | 4 | Friuli Earthquake 1st Shock | 06/05/1976 | 6.4 | n/a | 48 | B |
| | 170 | 47 | Irpinia Earthquake | 23/11/1980 | 6.9 | n/a | 54 | B |
| | 178 | 47 | Irpinia Earthquake | 23/11/1980 | 6.9 | n/a | 36 | B |
| | 8 | 4 | Friuli Earthquake 1st Shock | 06/05/1976 | 6.4 | n/a | 48 | B |
| | mean: | | | | 6.6 | | 51 | |
| SET | Waveform ID | Earthquake ID | Earthquake Name | Date | M | Fault Mechanism | R [km] | EC8 Site class |
| 14 | 803 | 178 | L'aquila Mainshock | 06/04/2009 | 6.3 | n/a | 33 | A |
| | 132 | 35 | Patti Gulf Earthquake | 15/04/1978 | 6 | n/a | 60 | A |

Appendix B

Earthquake ground motions used for analysis

| | | | | | | | | |
|------------|--------------------|----------------------|-----------------------------|-------------|----------|------------------------|---------------|-----------------------|
| | 165 | 47 | Irpinia Earthquake | 23/11/1980 | 6.9 | n/a | 77 | E |
| | 165 | 47 | Irpinia Earthquake | 23/11/1980 | 6.9 | n/a | 77 | E |
| | 383 | 100 | Umbria-Marche 2nd Shock | 26/09/1997 | 6 | n/a | 35 | A |
| | 178 | 47 | Irpinia Earthquake | 23/11/1980 | 6.9 | n/a | 36 | B |
| | 394 | 100 | Umbria-Marche 2nd Shock | 26/09/1997 | 6 | n/a | 65 | C |
| | mean: | | | | 6.4 | | 55 | |
| SET | Waveform ID | Earthquake ID | Earthquake Name | Date | M | Fault Mechanism | R [km] | EC8 Site class |
| 15 | 413 | 192 | Kalamata | 13/09/1986 | 5.9 | normal | 10 | B |
| | 414 | 192 | Kalamata | 13/09/1986 | 5.9 | normal | 11 | B |
| | 414 | 192 | Kalamata | 13/09/1986 | 5.9 | normal | 11 | B |
| | 413 | 192 | Kalamata | 13/09/1986 | 5.9 | normal | 10 | B |
| | 230 | 108 | Montenegro (Aftershock) | 24/05/1979 | 6.2 | thrust | 8 | B |
| | 159 | 72 | Friuli (Aftershock) | 16/09/1977 | 5.4 | thrust | 7 | B |
| | 1928 | 276 | Patras | 14/07/1993 | 5.6 | strike slip | 10 | B |
| | mean: | | | | 5.8 | | 10 | |
| SET | Waveform ID | Earthquake ID | Earthquake Name | Date | M | Fault Mechanism | R [km] | EC8 Site class |
| 16 | 104 | 28 | Friuli Earthquake 4th Shock | 15/09/1976 | 5.9 | n/a | 5 | B |
| | 104 | 28 | Friuli Earthquake 4th Shock | 15/09/1976 | 5.9 | n/a | 5 | B |
| | 900 | 183 | L'aquila Earthquake | 07/04/2009 | 5.6 | n/a | 5 | B |
| | 605 | 136 | App. Lucano | 09/09/1998 | 5.6 | n/a | 7 | B |

Appendix B

Earthquake ground motions used for analysis

| | | | | | | | | |
|------------|--------------------|----------------------|-----------------------------|-------------|----------|------------------------|---------------|-----------------------|
| | 605 | 136 | App. Lucano | 09/09/1998 | 5.6 | n/a | 7 | B |
| | 899 | 183 | L'aquila Earthquake | 07/04/2009 | 5.6 | n/a | 6 | C |
| | 899 | 183 | L'aquila Earthquake | 07/04/2009 | 5.6 | n/a | 6 | C |
| | mean: | | | | 5.7 | | 6 | |
| SET | Waveform ID | Earthquake ID | Earthquake Name | Date | M | Fault Mechanism | R [km] | EC8 Site class |
| 17 | 289 | 146 | Campano Lucano | 23/11/1980 | 6.9 | normal | 48 | B |
| | 289 | 146 | Campano Lucano | 23/11/1980 | 6.9 | normal | 48 | B |
| | 153 | 67 | Caldiran | 24/11/1976 | 7 | strike slip | 52 | B |
| | 6496 | 497 | Duzce 1 | 12/11/1999 | 7.2 | oblique | 45 | B |
| | 153 | 67 | Caldiran | 24/11/1976 | 7 | strike slip | 52 | B |
| | 202 | 93 | Montenegro | 15/04/1979 | 6.9 | thrust | 56 | B |
| | 202 | 93 | Montenegro | 15/04/1979 | 6.9 | thrust | 56 | B |
| | mean: | | | | 7.0 | | 51 | |
| SET | Waveform ID | Earthquake ID | Earthquake Name | Date | M | Fault Mechanism | R [km] | EC8 Site class |
| 18 | 168 | 47 | Irpinia Earthquake | 23/11/1980 | 6.9 | n/a | 42 | B |
| | 168 | 47 | Irpinia Earthquake | 23/11/1980 | 6.9 | n/a | 42 | B |
| | 176 | 47 | Irpinia Earthquake | 23/11/1980 | 6.9 | n/a | 46 | B |
| | 176 | 47 | Irpinia Earthquake | 23/11/1980 | 6.9 | n/a | 46 | B |
| | 8 | 4 | Friuli Earthquake 1st Shock | 06/05/1976 | 6.4 | n/a | 48 | B |
| | 8 | 4 | Friuli Earthquake 1st Shock | 06/05/1976 | 6.4 | n/a | 48 | B |
| | 167 | 47 | Irpinia Earthquake | 23/11/1980 | 6.9 | n/a | 59 | B |

Appendix B

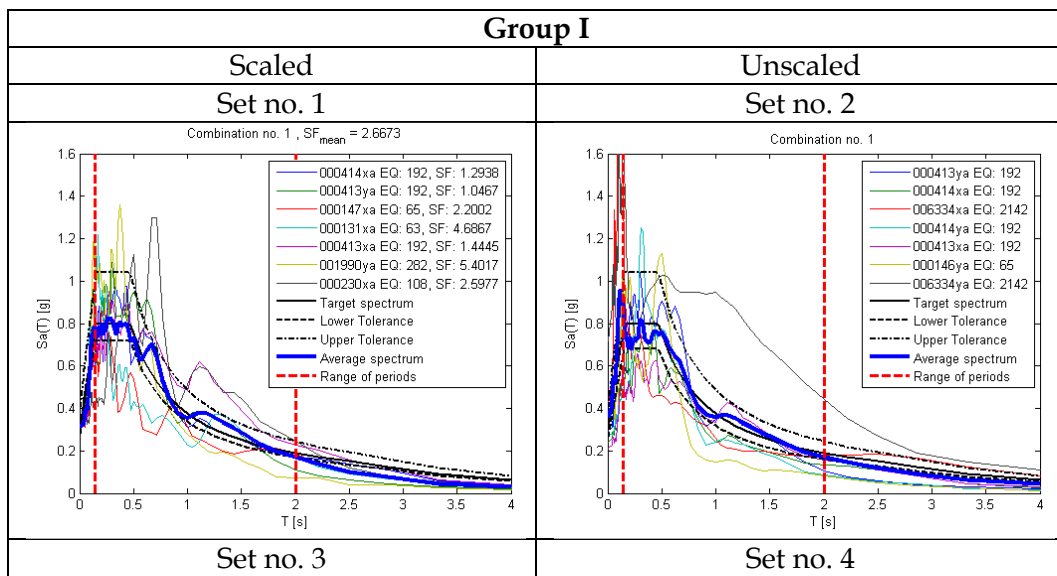
Earthquake ground motions used for analysis

| | | | | | | | | |
|--|-------|--|--|--|-----|--|----|--|
| | mean: | | | | 6.8 | | 47 | |
|--|-------|--|--|--|-----|--|----|--|

Appendix C

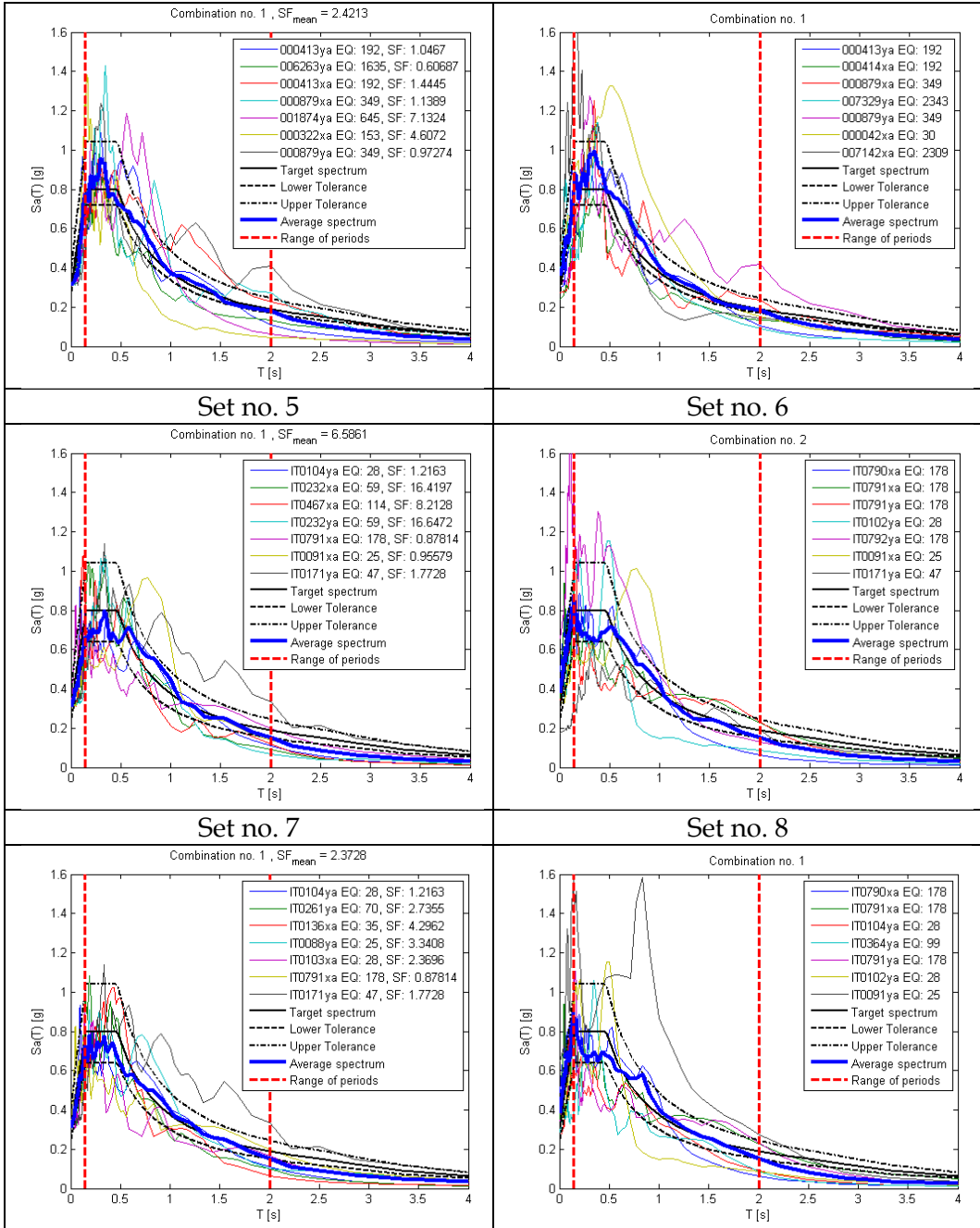
Ground motions sets used for analysis

In this appendix, plots regarding the real record selected and used in the study (Chapter 2) are reported. In the following figures, thick solid lines are the average of the set and the target spectrum, while the dashed are the tolerance and period range bounds where compatibility is ensured. Solid thin lines are the seven individual spectra of the set.



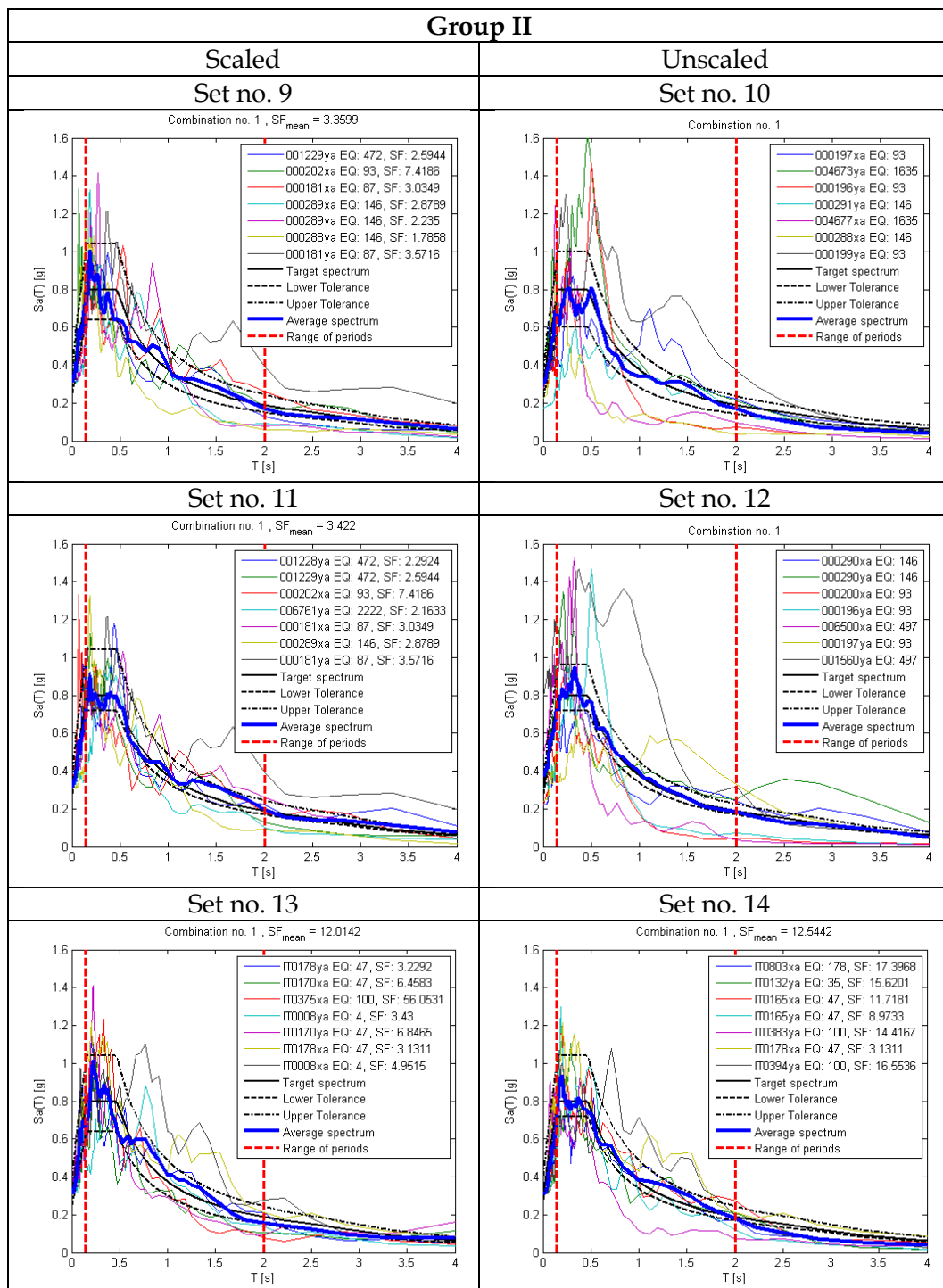
Appendix C

Ground motions sets used for analysis



Appendix C

Ground motions sets used for analysis

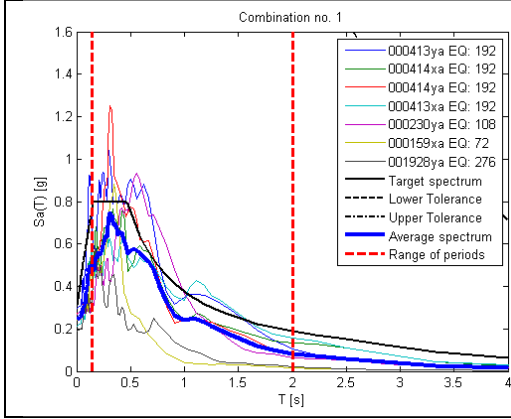


Appendix C

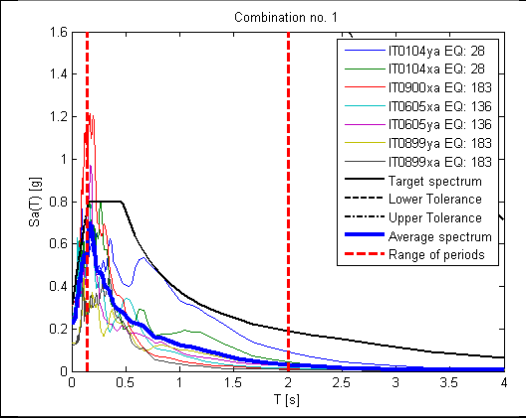
Ground motions sets used for analysis

Group III

Set no. 15

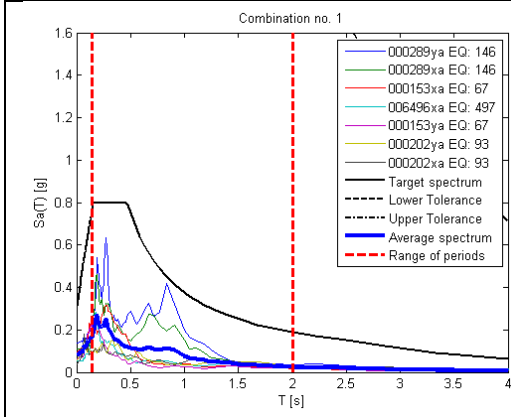


Set no. 16



Group IV

Set no. 17



Set no. 18

